

Public-data File 86-59

FLUID GEOCHEMISTRY AND FLUID-MINERAL EQUILIBRIA IN TEST WELLS AND
THERMAL-GRADIENT HOLES AT THE MAKUSHIN GEOTHERMAL AREA,
UNALASKA ISLAND, ALASKA

By

R.J. Motyka¹, L.D. Queen¹, C.J. Janik², D.S. Sheppard³,
R.J. Poreda⁴, and S.A. Liss¹

Alaska Division of
Geological and Geophysical Surveys

July, 1986

THIS REPORT HAS NOT BEEN REVIEWED FOR
TECHNICAL CONTENT (EXCEPT AS NOTED IN
TEXT) OR FOR CONFORMITY TO THE
EDITORIAL STANDARDS OF DGGS.

794 University Avenue, Basement
Fairbanks, Alaska 99709

- ¹Alaska Division of Geological and Geophysical Surveys, Fairbanks, Alaska.
²U.S. Geological Survey, Menlo Park, California.
³Department of Science and Industrial Research, Wellington, New Zealand.
⁴Scripps Institute of Oceanography, University of California, La Jolla, California.

CONTENTS

Introduction.....	3
Geologic Setting.....	8
Drilling History.....	11
Fluid Geochemistry.....	14
Sampling procedures.....	14
Methods of analyses.....	16
Water chemistry.....	18
Gas chemistry.....	20
Reservoir fluid composition.....	22
Fluid saturation.....	23
Isotope Analyses.....	26
Oxygen 18 and deuterium.....	26
Tritium.....	28
Carbon 13.....	30
Helium 3.....	31
Geothermometry.....	33
Hydrothermal Alteration.....	36
Methods.....	36
Surface alteration.....	37
Authigenic minerals in the core.....	38
Paragenesis and alteration assemblages.....	45
Fluid Inclusions.....	51
Methods.....	51
Fluid salinity.....	53
Homogenization temperatures.....	54
Alteration Equilibrium.....	58
Glacier Unloading: Cause of Recent Change in the Geothermal System.....	59
Discussion of Premier Geophysics Electrical Resistivity Study.....	63
Model of Makushin Geothermal System.....	68
References.....	72
Tables.....	87
Figures.....	
Appendix A: Fluid Geochemistry Data Tables for Fumaroles and hot springs	

INTRODUCTION

The Makushin geothermal area is located on northern Unalaska Island in the east central Aleutian Chain (fig. 1). The explored portion of the geothermal field lies on the east and southeast flanks of Makushin volcano, about 20 km west of the villages of Unalaska and Dutch Harbor. Surface manifestations of the hydrothermal system include numerous fumaroles, bicarbonate-sulfate thermal springs, and zones of intense alteration at the heads of Makushin and Glacier valleys (fig. 2). Additional fumaroles occur on the north and south flanks of the volcano and areas of warm ground are found near Sugarloaf and at the head of Nateekin Valley. Results of reconnaissance investigations indicated these thermal areas are underlain by a boiling hot-water reservoir capped by a shallow vapor-dominated zone (Motyka and others, 1981; Motyka and others, 1983).

A state-funded exploration drilling program was initiated in 1982 by Republic Geothermal, Inc. (RGI) of Santa Fe Springs, California under contract to the Alaska Power Authority (APA) (RGI report, 1983). In late August, 1983 a test-well located near the head of Makushin Valley (ST-1, fig.2) intersected a large fracture at a depth of 593 m from which

hot waters were successfully produced at the well-head. The well was flowed over a five day period then shut down until early July of 1984, then re-opened and allowed to flow for period of 45 days. The flowing bottom hole temperature (BHT) in both cases measured 193 °C. Although fluid enthalpy is relatively low, results of the reservoir engineering tests indicated the productivity of the fracture was sufficient for at least two production wells which could each drive 5 MW generators (RGI report, 1985).

Through the cooperation of RGI and APA, the authors were able to obtain samples of ST-1 fluids at the well-head during the initial testing of the well in 1983 and again in August of 1984 after the well had flowed for approximately 40 days. Rock cores extracted from a thermal gradient hole (TGH) drilled near Sugarloaf in 1984 (A-1, fig. 2) were shipped to Fairbanks, examined for mineral alteration, and compared to well-logs for ST-1 and TGH E-1, D-1, and I-1 which were previously examined by Queen, 1984. This report presents the findings of our geothermal fluid, mineral alteration, and fluid-mineral investigations of well ST-1 and the thermal gradient holes. Appendix A of this report also includes updated geochemical data on fumaroles, thermal springs, and cold waters in the Makushin geothermal area that were first discussed in Motyka and others, 1983.

Objectives of our investigations included:

- 1) Determination of reservoir fluid geochemistry.

- 2) Provision of pre-development geochemical data base.
- 3) Study of fluid-mineral equilibria.
- 4) Information on deeper reservoir characteristics and on the origin of chemical constituents in the reservoir fluids.
- 5) Geothermometry.
- 6) Mixing relationships.
- 7) Determination of potential scaling and environmental problems.
- 8) Comparison of isotopic and chemical composition of ST-1 fluids to neighboring fumaroles and springs.
- 9) History of the hydrothermal system.

The Makushin geothermal system is the first in the Aleutian arc of active volcanism to have been successfully drilled and produce fluids at temperatures above atmospheric boiling. As such, the Makushin program has provided us with a unique opportunity to study arc-related hydrothermal systems and the dynamic interactions between volcanism, glaciation, and hydrothermal systems.

The findings of our studies, discussed below, combined with our previous observations, and with results of volcanic investigations by Nye and others (1985), with measurements and tests made by RGI on the thermal gradient holes and test well (RGI reports, 1983, 1984, and 1985), and the results of

an electrical resistivity survey conducted in 1984 by Shore (1985) have led us to the following model for the Makushin geothermal system:

1) The heat source driving the hydrothermal system is presumed to be a shallow-lying body of magma as suggested by the caldera at the summit of Makushin volcano. The magma chamber is thought to be related to the post-Pleistocene outpouring of homogeneous lavas on the northeast flank of Makushin volcano and the pyroclastic flows at the head of Makushin Valley.

2) The main hydrothermal reservoir has a temperature of 250°C and is located over the heat source. Hot waters from the reservoir ascend through the core region of the volcano then cool as they spread laterally. Steam and gases that evolve from the boiling of the outflowing plume of hot water as it nears the surface feed the fumaroles and bicarbonate-sulfate thermal springs that abound at mid-elevations on the south and east flanks of the volcano.

3) The reservoir is charged by meteoric waters that infiltrate into the system along fractures located at mid- to lower elevations of the volcano. The reservoir waters obtain their chemical composition partially from release of volatile gases from the underlying magma system but mainly from interaction with the reservoir rock. ST-1 waters are moderately rich in sodium and chloride and have relatively high concentrations of calcium. The latter is attributed

to the interaction of hot waters with the gabbro-noritic intrusive that appears to be acting as the host rock for at least a portion of the reservoir waters.

4) Fluids being produced from ST 1 are out of equilibrium with the measured flowing BHT. Geothermometry indicates the waters were hotter and must have cooled upon ascent. Results of tritium studies rule out mixing of meteoric waters as the cause of the cooling. Fluids at the bottom of ST-1 are below the pressure boiling point. The remaining alternative is that the waters cooled conductively upon ascent and passage through bedrock.

5) Results of electrical resistivity surveys, conducted by Premier Geophysics of Vancouver, British Columbia, indicate that the hydrothermal system at the head of Makushin Valley is bounded by faults and fractures north and east of ST-1 and that the hydrothermal system extends west and south of ST-1 and E-1. The electrical resistivity survey showed no evidence for any hydrothermal system east of fumarole field 1 nor for any linear hydrothermal system offset to the east from the main volcano. These findings indicate that any future production wells should be sited at or up-valley of ST-1.

6) A wealth of evidence derived from mineral alteration and fluid inclusion studies indicates that the Cl- rich hot-water system extended to the surface at the heads of Makushin and Glacier Valleys in the recent past and that the

near-surface system temperature reached 250 °C. The change in hydrostatic pressure caused by the advance and retreat of Holocene glaciers is proposed as the cause of these changes in the near-surface regime of the hydrothermal system.

7) Paleotemperatures determined from fluid inclusions trapped in hydrothermal quartz veins are substantially higher than present-day temperatures in ST-1 and E-1. The temperature change indicates that at least the upper portion of the geothermal system has cooled. Nevertheless, ample energy should still be available for geothermal resource development for the foreseeable future.

GEOLOGIC SETTING

The Makushin area is one of over 70 major volcanic centers that comprise the Aleutian arc of active volcanism. The Aleutian Chain lies immediately north of the Aleutian Trench, a convergent boundary between the North American and the Pacific lithospheric plates. The eruption of Aleutian magmas appears to be intimately tied to the subduction of the Pacific plate beneath the North American plate.

Makushin Volcano (2,000 m) is a large composite, polygenetic volcanic center that dominates northwestern Unalaska Island.

The broad domed-shaped summit is capped by a ~ 5 km diameter ice-filled caldera and has glaciers that descend the larger valleys to elevations as low as 300 m. Four satellitic late-Pleistocene to Holocene volcanic cones also occur in the area and are aligned in a northeasterly trend, roughly subparallel to the strike of this portion of the Aleutian arc.

Geology of the Makushin study area, generalized from Nye and others (1984), is shown in figure 2. The oldest unit exposed in the study area is the Unalaska Formation which consists of Miocene to early Pliocene volcanoclastic rocks, dikes, sills, lava flows, and minor sedimentary rocks. The upper part of the formation consists primarily of pyroclastic rocks while lava flows dominate the lower section. The formation has been metamorphosed to grades as high as the pyroxene hornfels facies near contacts with an unzoned gabbro-noritic stock that is extensively exposed at the heads of Makushin and Glacier Valleys. The intrusive is medium-grained, equigranular to porphyritic, and consists primarily of plagioclase (50 to 75 modal percent, An_{50} to An_{70}) with subequal amounts of clinopyroxene and orthopyroxene (Nye and others, 1984). The gabbro-norite is thought to be roughly correlative with other intrusives exposed on the island and which have been dated at 10 - 13 m.y.b.p.

Fumaroles and hot springs at the heads of Makushin and Glacier Valleys emanate almost exclusively from the gabbro-norite and hornfelsic border zone. The gabbro-norite was encountered in all five holes drilled at the Makushin geothermal area and appears to be acting as the primary reservoir rock at least in the explored portions of the field. Interdigitation of the Unalaska Formation with the gabbro-norite is common, suggesting that only the roof of the stock has been exposed.

The volcanic rocks which comprise Makushin Volcano and the satellitic vents are discussed in detail by Nye and others (1985). Makushin Volcano is a polygenetic composite stratovolcano that is primarily composed of basalt and andesite flows, lahars, and pyroclastic flows. Available K Ar ages on the Makushin lavas are less than 1 m.y. indicating that the Makushin volcanics in the study area are exclusively Quaternary.

The satellitic cones are post-Wisconsinan monogenic vents consisting primarily of chemically homogeneous basaltic to andesitic flows and pyroclastic flows and cinders. A thick series of chemically homogeneous valley-filling, post Wisconsinan andesite flows also issued from the east flank of Makushin Volcano, enveloping Sugarloaf and filling Driftwood Valley. This large outpouring of post-Wisconsinan lavas and pyroclastic rocks suggests a Holocene magmatic pulse of exceptional volume. However, trace element

geochemical studies (Nye and others, 1985) indicate that the satellitic cones had source regions and plumbing systems separate from the ones supplying Makushin Volcano. The huge amount of lavas represented in the east flank Holocene Makushin eruption suggests that a large volume of residual magma may have lodged in the subcrustal region of the volcano and may be acting as the heat source for the present-day hydrothermal system.

DRILLING HISTORY ST-1

Test well ST-1 is located near the head of Makushin Valley (fig. 2). The wellhead sits upon the upper edge of an apron of pyroclastic debris that fills the bottom of upper Makushin Valley. Details of the procedures followed in the drilling of test well ST-1 (and TGH A-1) can be found in RGI's 1984 report to the Alaska Power Authority. The site chosen for ST-1 was based on the following factors: 1) proximity to E-1, which was the hottest of the thermal gradient holes drilled in 1982; 2) proximity to fumarole fields 1 and 2 and to a fault which runs up-canyon from ST 1; and 3) convenient logistical staging area for drilling. The upper part of ST-1 was drilled to a diameter of about 15 cm to a depth of about 215 m . Hole diameter below 215 m

down to well bottom is approximately 7.6 cm. Except for the top 10 m which are composed of pyroclastics, ST-1 penetrates the gabbro-norite to a depth of 593 m (Queen, 1984).

The drillers encountered a pressurized steam-filled fracture at a depth of 210 m. Well-head pressures after shut-in indicated steam temperatures of 140 to 150 °C. Samples of gases and steam evolving from the fracture were obtained from a well-head release valve. Subsequent drilling and downhole pressure measurements showed the pressurized hydrothermal system water table to lie at a depth of ~ 30 m below this fracture. Thus the steam in the fracture probably evolved from boiling of the water table.

The steam fracture was sealed and drilling continued. No additional open fractures were encountered until 585 m below the surface. The well was shut and pressure allowed to build. Upon opening of the well hot waters spurted intermittently from the well-head exhaust but continuous flow was not sustainable. Field measurements of chloride concentrations in the flashed waters ranged from 5,000 to 7,000 ppm.

Drilling was continued to a depth of 593 m whereupon the drill string dropped an estimated 1 m, indicating a major open fracture had been intersected. The well was immediately shut and the well-head pressure allowed to increase until it stabilized at approximately three bars. The well was then opened on August 27, 1983 and the resultant

fluid-flow up the borehole became self-sustaining. The well was briefly flowed and exhaust-end water samples collected for chemical analyses to determine whether any adverse environmental effects would occur upon discharge of the well waters into a local stream. After approval for discharging the waters was obtained from the appropriate agencies the well was re-opened on August 29 for a five-day flow test which included downhole pressure and temperature measurements by RGI staff scientists. During this period the authors collected five separate suites of water and gas samples.

The well was then shut down and well-head pressure monitored through the winter months. Static down-hole pressure and temperature measurements were made on July 5, 1984 and the well was re-opened on July 7. The well was flowed almost continuously over a 45-day period until shut-down on August 10, 1984. Samples of the well fluids were obtained by the authors on August 7 and again on August 9, 1984. Plans for 1984 originally called for a deepening of ST-1 after the flow test. The APA decided against the deepening in order to maintain the well for demonstration purposes. Flowing bottom hole temperatures measured 193 °C in both 1983 and 1984 (RGI report, 1985). The static hole temperature measurements made by RGI on July 5, 1984 gave a maximum down-hole temperature of ~ 198 °C at a depth of ~ 460 m. Static bottom hole temperature measured ~ 195°C.

FLUID GEOCHEMISTRY

Sampling Procedures

Samples of fluids produced from the test-well were collected both in 1983 and 1984. The majority of the samples are of fluids from the major production zone at 593 m depth. These samples were obtained between August 27, 1983 and Sept. 3, 1983 and between August 1, 1984 and August 7, 1984. The test-well was shut from Sept. 3, 1983 until July 4, 1984, then run continuously until shut-down on August 8, 1984.

Samples of gases and waters from ST-1 were collected using a Webre type mini-cyclone separator. Design and use of the separator are described in Nehring and Truesdell, 1982. Figure 3 shows the separator as used at ST-1. The separator was attached to the side of the exhaust manifold at a point about 5 m from the wellhead and 2 m before the throttling orifice. Separator pressure was monitored with a high pressure gauge located before the separator's water exhaust valve. Fluid collection pressures and temperatures together with sampling dates and steam fractions are given in table 1.

The separator was first adjusted for collection of the water fraction. Fluids emerging from the water exhaust port of the separator were routed through a condensing coil immersed in an ice bath, then collected and filtered through 0.45 micron filters. The sample suite normally consisted of 1 liter filtered untreated, 1 liter filtered acidified (HCl), 1 liter filtered and treated with formaldehyde for $S^{18}O-SO_4$ determinations, 100 ml of water at a dilution of 1:10 and 1:5 for silica determinations, 1 liter of untreated water for tritium determinations, and 30 ml of water for stable isotope determinations. In addition, raw untreated samples were collected for in-field determination of HCO_3 , pH, H_2S , and NH_3 . In two cases (samples 77 and 02), waters were filtered through 0.1 micron filters and treated in the field for Al analysis following methods described by Presser and Barnes, 1974.

As an additional check on water chemistry, water samples were collected from the end of the exhaust manifold. This was done by placing a large polyethelene beaker beneath the pipe-end and allowing the flashed water to flow into the container.

Steam and gas samples were collected after first adjusting the separator for pure steam phase flow. The steam and gases were routed through the condensing coil then collected in sodium hydroxide charged evacuated flasks. Additional samples were collected in uncharged evacuated flasks for

$^3\text{He}/^4\text{He}$ analyses. A 500 ml sample of the steam condensate was collected for Cl analyses as a check against water phase contamination. Thirty ml samples of the condensate were also collected for stable isotope analyses.

Methods of Analyses

Water

HCO_3 , pH, H_2S , and NH_3 were determined in the field following methods described in Presser and Barnes (1974). The remaining constituents were analyzed at the DGGs water laboratory in Fairbanks. Major and minor cation concentrations were determined using a Perkin Elmer atomic absorption spectrometer and following standard procedures. Sulfate and bromide were determined on a Dionex ion chromatograph. Fluoride was determined using specific ion electrode methods. Chlorides were analyzed by Mohr titration and boron by carminic acid spectroscopy. Silica concentrations were determined by the molybdate blue method.

Stable isotopes ($^{18}\text{O}/^{16}\text{O}$ and D/H) were analyzed at Southern Methodist University, Dallas, Texas and at U.S. Geological Survey, Menlo Park, California. Tritium concentrations were

determined at the Tritium Laboratory, University of Miami, Miami, Florida.

Gases

Residual gases, i.e., gases not absorbed in the sodium hydroxide solution (He , H_2 , Ar , O_2 , N_2 , and CH_4) were analyzed on a dual-column gas chromatograph with both argon and helium carrier gases at the U.S. Geological Survey, Menlo Park, California. Moles of residual gas were calculated from measured gas pressures and head space volumes. CO_2 and H_2S concentrations in the sodium hydroxide solutions were determined by titration and by ion chromatography respectively. Concentrations of these gases were also checked by gravimetric methods using SrCl_2 and BaCl_2 to precipitate SrCO_3 and BaSO_4 . The SrCO_3 precipitate was then reacted with phosphoric acid to determine CO_2 yield. The evolved gas was saved and analyzed for $^{13}\text{C}/^{12}\text{C}$. Steam content of the gases was determined by weight difference before and after sampling. Ammonia was analyzed by specific ion electrode method.

Adjustments were made for head space gases dissolved in the solution using Henry's Law. Moles of each constituent collected were then determined and the mole percent of each constituent was calculated. A correction was made for air

contamination by using the ratio of oxygen in the sample to oxygen in air. The gas concentrations in mole percent were then recalculated on an air-free basis.

Helium isotope ratios ($^3\text{He}/^4\text{He}$) were determined at the Scripps Institute of Oceanography, La Jolla, California. Carbon isotope ratios in CO_2 ($^{13}\text{C}/^{12}\text{C}$) were analyzed at the U.S. Geological Survey, Menlo Park, California.

Water Chemistry

Results of geochemical analyses of ST-1 waters obtained from the Webra mini-cyclone separator and from the end of the exhaust pipe are given in tables 2 and 3. Total discharge water chemistries, given in tables 4 and 5, were calculated using separator water and steam fractions given in table 1. The latter were based on separator pressure and a discharge enthalpy of 821 kJ/kg which corresponds to the measured flowing bottom-hole temperature of 193 °C.

End-of-exhaust water analyses give total discharge concentrations of constituents 10 to 15 percent higher than separator values if the exhaust water fraction is calculated on the assumption of atmospheric pressure-boiling point conditions. However, flashing at the exhaust end apparently occurs at pressures well below atmospheric (D. Michaels,

pers. comm., RGI, 1984). Supporting evidence for the latter comes from a temperature measurement of the center of fluid flow from the exhaust made by P. Parmentier (RGI). The temperature measured was 60°C indicating that low-pressure effects that are not well understood are causing increased flashing of the exhaust fluid. Using the 60°C temperature results in an exhaust-end water fraction of 0.75. Applying this water fraction to exhaust analyses gives total discharge chemistries that are in close harmony with those obtained from the separator method (table 6.).

Additional support for basing total discharge chemistry on the separator water analyses comes from RGI's reported analyses of 1983 ST-1 water samples. Two of their samples were obtained under high pressures using an entirely different technique than the mini-cyclone separator method (RGI Final Report, 1984, pg. XII). These samples yielded total discharge chemistries nearly identical to our separator samples.

The ST-1 waters are moderately saline and low in bicarbonate. Comparison of 1983 to 1984 chemistries show the waters to be nearly identical ; the 1984 waters are slightly less saline and slightly richer in HCO_3 . Although the ST-1 waters are moderately saline when compared to other geothermal systems in the world, they nevertheless contain more chloride than can be reasonably accounted for by leaching from the basic gabbro-noritic wallrock. Apparently

the reservoir waters either circulate through marine-laid deposits within the Unalaska Formation or the reservoir is being contaminated by seawater infiltration. A third possibility is that the chloride originates from the siliceous magmatic heat source.

The ST-1 waters are high in arsenic which could pose a potential water pollution problem for salmon spawning areas if exhaust waters are discharged directly into Makushin Valley streams. Compared to waters in other geothermal systems, ST-1 waters are relatively rich in calcium. The source of calcium is probably alteration of plagioclase in the gabbro-noritic host reservoir rock. The plagioclase has a composition of An₅₀-An₇₀ so more calcium than sodium should be dissolved by the waters. Much of the dissolved calcium must therefore be removed from the reservoir waters through reactions involving precipitation of anhydrite, calcite, and formation of zeolites.

Gas Chemistry

Air corrected analyses of gases collected from test-well ST-1 in mole percent are given in table 7. Gas content in total discharge is given table 8. Of the 1984 samples, MVTW-2G-B is the least air-contaminated and its analysis is

considered the most reliable and representative of the August, 1984 geothermal system.

Gas concentrations in total discharge are extremely low, ~ 0.02 percent, with a slight decline in total gases occurring between 1983 and 1984. Hydrogen content in particular seems to have dropped significantly, nearly an order of magnitude since the well was first opened. Methane concentrations appear to have also declined and was present in only trace amounts in the 1984 samples. Hydrogen sulfide, although 2 - 2.5 percent of the total non-steam gases, is in such low concentration in the total discharge it should not pose any significant health or pollution problems.

The $\text{CO}_2\text{-H}_2\text{S-N}_2$ composition of ST-1 gases are plotted on a tri lateral diagram which also shows compositions of fumarolic gases in the Makushin geothermal area (fig. 4). The ST-1 gases are similar in composition to gases from fumarole fields 1 and 2 suggesting they are derived from a common source at depth. Gases from the superheated fumarole (3sh, 150°C) show the highest relative concentrations of H_2S . Gases from other fumaroles and from ST-1 follow a trend towards increasingly greater proportion of N_2 indicating that the H_2S in these discharges is being selectively removed by oxidation with air or air dissolved in water. At ST-1 H_2S may also be being removed by reactions with the drillhole casing.

The ratio of N_2 to Ar is plotted against H_2 to Ar in figure 5. The N_2 /Ar ratios in the atmosphere and for air dissolved in water at 25°C are also shown for comparison. Except for 688, all ST-1 samples fall between these two values indicating air is the primary source of N_2 dissolved in the reservoir waters. Also note the early fluctuation then the trend of decreasing H_2 with time on this graph. As with H_2S , the concentration of H_2 may be affected by interactions of hot fluids with the steel drillhole casing. Alternatively, the decrease in H_2 may indicate a preferential outgassing of the lighter gases from the reservoir fluids early in the well-test.

Reservoir Fluid Composition

Concentrations of chemical species dissolved in the aquifer waters feeding ST-1 at the 593 m fracture were calculated using ENTHALP, a program originally developed by Truesdell and Singers (1973) and recently updated by Singers and Henley (pers. comm., 1984). Results of the computer calculations in molal units are given in table 9. The pH of the ST-1 waters at the reported flowing down-hole temperature is ~ 5.8, which is slightly alkaline compared to neutral pH of 5.65 for waters at this temperature.

The partial pressures of CO_2 and H_2S in the aquifer waters are given in table 10. The average PCO_2 in 1983 was 0.58 bars compared to 0.47 bars for 2G-B in 1984. PH_2S also declined from 0.005 bars in 1983 to 0.003 bars in 1984.

The oxygen partial pressures, PO_2 , of the ST-1 fluids can be estimated from the relationship between temperature and PO_2 determined by D'Amore and Panichi (1980),

$$\log \text{PO}_2 = 8.20 - (23643/T) \quad (1)$$

where T is the fluid temperature in °K. For 193 °C, the PO_2 of the ST-1 fluids is on the order of 10^{-43} atm. A check can be made on PO_2 using the equation

$$\begin{aligned} \log \text{PO}_2 = & 12.5 - 26888/T - 9/7 \log (\text{PH}_2\text{S}/\text{PCO}_2) \\ & + 6/7 \log \text{PCO}_2 \end{aligned} \quad (2)$$

(D'Amore and Panichi, 1980). Inserting values from table 10 into equation (2) gives results nearly identical to those derived using equation (1).

Fluid Saturation

Three hydrothermally deposited minerals were found layered on the gabbro-norite wallrock retrieved from the open fracture at the bottom of ST-1. The innermost layer was

composed primarily of quartz; the second layer was mostly calcite; while the outermost layer consisted primarily of anhydrite. The degrees of saturation of SiO_2 , CaCO_3 , and CaSO_4 were examined to determine whether any of these minerals are presently being deposited in the system.

The solid curve in figure 6 is the solubility of quartz in water at the vapor pressure of the solution from Fournier and Potter, 1982. All the samples obtained from ST-1 are slightly supersaturated with respect to the measured bottom hole temperature of 193°C . The quartz - silica equilibrium temperature for the ST-1 waters is $\sim 207^\circ\text{C}$ which suggests that the waters have cooled before entering the borehole.

The solid curve in figure 7 is the calcite saturation curve and the crosses are the values for ST-1 waters as determined by ENTHALP. The ST-1 waters are all undersaturated at 193°C . However, calcite was found deposited on an instrument cable that was left in the borehole for several days in mid-July, 1984. The ST-1 waters apparently became supersaturated with respect to calcite as they boiled upon ascending the borehole. The potential for calcite scaling of production well boreholes therefore exists and must be reckoned with in future development.

An estimate of the temperature of deposition of the calcite was obtained by determining the degree of fractionation of ^{18}O between the water and the calcite. The $\delta^{18}\text{O}$ of the calcite sinter was analyzed by the stable Isotope Laboratory

at Southern Methodist University and determined to be +0.6 with respect to standard mean ocean water (SMOW). Using a value of -10.2 for $\delta^{18}\text{O}$ of the water (cf. table 13) and the fractionation equation of O'Neil and others (1969), gives a temperature of deposition of $\sim 177^\circ\text{C}$.

The state of anhydrite saturation in ST-1 waters is shown by crosses in figure 8. The anhydrite equilibrium solubility curve (solid) is taken from Helgeson (1969), with the activity product of anhydrite as defined by Helgeson plotted on the Y-axis. Activity coefficients and molal concentrations for Ca and SO_4 ionic species were determined using ENTHALP. As can be seen from the figure, the waters would have to be somewhat warmer for anhydrite deposition to occur at ST-1.

An estimate of the temperature at which the anhydrite deposition occurred was obtained by determining the degree of fractionation of ^{18}O between the anhydrite and the reservoir waters (table 11). Using the fractionation equation of Chiba and others (1981) and assuming a $\delta^{18}\text{O}$ of -10.2 for the reservoir waters gives a temperature of deposition of $\sim 208^\circ\text{C}$ for anhydrite found at the bottom hole fracture. In contrast, using the same technique, anhydrite found in a vein at 592.5 m depth has an estimated temperature of deposition of 226°C while anhydrite found in a vein at 148 m depth has an estimated temperature of deposition of 249°C .

ISOTOPE ANALYSES

Oxygen 18 and Deuterium

Results of oxygen and deuterium isotope analyses of water and steam samples that were collected using the mini-cyclone separator at the ST-1 well-head are given in table 12. The corresponding pre-flash isotopic compositions of ST-1 waters are given in table 13 and plotted in figure 9. Because of suspected sampling and analyses problems, samples 76 and 84 are not included on figure 9. Also plotted on figure 9 are isotopic compositions of locally derived meteoric waters (LDMW), low Cl, high $\text{HCO}_3\text{-SO}_4$ thermal spring waters, Cl rich thermal spring waters, the meteoric water line defined by Craig (1961), and the Adak precipitation line (Motyka, 1982).

The majority of meteoric and low chloride thermal spring water samples plot to the left of both meteoric water lines while the chloride thermal spring and ST-1 waters plot to the right of the lines. Meteoric stream waters whose source regions lie at mid- to lower elevations on the volcano have heavier isotopic compositions than meteoric stream waters

whose source regions are at higher elevations. The range of isotopic compositions for low chloride thermal spring waters directly overlaps the mid-range for meteoric waters indicating the thermal waters are locally derived meteoric waters at mid-elevations.

On the basis of similarities in deuterium composition of meteoric and thermal waters, reservoir waters in the majority of explored hydrothermal systems are thought to be derived mostly from meteoric sources (Craig, 1963). The Makushin system is no exception although the high chloride concentration suggests a small amount of seawater contamination. Th seawater mixing would tend to shift the deuterium to slightly heavier values. The deuterium values of the ST-1 waters correlate with the mid- to upper range for meteoric waters which suggests that the waters charging the reservoir feeding ST-1 originated as precipitation on the mid- to lower flanks of the volcano if seawater contamination is minimal. These meteoric waters probably infiltrate into the reservoir system through fractures on the periphery of the hydrothermal system.

The ST-1 waters show a positive shift of 1 mil in $\delta^{18}\text{O}$ with respect to the two meteoric water lines and a shift of about 1.5 mils with respect to Makushin meteoric waters. Such shifts are commonly observed in geothermal systems and are caused by high-temperature oxygen isotope exchange between the thermal waters and the reservoir rock. Similar shifts

are not seen for deuterium because of the lack of hydrogen bearing minerals. The magnitude of an oxygen isotope shift is a function of water temperature, duration of contact, and the magnitude of the difference in the water vs. rock isotopic compositions. The gabbro-norite reservoir rock at Makushin was found to have a $\delta^{18}\text{O}$ composition ranging from -4.0 for highly altered rocks to +2.8 for slightly altered rocks (table 14). The difference in unaltered vs altered composition indicates isotope exchange has occurred in the Makushin hydrothermal system and thus the $\delta^{18}\text{O}$ shift observed for the ST-1 waters is probably due to high temperature exchange. However, a part of the shift could also be due to seawater mixing.

Tritium

Results of tritium analyses for waters collected from ST-1 and from various springs and streams are given in table 15 and plotted in figure 10. Panichi and Gonfiantini (1978) have reviewed the use of tritium as an indicator of age and mixing of waters in geothermal systems. Tritium was introduced into the atmosphere in large quantities during the years of thermo-nuclear weapons testing following 1952. Since the test ban treaty of 1963, tritium in the atmosphere has steadily declined, but still remains at levels much

greater than pre-1952. Because of its relatively short half-life (12.3 yrs), tritium provides a good marker for waters of recent age. To provide a comparison for Makushin waters, the tritium levels in 1980 precipitation at Anchorage (the nearest station and most recent year for which data is available) are also plotted on figure 10. The weighted-average tritium content of precipitation in Anchorage in 1980 was 29 Tritium Units (T.U.), with a seasonal variation ranging from a winter minimum of 16 T.U. to a late-spring maximum of 51 T.U.

A water sample collected from a cold spring fed by snow melt has tritium level of 11 T.U., which is consistent with winter precipitation. Tritium concentrations in low-Cl $\text{HCO}_3\text{-SO}_4$ thermal springs ranged from 16 to 36 T.U. which indicates these waters are very young and probably originated as local precipitation. The two samples collected from Cl-rich thermal springs, although lower in tritium (6 and 10 T.U.) than any of the other spring waters sampled, are still high enough in tritium to indicate that thermal waters are probably mixing with meteoric waters near the surface before emerging as springs.

In contrast, two water samples collected from ST-1 gave tritium concentrations of 0.3 and 0.5 T.U. Concentrations this low indicate the waters are at least 25 years in age and probably older (Panichi and Gonfiantini, 1978). Furthermore, the low level of tritium in the ST-1 waters

strongly argues against any substantial cold-water mixing at ST-1. Tritium concentrations in waters older than 60 yrs would be expected to be <0.1 T.U. (Truesdell and Hulston, 1980). If we assume this value as the limit for deep thermal waters at Makushin and use 29 T.U. for a cold water end member then the cold water fraction in any mixing would be at most 1.4 percent.

Carbon 13 in Carbon Dioxide

Results of analyses of $\delta^{13}\text{C}$ composition of CO_2 gas collected from ST-1 are given in table 16 and plotted in figure 11. Also plotted are $\delta^{13}\text{C}$ compositions of CO_2 gas collected from various fumaroles and hot springs. Mantle-derived CO_2 is thought to have $\delta^{13}\text{C}$ compositions ranging from -4 to -8 permil (Craig, 1953; Welhan, 1981), while CO_2 from organic-sedimentary sources have $\delta^{13}\text{C}$ values < -11 permil. The highest $\delta^{13}\text{C}$ compositions at the Makushin geothermal area were found for the samples from the summit and from the superheated fumarole in field 3. The majority of the sampled gases including those from ST-1 in 1983 fall in the narrow range of -11.5 to -13.5 permil which lies at the upper end of values for organic-sedimentary CO_2 . For reasons yet unknown the $\delta^{13}\text{C}$ - CO_2 in 1984 ST 1 fluids was found to be -15 permil, 1.5 mils less than the 1983 values.

The $\delta^{13}\text{C}-\text{CO}_2$ compositions at Makushin suggest that the CO_2 is in part being generated from thermogenic breakdown of organic-sedimentary material underlying the volcano with a magmatic intrusion acting as the heat source. These thermogenic gases then mix with CO_2 outgassing from the magma body itself and migrate into the hydrothermal reservoir.

Helium Isotopes

Samples of gases obtained from ST-1 were analyzed for helium isotope compositions. Enrichments in ^3He with respect to atmospheric levels have been correlated with magmatic activity on a worldwide basis with the excess ^3He thought to be derived from the mantle (Craig and Lupton, 1981). Samples of gases for $^3\text{He}/^4\text{He}$ testing were collected in 50-cc glass flasks (Corning 1720) fitted with high-vacuum stopcocks. The procedures followed for gas extraction, measurement of absolute helium amounts, mass spectrometer measurement of $^3\text{He}/^4\text{He}$ ratios, and application of He/Ne correction for air contamination are described in Lupton and Craig (1975), Torgersen and others (1982), and Poreda (1983).

Table 17 presents helium isotope data for ST-1 and for gases collected from fumaroles and hot springs in the Makushin

geothermal area. The R/R_a value ($^3\text{He}/^4\text{He}$ ratio of sample vs air) of 7.8 obtained for the summit fumaroles falls within the range of values of 5 to 8 found at other volcanic vents in the Aleutian Arc and from convergent margin volcanic arc settings elsewhere in the world (fig. 12) (Craig and others, 1978; Poreda, 1983). R/R_a values for gases from the flanks of Makushin are all lower than that from the summit, with the lowest values occurring at fumarole field 3 and for ST-1.

Variations in R/R_a have been found at other volcanically related geothermal systems (Craig and others, 1978; Welhan, 1981; Torgersen and others, 1982; Torgerson and Jenkins, 1982). A high value for R/R_a in gases from geothermal systems suggests a more direct connection to magmatic sources with little or no crustal contamination -- although it may also result from leaching of young volcanic rock (Truesdell and Hulston, 1980). Lower values indicate a greater crustal influence of radiogenic ^4He .

If the summit value of R/R_a is taken to represent the $^3\text{He}/^4\text{He}$ ratio of the parent cooling magma, then the R/R_a values for sites on the flanks of the volcano represent varying degrees of mixing with a crustal ^4He component. One effective method for increasing the amount of ^4He present in the gases is by hot-water interaction with and leaching of reservoir wall rock. At Makushin the host reservoir rock is a gabbro-noritic pluton. Calculations by Torgersen and

Jenkins (1982) indicate that the R/R_a ratio in an intrusive would fall to <0.1 through radiogenic decay of U and Th for emplacement ages >1.0 m.y. A mixing of 55 percent crustal He and 45 percent magmatic He would produce an R/R_a value of 3.7 with 7.8 for the magmatic component and 0.1 for the crustal component.

GEOOTHERMOMETRY

The results of applying water, isotope, and gas geothermometers to ST-1 thermal fluid geochemistry are given in tables 18, 19, and 20 and compared in figure 13. Only two of the geothermometers, the chalcedony geothermometer of Fournier (1981) and the Na/Li geothermometer of Foullic and Michard (1981), give temperatures in agreement with the flowing bottom hole temperature of 193°C reported by RGI. Free quartz is found in the gabbro-norite and for temperatures greater than 180°C quartz is the silica phase most likely to control dissolved silica (Fournier, 1981). Thus for ST-1 the quartz temperatures which average about 207°C are the more appropriate estimates to use.

The Na/K geothermometer of Arnorsson (1983) for basaltic rocks is chosen as the most appropriate for ST-1 since the

host reservoir rock is a gabbro-norite. The average temperature of 225°C given by this geothermometer is in close agreement with the average temperature of 226°C given by the Na-K-Ca geothermometer of Fournier and Truesdell (1973). The water-sulfate oxygen isotope geothermometer of McKenzie and Truesdell (1977) predicts even higher temperatures (table 19.). Using the isotopic composition of ST-1 waters (cf. table 13) this geothermometer gives reservoir temperatures of ~ 247°C.

Results of applying three different gas geothermometers to ST-1 fluids are given in table 20. The gas geothermometer of D'Amore and Panichi (1980) is based on an empirical relationship between ratios of H_2S , H_2 , and CH_4 to CO_2 and the partial pressure of CO_2 in the reservoir. For analyses in which CH_4 was present in only trace amounts a value of 0.001 mole percent was used in the computations. The H_2S geothermometer of D'Amore and Truesdell (1983) is based on equilibria between constituents affecting H_2S concentrations. The CO_2 geothermometer of Arnorsson and others (1983) is based on an empirical relationship between temperature and PCO_2 observed in geothermal waters from drillholes in Iceland.

Discounting the 250°C temperature given by the D'Amore Panichi geothermometer for MVTW-2A, the average temperatures given by the gas geothermometers are 211, 216, and 219°C, respectively. These temperatures fall between the

temperatures predicted by the quartz and cation geothermometers.

Almost all the geothermometers that were applied to ST-1 predict temperatures substantially higher than the reported flowing bottom hole temperature of 193°C, which indicates the fluid chemistry is out of equilibrium with the measured temperature. Such differences in geothermometer temperatures, particularly between the quartz, cation, and sulfate-water oxygen isotope geothermometers, have been observed at numerous other high-temperature hot-water systems and have been commonly attributed to the combination of cooling of the thermal fluids upon ascent and the differences in the re-equalibration times of the various geothermometers (Fournier, 1981). For example, quartz equilibrates fairly rapidly, on the order of days to weeks at $T \sim 200^\circ\text{C}$, while the cation geothermometers equilibrate on the order of weeks to months for $T \sim 200^\circ\text{C}$.

In contrast, the sulfate-water oxygen isotope geothermometer takes much longer to equilibrate at lower temperatures. Experimental studies by Chiba and Sakai (1985) on the fractionation of ^{18}O between H_2O and SO_4 showed the equilibration time to be weakly dependent on pH and strongly dependent on temperature. For a pH of 6 (similar to ST-1 waters) and a temperature of 250°C, the equilibration half time, $t_{1/2}$, is on the order of several weeks while for a temperature of 200°C, $t_{1/2}$ is on the order of 10 - 20 years.

Thus the sulfate-water oxygen isotope geothermometer is a good indicator of deep reservoir temperatures.

The correlation of lower calculated temperatures with shorter equilibration times for the geothermometers applied to ST-1 fluids indicates the thermal waters have slowly cooled upon ascent, before entering the ST-1 borehole. As seen from the results of the tritium analyses any cooling attributable to mixing with cold meteoric waters appears minimal. Temperature-pressure conditions preclude boiling at the bottom of ST-1 thus leaving conduction as the most likely process by which the ST-1 waters have cooled.

HYDROTHERMAL ALTERATION

Methods

The description of the lithology and minerals is based largely on hand-samples. As a control, selected samples were chosen for additional study by x-ray diffraction and optical petrography. The location of the samples taken from the cores are shown on the core logs (figs. 14, 15, 16, 17, 18). Alteration minerals that could not be immediately identified by physical properties due either to their fine-grained nature (clays) or their rarity (zeolites) were identified using x-ray diffraction. Once positively

identified it was possible to find these minerals elsewhere in the core by their physical properties. Thin sections of representative samples from both the core and similar rocks from the surface were used to assist in the description of the lithology. The lithologic units used in this paper are those of Nye and others(1984).

Surface Alteration

Alteration minerals related to the active hydrothermal system in the Makushin area occur both at the surface and at depth. The alteration minerals at the surface reflect the vapor-dominated nature of the upper portion of the Makushin hydrothermal system. Since surface alteration may not reflect the conditions of the deep production zones this study focused mainly on the subsurface alteration. The distribution and mineral assemblages of the surface alteration are discussed in Parmentier and others(1983). A brief discussion of the surface alteration follows.

At the surface hydrothermal alteration is restricted to areas around fumarole fields both active and fossil. Alteration minerals also occur to a lesser degree near active and fossil hot springs. Both active and fossil fumarole fields exhibit the same alteration assemblage. Kaolinite is the dominate mineral in the fumarole fields with lesser amounts of pyrite, iron oxides, and amorphous

silica. Sulfur and pickeringite have been identified from the fumarole encrustations. Pyrophyllite is also locally present. Outside the area of the main vents montmorillonite becomes the major clay mineral. This assemblage is interpreted to be a result of acid alteration caused by the shallow vapor-dominated zone (Parmentier and others, 1983; Reeder, 1982).

The active hot-springs in the area are low chloride bicarbonate, sulfate springs. Active formation of authigenic minerals around these springs appears to be restricted to travertine. However, in Glacier Valley there are several altered zones, interpreted to be fossil hot spring deposits, in Recent morainal deposits which contain significant amounts of halite. Motyka and others (1983) suggest that this is evidence that in the recent past chloride-rich hot-springs did exist in the area.

Alteration Minerals in the Core

Quartz is common in all the alteration groups. Its habit varies from grey cryptocrystalline veins to clear, doubly terminated, 1-2 cm long crystals in an anhydrite matrix. The most common occurrence is as veins ranging in size from 0.5 mm to 2.0 cm in width. The quartz in the veins is often an opaque milky-white. The grains of quartz in the veins are anhedral to euhedral and range in size from

cryptocrystalline to 1 cm in length. The finer grained material typically contains numerous fluid and clay inclusions while the larger euhedral crystals contain only a few scattered fluid inclusions. The quartz veins occasionally show fracturing and resealing by second generation quartz, but more frequently the quartz veins are cut by calcite and anhydrite veins.

Calcite occurs in veins, as fine-grained mixtures with clay alteration, and as euhedral crystals in open-space quartz and calcite veins. Most of the calcite veins are thin (1-2 mm) and have fine-grained (<0.5 mm), anhedral calcite. The calcite crystals in open-space veins are principally scalenohedral, but in the upper parts of well A-1 bladed calcite crystals also occur. At the bottom of well D-1 calcite is present in the brecciated hornfels as a sparry breccia filling with pyrite. The sparry calcite is translucent and is relatively free of inclusions. These calcite grains are anhedral and are about 2mm in diameter.

Anhydrite is present in two distinct habits. The more common habit is as a fine-grained vein filling. These anhydrite veins also contain calcite, quartz, pyrite, and occasional zeolites. Some of the veins are vuggy and are lined with terminated anhydrite crystals. The fine grain anhydrite veins are 1-20 mm wide and are composed of subhedral anhydrite blades 0.5-1.0 mm wide and 1-3 mm long. The alteration around these anhydrite veins is about equal

to the thickness of the veins. Plagioclase in the alteration envelope is typically altered to montmorillonite. The mafic minerals are altered to either chlorite or pyrite.

The second habit of anhydrite is as sparry, coarsely crystalline (to 3 mm wide and 15 mm long) vein and breccia fillings. The sparry anhydrite occurs with quartz, calcite, and magnetite. Vugs containing euhedral crystals of anhydrite, quartz and calcite are common in the breccia zone of ST-1. The veins and breccia clasts commonly exhibit an alteration envelope of chlorite rather than montmorillonite. The fine-grain anhydrite veins are younger than the sparry anhydrite veins.

Epidote occurs both in veins and as disseminated anhedral grains in the gabbro. When present in a vein it is never the dominate mineral. Epidote is absent from the fine-grained anhydrite veins and is uncommon in the other vein types. The epidote bearing quartz and calcite veins are among the oldest veins in the core and many show multiple stage fracturing and deposition. Epidote occurs as euhedral crystals in irregularly shapedmiarolitic, albite-epidote-quartz veins. It can make up to 10 percent of the mode in the albite-quartz-epidote veins. In the disseminated form epidote occurs as 0.5-1.0 mm diameter anhedral grains scattered throughout altered zones, especially those near the contacts between hornfels and gabbro.

Albite and K-feldspar are among the oldest alteration minerals. The albite occurs as white subhedral to euhedral crystals (0.5-1 mm) in short (1 cm) pegmatitic veins found scattered throughout the gabbro. K-feldspar occurs with the albite in these veins. The K-feldspar grains are typically larger (3-4 mm) than those of the albite and are a pinkish gray. It is always anhedral.

Chlorite and actinolite were logged together because of their intimate association in some assemblages and the general difficulty in distinguishing them in the hand samples. They are pale green and appear fibrous in hand sample. They occur in veins and as disseminated replacement of pyroxenes. The veins are generally short (0.5-1.5 cm), thin (<2 mm) and monomineralic. They lack alteration envelopes. The disseminated alteration is more common than the veins. Pyroxenes in much of the pluton have been completely altered to chlorite-actinolite. The alteration of pyroxenes is the only alteration present in some parts of the core.

The alteration of pyroxenes, particularly orthopyroxenes, to anthophyllite-cummingtonite is probably the most wide spread alteration in the core. It is difficult to see in hand specimen but in thin section it is readily apparent that most of the orthopyroxene has been altered to anthophyllite-cummingtonite and much clinopyroxene shows some degree of alteration. Like the chlorite-actinolite alteration, it

appears to be unrelated to hydrothermal vein alteration. The anthophyllite-cummingtonite is thought to be the oldest alteration in the area.

Sphene is locally present in the alteration envelopes around anhydrite veins and less commonly in the veins themselves. It is most abundant in the altered rock of the hydrothermal breccia found in ST-1. It commonly occurs as irregularly shaped aggregates of grains, although some subhedral crystals have been found in the veins.

Illite is found at a single occurrence, a clay zone in I-1 at a depth of 358 m. The clay is greenish grey and contains a mixture of montmorillonite, illite, chlorite and calcite.

Montmorillonite is the most abundant clay mineral in the Makushin Geothermal Area. It is the dominate mineral in the clay zones which occur throughout the upper portions of the cores. Generally the clay zones do not occur much deeper than 40 m below surface but in well I-1 montmorillonite clay zones occur to a depth of 450 m below surface. The clay zones are 2 to 20 cm wide fractures filled with a friable, fine-grained mixture of clay, chlorite and calcite. The clay mixture is grey-green to grey to blue-green.

Montmorillonite also replaces plagioclase in the alteration envelopes around the anhydrite veins. The montmorillonite forms soft, white pseudomorphs after plagioclase laths.

Kaolinite is rare in the core samples from Makushin, even though it is abundant in the fumarole fields in the area. It has been identified in some of the clay samples from the upper portions of wells ST-1 and E-1.

Laumontite is the most common zeolite from the core. It occurs as white, euhedral crystals in open-space calcite veins. The crystals are typically 2-3 mm in length and may locally form clusters.

Mordenite occurs as white acicular crystals in an open-space calcite-quartz vein in well I-1. The crystals are 6-7 mm in length.

Yugawaralite is restricted to two occurrences in well E-1. The yugawaralite occurs as tiny 0.5 mm euhedral crystals in an altered gabbro honey-combed with small vugs.

Wairakite has been identified in two samples from ST-1 and one from E-1. The sample from E-1 occurs at 426 m. The wairakite in this sample occurs as white, euhedral crystals on calcite crystals which in turn are on a quartz vein. The wairakite from ST-1, at 158 m and 202 m, forms massive, white alteration zones in the gabbro. In thin-section euhedral crystals of wairakite can be seen. The alteration zones are about 15-20 cm wide. The 202 m occurrence is associated with a steam producing fracture.

Stilbite is restricted to a single occurrence at 65 m in well ST-1. The stilbite forms numerous small (0.5mm)

euohedral crystals on the faces of quartz crystals in a vuggy quartz-clay vein.

Hematite is present as stains, small crystals lining fractures and rarely as replacement of magnetite. The hematite crystals are <0.5mm euohedral and metallic red. The occurrences seem to be restricted to the upper-cooler portions of the system.

Pyrite is ubiquitous throughout the core. The most common habit is as an anohedral replacement of the primary magnetite and pyroxenes. Pyrite also replaces some of the authigenic magnetite.

Pyrite may occur in veins as an accessory mineral. In the veins it occurs as small euohedral cubes(0.5-1.0 mm). Euohedral pyrite is also a common phase in the vein alteration envelopes.

Authigenic magnetite is present in all the walls except for E-1. The authigenic magnetite occurs as large sooty anohedral grains associated with sparry anhydrite. The magnetite grains commonly appear somewhat rounded. In polished section they are homogeneous and quite distinct from the ilmenite bearing primary magnetite. Rarely large grains of magnetite will occur in the gabbro seemingly removed from other alteration.

Marcasite has been found in several of the open-space quartz veins. The marcasite is tarnished and has cockscomb habit.

Paragenesis and Alteration Assemblages

The paragenetic sequence for the authigenic minerals was determined from the depositional sequence of vein minerals, cross-cutting relationships between veins, and replacement textures. Figure 19 is a paragenetic chart for all the authigenic minerals found in the drill core. Co-deposition of minerals as shown on this chart does not imply equilibrium among the phase being deposited. Local equilibrium is the rule in near-surface hydrothermal systems. Conditions can vary greatly over short distances. Minerals which cannot coexist can thus form at the same time in different parts of the system. The paragenetic chart, therefore, tells very little about equilibrium in the system.

The utility of the paragenetic chart is that allows one to see major changes in the Makushin hydrothermal area with time. For example, minerals such as biotite, hornblende and albite were deposited early on while the zeolites were deposited more recently. From the paragenetic chart and information about mineral stabilities, two major alteration events can be identified. The early alteration event is the result of deuteric alteration of the pluton and is unrelated to the active hydrothermal system. The late alteration is the work of the Makushin hydrothermal system.

The deuteric alteration comprises two assemblages: an albite ± biotite ± hornblende ± actinolite ± epidote ± quartz assemblage found in comagmatic breccias and aplite dikes, which occur randomly throughout the pluton, and an anthophyllite ± cummingtonite ± actinolite ± magnetite ± pyrite assemblage which replaces mafic phases, in particular the orthopyroxenes, in the gabbro and hornfels. The deuteric alteration occurs throughout the pluton so that it is difficult to find unaltered orthopyroxenes.

Perfit and others (1979) found that the rocks of the Captains Bay pluton showed depleted $^{18}\text{O}/^{16}\text{O}$ values with respect to normal igneous rocks. They interpreted this to be a result of the interaction of circulating meteoric water with the cooling pluton. Samples of the Makushin gabbro were analyzed for oxygen isotopes. The results are shown in table 14. Like those of the Captains Bay pluton they show depleted $^{18}\text{O}/^{16}\text{O}$ values compared to normal igneous rocks. It is therefore likely that the Makushin pluton also interacted with circulating meteoric water as it cooled. The greenschist metamorphism of the Unalaska Formation is also believed to be related to hydrothermal systems set up by the cooling plutons (Perfit and others, 1979).

The alteration related to the Makushin geothermal system is divided into two periods of deposition; an early and late period. The early period authigenic minerals seem to be a single assemblage of anhydrite ± magnetite ± calcite ±

pyrite \pm chlorite \pm epidote \pm sphene. This will be referred to as the "magnetite" assemblage. The authigenic minerals of the late period form two distinct assemblages; a montmorillonite \pm chlorite \pm calcite \pm pyrite assemblage, the "argillic" assemblage, and anhydrite \pm calcite \pm quartz \pm zeolite \pm epidote \pm pyrite \pm sphalerite \pm sphene assemblage, the "zeolite" assemblage.

The magnetite assemblage occurs principally in the hydrothermal breccias which are abundant in the upper 220 m of ST-1. The breccias occur less frequently in the other wells. The breccias consist of clasts of gabbro surrounded by a matrix of sparry anhydrite, anhedral magnetite, euhedral quartz crystals and rarely calcite crystals. The clasts are angular, 0.5-4 cm in diameter, and almost always have a chloritic alteration rind. In well D-1 the breccias are slightly different consisting of hornfels clasts in a matrix of sparry calcite and anhedral pyrite. The clasts are approximately the same size and shape and have chloritic alteration rinds.

The sparry anhydrite, as opposed to the finer grain anhydrite of the zeolite assemblage, and the magnetite serve to distinguish this assemblage. The anhydrite and magnetite appear to have formed together. This is most unusual for a geothermal system. While anhydrite is common in explored geothermal areas, authigenic magnetite has only been reported from two other geothermal areas: Tongonan,

Philippines and Tatun, Taiwan (Browne, 1978; Lan and others, 1980). The Tongonan system has temperatures of above 300° C, much higher than those so far encountered in the Makushin system.

The Makushin hydrothermal system clearly cannot have formed the magnetite assemblage under the present conditions. The breccias found in ST-1 are above the water table and the magnetite assemblage must have formed in a liquid dominated system. It also does not appear possible to deposit anhydrite and magnetite together at the present temperatures. Despite this, the magnetite assemblage does appear to be related to the Makushin system. No evidence of any early hydrothermal systems can be found in the Makushin area. Extensive exploration of the pluton at surface indicated only the deuteric alteration and the alteration around the fumaroles and hot springs. An unpublished geochemical study of the Makushin well drill chips by R. Bamford for Republic Geothermal, Inc. indicated no other hydrothermal activity other than the present system. Finally salinity data from the fluid inclusions (discussed later in this report) indicates the fluids that formed the magnetite assemblage are similar to the present fluids. Taken together this is good evidence that the magnetite assemblage was formed by the Makushin system at an earlier stage.

The zeolite and argillic assemblages are much easier to relate to the present system. The argillic assemblage is fairly typically of the vapor-dominated and cooler liquid-dominated portions of other geothermal systems (Ellis, 1979). It is basically confined to areas above the known water table to or liquid-dominated zones with temperature below ~ 100°C.

The zeolite assemblage is representative of the liquid dominated portions of the active system. The assemblage occurs in every core and is the most common of the hydrothermal assemblages. There is a rough temperature zoning for the zeolites. Mordenite was only found in I-1 and is assumed to be stable below 100°C. Laumontite is by far the most common zeolite in the Makushin system. It has been found at temperatures as low as 70°C. However, this may be a relict of the early stage. More reasonable is the occurrence in A-1 which starts at about 125°C. The upper temperature limit is probably around 190°C. Wairakite, like the laumontite, is found at temperatures that are too low to be reasonable for formation. In other systems wairakite first appears around 175°C and disappears at about 250°C. Yugawaralite is rare in the Makushin core but probably has stabilities similar to that of wairakite.

The only other zoning seen in the Makushin system is the zoning between bladed and scalenohedral calcite. In well I-1

bladed calcite occurs from 100 meters to about 340 m, below which point the calcite is scalenohedral.

As mentioned there are occurrences of the zeolite assemblage that are, like the magnetite assemblage, outside the stability limits for the assemblage. In ST-1 wairakite occurs at 137 m and at 190 m. Both of the zones are above the present water table and are at temperatures well below those reasonable for wairakite formation. The 190 m occurrence is gabbro altered to wairakite surrounding a steam producing fracture. In order for wairakite to form, the fluids must be supersaturated with respect to quartz. This impossible in a vapor-dominated system. Wairakite has been found in vapor dominated systems, but these occurrences are rare and always are at temperatures close to 200°C. The wairakite in ST-1 must have formed during an earlier period when the water table was higher than at present and the temperatures near the surface must have also been higher.

The evidence from the authigenic minerals, therefore, indicates that a change in the Makushin hydrothermal system has taken place. This change certainly involved a drop in the water table and a lowering of the temperature in the upper parts of the system.

FLUID INCLUSIONS

Methods

The fluid inclusion study was undertaken to determine the temperature and salinity of the fluids which formed the early hydrothermal minerals. Three samples from E-1, three samples from ST-1, and one sample from I-1 were selected for the homogenization and salinity investigation. The samples were selected on the basis of four criteria: (1) the samples had to contain quartz; (2) the quartz grains had to be larger than 2 mm in diameter; (3) the veins the quartz came from had to be of hydrothermal origin and (4) the sample depths had to be varied to allow a paleogeothermal gradient to be determined. Description of the samples are given in Table 21.

Although anhydrite and calcite also contain fluid inclusions and are abundant in the core, they were not used in the fluid inclusion study. They were judged unsuitable for the study for two major reasons. The first is grains of anhydrite and calcite large enough to have usable inclusions are not as abundant as large grains of quartz. The second reason is that anhydrite and calcite are thought to be more susceptible to possible re-equilibration during retrograde events than is quartz.

The fluid inclusion samples were prepared according to procedures outlined in Roedder(1984). Special care was

taken to avoid heating the samples above 80°C during preparation. The melting and homogenization measurements were done on a Linkam 600 heating-cooling stage. To determine fluid salinities the sample was cooled to -40°C, then heated at a rate of 10°C/min until the sample temperature reached -5°C. The sample was allowed to equilibrate at this temperature for one minute. Heating was then continued at 1.0°C/min until the last ice melted. After the last ice melted, heating was continued at the same rate to +12°C in order to check for clathrates.

To measure homogenization temperatures the sample was heated at 20°C/min until the sample temperature reached 180°C. The sample was allowed to remain at 180°C for one minute. The rate of heating was then reduced to 5°C/min and heating continued until homogenization was achieved. Multiple homogenization runs were made on selected inclusions to determine the repeatability of the results. Homogenization temperatures measured at heating rates of 1°C/min were within $\pm 1^\circ\text{C}$ of homogenization temperatures measured at heating rates of 5°C/min.

The inclusions used in the study ranged from .01 mm to .5 mm in diameter. Most of the inclusions were primary but some psuedo secondary and secondary inclusions were also used. The vapor fillings were between 5 and 10 percent. The vapor bubbles were slightly darker than one would expect for pure H₂O vapor. Typical inclusions are shown in figure 20.

About half the inclusions contained thin, transparent, daughter minerals (fig 21). The daughter mineral did not show any visible dissolution even at 400°C. This may indicate that the minerals are accidental inclusions and not true daughters.

Fluid Salinity

Figure 22 shows the temperature of last ice melting for 80 inclusions from five samples (ST-1:277, ST-1:295, E-1:791, E-1:1155, E-1:1396). The variation shown by the melting temperatures is within the error limits for the cooling stage. Thus it is reasonable to assume that the compositions of the fluid inclusions is constant.

Using the equation given by Potter and others (1978) to determine the inclusion salinity in NaCl molar equivalents from the temperature of last ice melting, one obtains for the mean temperature a salinity of 0.106 M NaCl or 6194 ppm. The measured salinity of the ST-1 waters is 0.098 M NaCl or 5868 ppm. Even ignoring the difficulty in measuring the salinity of low salinity inclusions, the agreement between present system salinities and the fluid inclusion salinities is remarkable.

After the last ice melted the samples were checked for clathrates. Although the dark vapor bubble indicated the presence of some CO₂, no clathrates were observed. The

active hydrothermal system has CO_2 partial pressures of 0.5 bars which are much too low to allow clathrate formation.

Thus for the compositional information that can be obtained from freezing the inclusions, the paleofluid and the present fluids appear the same. This seems to rule out any major changes in composition during the life of the Makushin hydrothermal system. Although it would be desirable to obtain quantitative chemical analysis of the fluid inclusion, this seems unlikely at the present due to the dilute nature of the fluid inclusions.

Homogenization Temperatures

Figures 23a, b, and c show the fluid inclusion homogenization temperatures at the appropriate sample depth in each well. Also shown are the measured thermal gradients (MTG) and the hydrostatic reference boiling curve (RBC).

The degree of vapor filling in the inclusions at 40°C was essentially constant, being between 5 and 10 percent by volume. All of the inclusions homogenized to a high density fluid (i.e. the vapor bubble shrank). These observations are generally taken to indicate that the fluid inclusions were formed in a liquid-dominated environment and that the liquid was not boiling. However, experience in other geothermal fields indicates that similar inclusions can form from

fluids which are boiling (Roedder, 1984). Therefore one can not say that boiling has not occurred, but only that there is no evidence for boiling.

The lack of evidence of boiling prevents the determination of the pressure correction to be applied to the homogenization temperatures to get the true temperature of trapping. However, in many explored geothermal system the pressure is close to hydrostatic. Since the Makushin samples came from fairly shallow depths the pressure correction should be small. Never the less the homogenization temperatures should be regarded as minimum temperature of trapping.

The most striking feature of the homogenization temperatures is that they are all above the measured well-temperatures for the sample depth. In some samples the highest homogenization temperatures are $>100^{\circ}\text{C}$ above the maximum bottom-hole temperature so far measured in the Makushin system. Despite this the inclusions do probably represent the conditions of the early Makushin Geothermal System. As discussed earlier in this report the evidence strongly suggests that all the hydrothermal alteration in the wells is related to one hydrothermal system.

Fluid inclusion homogenization temperatures are often significantly greater than the present measured temperatures for a well (Bargar and others, 1984a; Bargar and others, 1984b; Keith and others, 1984; Huang, 1984; Taguchi and

others, 1980; Taguchi, 1983). The lower homogenization temperatures are, however, in most fields within $\pm 5^{\circ}\text{C}$ of the preproduction measured temperature curve. The higher homogenization temperatures are, therefore, usually interpreted as evidence that the geothermal system has cooled. Thus the fluid inclusion homogenization temperatures suggest that the Makushin geothermal field has cooled as much as 100°C in places.

The difficulty with this interpretation lies in that most of the homogenization temperatures lie above the hydrostatic boiling curve. As can be seen in figures 23a, b, and c the mean temperature of homogenization of all the samples is at or exceeds the hydrostatic boiling curve indicating boiling should have taken place. The fluid inclusion data does not rule out boiling at the time of the inclusion trapping, but if boiling were taking place the homogenization temperatures could not exceed that of the boiling curve. The boiling curve must have, therefore, been shifted toward higher temperatures for a given present depth in the early geothermal system.

A shift of the boiling curve can be effected by an increase in salinity or an increase in pressure. For the Makushin geothermal system the increase in salinity can be ruled out based on the fluid inclusion freezing data. This means the shift in the boiling curve must have been due to increased pressure in the past. Additional pressure can be supplied if

the system is self-sealed so that lithostatic pressures rather than hydrostatic apply. The lithostatic pressures are, however, still too small to prevent boiling in all but deepest the samples. Self-sealed geothermal systems can over-pressure, however the over-pressure can not exceed the lithostatic pressure by more than approximately 30 per cent (Muffler and others, 1971). In the case of the Makushin system the over-pressure required to prevent boiling in the upper samples exceeds the lithostatic pressure by a factor of 3.

We must therefore invoke a mechanism to increase the hydrostatic and/or the lithostatic pressure. This can only be done by increasing the overburden on the system. In many fossil systems the overburden is assumed to be rock. If we assume that the Makushin system was solely under hydrostatic pressure then the amount of rock that has been eroded must exceed 300 meters. A lithostatic load would require 100 meters of rock.

This is probably an unreasonable amount of material to erode during the expected lifetime of this geothermal system. Rates of erosion by two large glaciers in Iceland were calculated to be 6.4cm and 55cm/ 100 yr respectively (Okko, 1955). Assuming these values to be a upper and lower limit to the erosion rate in the Makushin area we can estimate the amount of time require to erode the 100 to 300 m of rock over-burden. The result is it would require between

approximately 20,000 to 500,000 years. While these numbers are reasonable given the amount of time the geothermal system could exist the surface alteration suggest that this is not what occurred.

If the additional pressure were supplied by rock now eroded away one would expect to find evidence of the liquid dominated system at the surface. The evidence would be in the form of veins and liquid-dominated type alteration. As was discussed earlier the surface alteration is confined to vapor-dominated type alteration. Thus it does not seem likely that rock is the source of the additional pressure.

Instead, as we will discuss in a subsequent section, we propose that the additional pressure was supplied by glacial loading.

Alteration Equilibrium in the Makushin System

Having established the likely temperatures and pressures of the paleogeothermal system it is now possible to apply thermodynamic data to the alteration mineral assemblages and check for consistency.

The authigenic minerals of a hydrothermal system are the end result of the interaction among several physical-chemical factors. Browne(1978) grouped these factors under six major

headings: (1) temperature (2) pressure (3) rock type (4) fluid composition (5) permeability and (6) duration of activity. These factors vary from field to field and in most cases vary greatly even within an individual field. Most of these factors can be more or less directly measured to determine the present conditions. Chemical thermodynamics allows use to predict the results of some of the factors. The model created by the chemical thermodynamic data can then be compared to what is actually seen.

Figure 25 is a chemical potential diagram for the system $\text{CaO-Al}_2\text{O}_3\text{-SiO}_2\text{-H}_2\text{O}$. The phases shown are all found in the Makushin system. Good thermodynamic data is unavailable for some of the phases. This precludes their being shown on a standard activity diagram. One can, however, obtain information about the system from the shape of their fields and their location on chemical potential diagrams. There are some restrictions which can be applied to the chemical potential diagram shown.

Wairakite is known to form only at or above quartz saturation. This means that for a given temperature all the phases to the right of wairakite form at silica activities above quartz saturation. Margarite is also known to form only at silica activities below quartz saturation. Thus one would not expect to find zeolites and margarite together. Indeed this is the case. Zeolites are present in the Makushin system while margarite and gibbsite are absent.

Prehnite is also absent in the system. This could indicate that Ca activity is limited by some mechanism.

The zoning of zeolites on the diagram reflect the zoning of zeolites with temperature shown in the system. Similar zoning patterns are seen in other systems. The mechanism for this zoning appears to be related to the change in the silica activity buffer with temperature. At temperatures above 180°C, water is usually saturated with respect to quartz; at lower temperatures, however, the stable silica phase becomes chalcedony or opal (Arnorsson, 1975). This allows the higher silica zeolites to form at the lower temperatures and thus creates the zoning pattern (Browne, 1978; Henley and Ellis, 1983).

Figure 25 is the activity diagram for the $\text{Ca-Al}_2\text{O}_3\text{-SiO}_2\text{-H}_2\text{O}$ system at 200°C. As one can see the Makushin water plots in the kaolinite stability field. Kaolinite is not an abundant mineral in the cores, however. This might be due to one of three things: (1) The actual temperature of the water is 195°C and thus the diagram is at an inappropriate temperature. (2) Kaolinite is present but in such small amount it was overlooked. (3) The water does not plot correctly. This last problem appears to be the case. The difference in temperature between the actual temperature of the fluid and the diagram is not enough to change the relative position of the point in the fields. If kaolinite is present in small quantities that have been overlooked

then it would indicate a non-silicate mineral represents the bulk of the calcium bearing alteration. This is possible but would be unusual for most geothermal systems. The water is saturated with respect to quartz at about 207°C. While the change from 207°C to 195°C would allow the silica activity to rise it is not sufficient to allow the deposition of wairakite. It would be enough to allow for the deposition of laumontite. Laumontite is close to its upper thermal boundary at 200°C but in the Makushin system it does appear to be stable.

Laumontite might well be the stable zeolite in the Makushin system under the present conditions. The wairakite may have formed shortly after the formation of the magnetite assemblage while the system was cooling. If this was accomplished in a rapid fashion (i.e. boiling) then the silica activity would be allowed to rise considerably above the quartz saturation limit. This would in turn allow the formation of wairakite. Thus the wairakite may be more indicative of the past conditions than of the present.

Figures 26 and 27 are activity diagrams for the systems $K_2O-Al_2O_3-CaO-H_2O$ and $Na_2O-Al_2O_3-Ca-H_2O$ respectively. The Makushin waters in these diagrams fall in the white mica fields. Although white mica is not shown in the alteration charts it is present in the cores. The plagioclase around some of the recent veins always has some white mica alteration. The amounts are small but significant. White

mica has also been reported as the most recent mineral from vein material recovered from the bottom fracture of ST-1. In this case it does seem likely that the active diagrams do reflect the equilibrium in the present system.

A final phase diagram has been drawn to help explain the unusual magnetite assemblage from the ST-1 breccias. All the available evidence indicates the magnetite breccias formed during or shortly after the end of the high temperature stage of the Makushin hydrothermal system. Figure 28 is a fO_2 -pH diagram for the system Fe-O-S at 250°C. Also shown are the calcite and anhydrite insoluble lines. From the homogenization temperatures, 250°C is a reasonable guess at the temperature of the high temperature stage.

The original fluid must have had a pH and fO_2 such that calcite and anhydrite were soluble. Furthermore the fO_2 cannot have been lower than the pyrite-pyrrhotite line, since pyrrhotite is not present in the Makushin system. For geothermal systems at 250-300°C, Ellis and Mahon(1977) have proposed fO_2 values of between 10^{-40} and $10^{-37.5}$. These are our assumed conditions of the origin system. Clearly under these conditions anhydrite, calcite and magnetite could not formed.

Deposition could be accomplished by changing the fO_2 values but changes in oxidation are difficult and slow at these conditions. Instead it much easier to change the pH. One

simply allows the fluids to boil. The pH change in the present Makushin waters due to boiling is over 2.0 pH units. Since fluid inclusion data indicates that the composition of the paleofluids were similar to the present fluids, it is reasonable to assume similar change in pH if the early Makushin system boiled rapidly. Such a change could result in the deposition of anhydrite, magnetite, calcite and quartz.

GLACIER UNLOADING: CAUSE OF RECENT CHANGE IN THE GEOTHERMAL SYSTEM

We have accumulated compelling evidence indicating that a rapid decline in the water table and a cooling of the upper part of the Makushin hydrothermal system occurred in the geologically recent past. The current depth to the pressurized hydrothermal system as determined from drill holes, lies at 230-240 m below the the surface in upper Makushin Valley. A vapor-dominated zone presently extends from this depth to the surface. By inference a shallow vapor-dominated zone of similar magnitude is thought to exist at the head of Glacier Valley in the vicinity of fumarole field 3. Yet halite was found coating

hydrothermally cemented rocks in neoglacial moraines and outwash deposits in the upper part of Glacier Valley (Motyka and others, 1983). These salt deposits are thought to be relicts of fossil chloride-rich thermal springs and indicate a hot-water system reached the surface in recent times in a region that is now dominated by fumarole activity and $\text{HCO}_3\text{-SO}_4$ thermal springs.

The hydrothermal alteration mineral assemblages found in the upper parts of holes E-1 and ST-1 (which include quartz, calcite, anhydrite, wairakite, and montmorillonite) could only have been formed under hot-water neutral to slightly alkaline conditions and not the acid-steam conditions that presently exist in this zone. Furthermore, trace-element enrichment and depletion studies of core from the Makushin geothermal area also indicate neutral pH hot-water rather than acid-steam conditions in the upper parts of the drill holes (Isselhardt and others, 1983). The apparent lack of steam-dominated mineral assemblages and trace-element geochemistry in these zones indicates the hydrothermal system water level dropped fairly recently.

The evidence from our fluid inclusion studies indicates that the temperature of the hot-water hydrothermal system at the time the fluid inclusions were entrapped in vein -deposited quartz in the upper parts of the system were substantially hotter than present-day temperatures. Examination of figure 23 shows that paleotemperatures at depths as shallow as 100

m below the present day surface were as high as 250°C. The studies also indicate that the waters from which the quartz was precipitated had a salinity nearly the same as the present-day system. If the paleo-fluid is assumed to have had a $S^{18}O$ composition similar to the present day reservoir waters we can then apply the equilibrium fractionation equation of Chiba and others (1981) to anhydrite found in a vein at a depth of 149 m (cf. table 11). The result gives a temperature of formation of ~ 250°C which is similar to the temperatures of formation of fluid inclusions in the associated quartz.

The pressure required to sustain such high temperatures at saturation boiling point conditions is about 40 bars which is equivalent to a hydrostatic head of over 400 meters. To produce such high pressures the system must have either been self-sealed or some other mechanism of pressure loading must have been in effect. We reject the hypothesis of lithostatic self-sealed pressurization because of the high pressures involved and because of the highly fractured nature of the host gabbro-norite as evidenced by the numerous fumaroles and hot-springs that presently exist throughout the area.

Instead we prefer to invoke ice-loading of the hydrothermal system during a neo-glacial advance to explain the anomalously high temperatures recorded by the fluid inclusions. Ice-thicknesses of 400 - 500 m are commonly

found in present-day valley type glaciers in Alaska and it is reasonable to assume such ice-thicknesses existed in Makushin and Glacier Valleys in neo-glacial times. The increased hydrostatic pressure exerted by the ice would be sufficient to produce the elevated temperatures recorded by the fluid inclusions. Such interactions between ice loading and hydrothermal systems exist today in Iceland, particularly in the Vatnajökull Grímsvötn caldera area (Björnsson, 1975) and are also thought to have occurred during glacier advances and retreats in the Yellowstone National Park geothermal areas (Muffler and others, 1971; R. Fournier, USGS, pers. comm.)

The thermal fields at Makushin lie at the heads of valleys on the flanks of a volcano which still maintains a sizeable ice-cap and a system of valley glaciers. At least two neoglacial advances that reached tide water have been documented elsewhere in the Aleutians (Black, 1983) and it is reasonable to assume that correlative glacial advances occurred at Makushin. There are in fact abundant neoglacial moraines, outwash deposits, and glacial scouring marks in Glacier, Makushin, and Driftwood Bay Valleys. The most recent advance and retreat in the Aleutians is estimated by Black (1983) to have occurred about 3,000-4,000 years b.p.

At the Vatnajökull in Iceland, meltwater generated by subglacial geothermal heating becomes entrapped in large,

hydrostatically sealed subglacial chambers. The seals on these subglacial meltwater reservoirs are periodically broken resulting in catastrophic release of the entrapped water known as jokulhlaups (Bjornsson, 1975). Similar pressure release phenomena probably occurred at the Makushin geothermal area during neoglacial times and could have caused the breccias found in the ST-1 and D-1 drill cores. As discussed previously, vigorous boiling would increase the pH could explain the curious co-precipitated mineral assemblage of quartz-calcite-anhydrite-magnetite that is found in the breccias in the upper parts of ST-1 and E-1.

Subsequent deglaciation would decrease the hydrostatic pressure causing boiling to increase in the upper part of the hydrothermal system. A net loss of water caused by the boiling and from the decrease in recharging glacier meltwater would in turn result in a decline of the system's water table.

If our hypothesis is correct, the drop in temperature in the upper part of the hydrothermal system may largely reflect an episode of intense boiling and water loss rather than overall cooling of the system. The sulfate-water oxygen isotope geothermometer does predict a deep reservoir temperature of $\sim 250^{\circ}\text{C}$ which is similar to fluid inclusion temperatures found in the upper part of the system.

DISCUSSION OF PREMIER GEOPHYSICS ELECTRICAL RESISTIVITY STUDY

At the recommendation of DGGS scientists, an electrical resistivity survey of upper Makushin Valley was incorporated into the geothermal exploration program for the summer of 1984. The rationale for the survey was that data on reservoir fluid composition and drill hole temperature profiles were now available to guide the survey and that the survey could potentially delimit the lateral boundaries of the subsurface hydrothermal resource. Economic feasibility of developing the resource would be greatly enhanced if the resource could be shown to exist further down Makushin Valley or at the head of Driftwood Valley. The electrical resistivity survey would also help test the proposed hypothesis that the geothermal system is offset east-southeast of Makushin Volcano as suggested by the regional alignment of fumarole fields and thermal springs.

The electrical resistivity survey was conducted by Premier Geophysics of Vancouver, Canada. The outcome of the electrical resistivity survey is discussed in detail by G. Shore of Premier Geophysics in Appendix E of RGI's final report of 1985. The surveyed area, reproduced in figure 29, covered all of upper Makushin Valley and the plateau at the

head of Driftwood Valley. The survey penetrated to depths of 2000 m. A brief summary of Shore's more pertinent findings are reviewed here:

1) The survey defined the north and east boundaries of a main resistivity anomaly which was taken to be indicative of the main hydrothermal reservoir. These boundaries, shown on figure 29, are located in Fox Canyon on the north and east of ST-1. The conductive zone extends west and south for at least two kilometers and is then beyond the range of the survey.

2) A sloping lower boundary separates the conductive reservoir rocks from an underlying higher resistivity regime as depicted in figure 30.

3) No resource is thought to underlie the part of Fox Canyon covered by the survey.

4) No other parts of the survey coverage area, including Sugarloaf, yielded results comparable to those of the known reservoir area.

5) A major near-vertical discontinuity in resistivity occurs in a zone extending south from Sugarloaf. The discontinuity is inferred by Shore to be a fault zone. An alternate explanation for the discontinuity is a change in bedrock mineralization.

We now attempt to resolve the conclusions of the resistivity survey with data from geologic mapping and geochemistry. No known geological boundary correlates with the change in resistivity demarcating the eastern edge of the main resistivity anomaly. The northern boundary is on strike with the block fault found to the southeast and perhaps is an extension of this fault. An alternate explanation for the discontinuity is that the canyon is the approximate boundary between the gabbroic intrusive and the hornfelsic metamorphosed Unalaska Formation border zone. Pyritization was found to occur mostly along the hornfelsic border zone and thus the resistivity change could reflect sulfide mineralization.

We believe the sloping contact between low and high resistivity zones found by the survey in the vicinity of E-1 and ST-1 is the large open fracture at bottom of ST-1. The surface location of the dipping horizon is constrained to be 50 m of the position shown in figure 30. However, the uncertainty in the slope of the boundary increases with depth and the boundary could be very well be placed at the bottom of ST-1.

It is possible that the fracture and the dipping horizon are related to the fault mapped through the canyon adjacent to fumarole field 2 (fig. 2). The fault dips steeply to the north northwest and its projection passes through the vicinity of fumarole field 1. The fault, which is also the

contact between Unalaska Formation rocks to the south and hornfelsic rocks to the north, could be acting as a conduit for thermal fluids that are feeding the fumaroles and hot springs.

No surface expression could be found of any major fault through the Sugarloaf region as suggested by the resistivity data. We prefer Shore's alternate explanation for the resistivity contrast, that of a steeply dipping contact between rock types. The nature of the subsurface contact between the two different Unalaska Formation rock types is concealed by the thick sequence of Holocene lavas that fill upper Driftwood Valley. The eastern valley wall consists mainly of Unalaska Formation lava flows while the west side is mostly pyroclastic flows. The pyroclastic flows were found to be much more altered and pyritized than the lava flows. Thus the change in resistivity could be due to a change in mineralization.

Although drill hole A-1 encountered temperatures as high as 180°C at a depth of ~ 580 m, the electrical resistivity survey found no indication of a hydrothermal resource in this area. Thus the ST-1 site and the region upvalley from it appear to offer the best potential for future resource development.

The results of the resistivity survey have strong implications regarding the source of the geothermal fluids. The resistivity models indicate the hydrothermal system

extends in a wedge shape towards the south and west of ST-1 and E-1. The boundaries on the main resistivity anomaly essentially rule out any major hydrothermal system offset from the volcano. Instead, the resistivity data support a model in which thermal fluids ascend from a reservoir overlying a centrally located heat source beneath the volcano. The fluids migrate upward then spread laterally as they approach the surface with fractures and faults acting as conduits which feed fumaroles and ST-1.

MODEL OF MAKUSHIN GEOTHERMAL SYSTEM

Our investigations lead us to believe that the Makushin geothermal system is geologically very young. Nye and others (1985) using geochemical evidenced derived from Makushin volcanic rocks, argue that prior to the late-Pleistocene, any shallow magmatic heat source at Makushin would have to have been relatively small, on the order of $1/2 \text{ km}^3$ or less in volume. A magma chamber of this size appears much too small to sustain geothermal activity over an area as large as that presently found at Makushin for any reasonable length of time. Instead, Nye and others (1985) suggest that the heat source driving the Makushin geothermal system formed relatively recently and is related

to a voluminous post-Pleistocene outpouring of chemically homogeneous lavas and pyroclastic flows that issued from the east flank of Makushin Volcano. The large volume and rapid outpouring of these flows and the fact that these volcanics are considerably more siliceous than Pleistocene Makushin volcanic rocks suggests that the post-Pleistocene flows had become fractionated in a newly formed and much larger shallow magma system than had previously existed.

Based on post-Pleistocene glacial history, the age of the lava flows filling Driftwood Valley are estimated to be 11,000 to 3,000 y.b.p. with 11,000 to 7,000 y.b.p. the most probable age. Thus, the shallow magmatic system would have been in place by the late-Pleistocene to early Holocene.

Evidence from investigations of hydrothermal alteration mineral assemblages and fluid inclusions indicate that there has been only one hydrothermal system that has been active at Makushin but that this system has undergone changes and has been affected by interactions with post-Pleistocene glaciers. The hot-water system at Makushin at one time extended to the surface and was substantially hotter than at present, at least within the explored upper portions. During a neo-glacial advance, the hydrostatic pressure exerted by glacier ice increased the boiling point causing temperatures to reach as high as 250°C at depths as shallow as 100 m below the ground surface at the head of Makushin

Valley. Periodic release of meltwaters trapped in geothermally generated subglacial vaults caused rapid decreases in pressures in the hydrothermal system. The ensuing vaporization caused explosive brecciation of the gabbro-noritic host rock near the ground surface. Increased pH and saturation of chemical constituents in the flashed waters caused co-precipitation of anhydrite, magnetite, calcite, and quartz. Subsequent deglaciation resulted in a gradual decline in pressure and a decrease of meltwaters that may have been charging the hydrothermal system. The combination of boiling and loss of charging waters lead to a general lowering of the hydrothermal system water table.

Although geothermometry predicts deep reservoir temperatures as high as 250°C, similar to the fluid inclusion temperatures found in near-surface quartz veins, an overall cooling of the hydrothermal system may also have occurred. Bottom-hole temperatures measured in both test well ST-1 and in TGH E-1 (~ 200°C) are well-below the pressure boiling point for their respective depths below the water table. Fluid inclusion studies of cores from both locations gave temperatures of formation of 250°C or higher throughout the cores. If cooling of the deeper system has not taken place since the formation of the fluid inclusions than hydrostatic boiling point temperatures would be expected throughout most of the depth of the drillholes unless the upper part of the system has become more fractured and therefore more open. In

this later case, pressures within the the system may not be sufficiently high enough to sustain the higher temperatures in the upper parts. Despite the apparent overall cooling of at least the upper part of the Makushin geothermal system, we hasten to point out that more than ample energy still exists for geothermal resource development for the foreseeable future.

The present-day Makushin geothermal system possesses many characteristics found at other geothermal systems associated with island-arc volcanoes elsewhere in the world. A model of such systems as proposed by Ellis and Henley (1983) is shown in figure 31. As discussed above, the heat source for the Makushin system is thought to be a relatively recently emplaced body of magma that is associated with the eruption of large volumes of magma during the early Holocene. The magmatic heat source is assumed to be approximately centrally located beneath the volcano although the east flank eruptions suggest that a portion of it may be slightly offset to the east. The deep hydrothermal system is assumed to reside over the heat source and that the heated waters ascend upwards and then spread laterally as they approach the surface.

As the hot waters ascend, the reduction in hydrostatic pressure causes boiling to occur. Steam and gases evolving from the boiling water table feed the numerous fumaroles

located at mid-elevations and heat perched aquifers which result in a profusion of bicarbonate-sulfate springs below the fumarole fields. A low water table and high relief of the volcano result in a scarcity of chloride hot springs except at low elevations some distance from the central upflow.

At Makushin, the hydrothermal system is charged primarily by meteoric waters which fall at mid- to lower elevations and infiltrate along fractures located on the periphery of the volcano. Much of the recharge may come from the west flank of the volcano which lies in the track of incoming storm systems. The large thickness of highly permeable volcanic flows found on the west flank allow percolation of the meteoric waters into the deeper portions of the volcano's interior. Such a system of recharge could effectively block establishment of fumarolic activity on the west flank.

The host rock in the explored portions of the hydrothermal reservoir is a gabbro-noritic pluton. Apparently this pluton possesses an optimum degree of fracture permeability which permits waters to reside long enough to become heated.

The Makushin hydrothermal system is moderately saline in comparison to other hydrothermal systems in the world but nevertheless contains more chloride than can be reasonably accounted for by leaching from the gabbro-norite. Apparently

the reservoir waters either circulate through marine-laid deposits within the Unalaska Formation or the reservoir is being contaminated by seawater infiltration. A third possibility is that the chloride originates from the siliceous magmatic heat source. The high concentration of Ca in the thermal waters is attributed to breakdown of calcium-rich plagioclase in the gabbro-noritic wall-rock.

The Makushin reservoir water has a relatively low concentration of gases and has a CO₂ partial pressure of approximately 0.5 bars. Helium isotope ratios reflect the magmatic influence on the hydrothermal system indicating some of the gases are of magmatic origin. Gas composition of the reservoir fluids is similar to that found for fumarole fields 1 and 2, suggesting a possible interconnection between these vents and ST-1. Carbon 13 isotope ratios in the reservoir CO₂ gas indicate an organic sedimentary origin for some of the CO₂ gas. Fluctuations and decline in H₂ found in the test well gas samples may be due to reactions of the hot waters and H₂S gas with drillhole casing.

Thermal fluids entering the borehole at ST-1 were found to be slightly out of equilibrium with the measured bottom-hole temperature. Application of various geothermometers to the ST-1 fluids gave temperature estimates of 207 to 226°C with 250°C estimated for the deep reservoir. These temperatures

suggest the thermal fluids cooled slowly by conduction before entering the borehole. The ST-1 Fluid was found to be oversaturated with respect to quartz and slightly undersaturated with respect to calcite and anhydrite.

Figure 32 is a schematic cross-section through the Makushin geothermal field which incorporates available geological, geochemical, and geophysical information. The cross-section is taken as close as possible to the thermal gradient holes, test well ST-1, and fumarole fields 1, 2, and 3 (AA' in fig. 2). Results of the electrical resistivity survey indicate the main geothermal reservoir lies south and west of E-1 and ST-1 and does not extend under the Fox Canyon plateau or the Sugarloaf area. The southwestern boundary of the main reservoir is constrained by drillhole data to lie upslope of I-1.

We believe the hydrothermal fluids which feed ST-1 are derived from a deep parent reservoir, approximately centrally located beneath the volcano. Fluid flow towards ST-1 is controlled primarily by fracture and fault related conduits and, in particular, by a large fracture that dips towards the volcano at $\sim 60^\circ$. As the fluid rises along this conduit it cools by conduction to adjacent wallrock. Some of the fluid ascends secondary fractures and, when the boiling point pressure is eventually reached, the resulting steam and gases continue to ascend to feed fumarole fields

1 and 2. Fortuitous intersection of the primary fracture by ST-1 lead to the successful confirmation of the Makushin geothermal field. Future production wells should be sited at or upvalley from ST-1.

REFERENCES CITED

- Arnorsson, Stefan, 1983, Chemical equilibria in Icelandic geothermal systems - implications for chemical geothermometry investigations: *Geothermics*, v. 12, no. 2/3, p. 119-128.
- Arnorsson, Stefan, Gunnlaugsson, Einar, and Svavarsson, Hordur, 1983, The chemistry of geothermal waters in Iceland. III. Chemical geothermometry in geothermal investigations: *Geochimica et Cosmochimica Acta*, v. 47, no. 3, p. 567-578.
- Bargar, K.E. and Beeson, M. H., 1984a, Hydrothermal Alteration in Research Drill Hole Y-6, Upper Firehole River, Yellowstone National Park, Wyoming, U. S. Geological Survey Professional Paper 1054-B, 24 p.
- Bargar, K.E., Fournier, R.O., and Theodore, T.G., 1984b, Particles resembling bacteria in fluid inclusions from Yellowstone National Park, Wyoming (abstr.), *Geol. Soc. Am. Abstr. Programs*, Vol. 16, no 1.
- Bjornsson, H., 1974, Exploration of jokulhlaups from Grimsvotn, Vatnajokull, Iceland: *Jokull*, v. 24, p. 1-26.
- Bjornsson, H., 1975: Subglacial water reservoirs, jokulhlaups, and volcanic eruptions: *Jokull*, v. 25, p. 1-11.
- Black, R.F., 1981, Late Quaternary climatic changes in the Aleutian Islands, Alaska, in Mahaney, W. C. ed., *Quaternary Paleoclimate: Norwich, U.K.*, Geoabstracts Ltd., p. 47-62.
- Black, R.F., 1983, Glacial chronology of the Aleutian Islands, in Thorson, R.M., and Hamilton, T.D., eds., *Glaciation in Alaska: Alaskan Quaternary Center, University of Alaska Museum, Occasional Paper No. 2*, p. 5-10.
- Browne, P.R.L., 1978, Hydrothermal alteration in active geothermal fields: *Ann. Rev. Earth Planet. Sci.*, v.6, p. 229-250.
- Chiba, Hitoshi, Kusakabe, Minoru, Hirano, Shin-ichi, Matsuo, Sadao, and Somiya, Shigeyuki, 1981, Oxygen isotope fractionation between anhydrite and water from 100

- 500 deg. C: Earth and Planetary Science Letters, v. 53., p. 55-62.

- Chiba, Hitoshi, and Sakai, Hitoshi, 1985, Oxygen isotope exchange rate between dissolved sulfate and water at hydrothermal temperatures: *Geochemica et Cosmochimica Acta*, v. 49, p. 993-1000.
- Craig, H., 1953, The geochemistry of the stable carbon isotopes, *Geochemica et Cosmochimica Acta*, v. 3, p. 53-92.
- Craig, H., 1961, Isotopic variations in meteoric waters, *Science*, v. 133, p. 1702.
- Craig, H., 1963, The isotopic geochemistry of water and carbon in geothermal areas, in Tongiorgi, E. (ed.), *Nuclear geology in geothermal areas*, Spoleto, 1963: Pisa, Italy, Consiglio Nazionale Delle Ricerche, Laboratorio di Geologia Nucleare, p. 17-53.
- Craig, H., Lupton, J. E., Welhan, J. A., and Poreda, R., 1978, Helium isotope ratios in Yellowstone and Lassen Park volcanic gases: *Geophysical Research Letters*, v. 5, no. 11, p. 897-900.
- Craig, H., Lupton, J. E., and Horibe, Y., 1978, A mantle helium component in Circum-Pacific volcanic gases: Hakone, the Marianas, and Mount Lassen, in *Terrestrial Rare Gases* (ed. E. C. Alexander and M. Ozima), Cent. Acad. Publ. Japan.
- Craig, H., and Lupton, J. E., 1981, Helium-3 and mantle volatiles in the ocean and oceanic crust: in *The Oceanic Lithosphere*, Vol 7, The Sea, John Wiley and Sons, 1981, pp. 391-428.
- Crerar, D.A., and Barnes, H.L., 1976, Ore solution chemistry V. Solubility of chalcopyrite and chalcocite assemblages in hydrothermal solution at 200° to 350°C: *Econ. Geol.*, v.71, p. 772-794.
- D'Amore, F., and Panichi, C., 1980, Evaluation of deep temperatures of hydrothermal systems by a new gas geothermometer: *Geochimica et Cosmochimica Acta*, v. 44, p. 549-556.
- D'Amore, F., and Truesdell, A. H., 1980, Gas geothermometry for drill hole fluids from vapor dominated and hot water geothermal fields: *Proc. 6th Stanford Geothermal Reservoir Engineering Workshop*, 351-360.

- Ellis, A. J., 1979, Explored Geothermal Systems, in Barnes, H. L., ed., *Geochemistry of Hydrothermal Ore Deposits*: New York, Wiley and Sons, p. 632-683.
- Fouillac, C., and Michard, G., 1981, Sodium/lithium ratio in water applied to geothermometry of geothermal reservoirs: *Geothermics*, v. 10, no. 1, p. 55-70.
- Fournier, R. O., and Truesdell, A. H., 1973, An empirical Na-K-Ca geothermometer for natural waters: *Geochimica et Cosmochimica Acta*, v. 37, p. 1255-1275.
- Fournier, R. O., 1981, Application of water chemistry to geothermal exploration and reservoir engineering, in Ryback, L., and Muffler, L. P. J., eds., *Geothermal systems: Principles and case histories*: New York, Wiley and Sons, p. 109-144.
- Fournier, R. O., and Potter, R. W. II., 1982, A revised and expanded silica (quartz) geothermometer: *Geothermal Resources Council Bulletin*, v. 11, no. 10, p. 3-12.
- Fournier, R. O., 1983, A method of calculating quartz solubilities in aqueous sodium chloride solutions: *Geochimica et Cosmochimica Acta*, v. 47, no. 3, p. 579-586.
- Helgesson, H. C., 1969, Thermodynamics of hydrothermal systems at elevated temperatures and pressures: *American Journal of Science*, v. 267, p. 729-804.
- Henley, R. W. and Ellis, A. J., 1983, Geothermal systems ancient and modern: A geochemical review: *Earth Science Reviews*, v. 19, no. 1, p. 1-50.
- Isselhardt, C.F., Matlick, J.S., Parmentier, P.P., and Bamford, R.W., 1983, Temperature gradient hole results from Makushin Geothermal Area, Unalaska Island, Alaska: *Geothermal Resources Council, Transactions*, v. 7, p. 95-98.
- Keenan, J. H., Keyes, F. G., Hill, P. G., and Moore, J. G., 1969, *Steam Tables (Int. ed. metric units)*: Interscience, New York, 162 p.
- Lan, C. Y., Liou, J. G., and Saki, Y., 1980, Investigation of drillhole core samples from the Tatun geothermal area, Taiwan: *Water-Rock Interaction Symposium*, 3rd, Edmonton, Canada, Proceedings, p. 183-185.

- Lloyd, R. M., Oxygen isotope behavior in the sulfate-water system: *Journal of Geophysical Research*, v. 73, p. 6099-6101.
- Lupton, J. E., and Craig, H., 1975, Excess ^3He in oceanic basalts: Evidence for terrestrial primordial helium: *Earth and Planetary Science Letters*, v. 26, p. 133-139.
- McKenzie, W. F., and Truesdell, A. H., 1977, Geothermal reservoir temperatures estimated from the oxygen compositions of dissolved sulfate in water from hot springs and shallow drillholes: *Geothermics*, v. 5, p. 51-61.
- Mizutani, Y. and Rafter, T. A., 1969, Oxygen isotopic composition of sulphates, 3. Oxygen isotopic fraction in the bisulfate ion-water system: *New Zealand Journal of Science*, v. 12, p. 54-59.
- Motyka, R. J., Moorman, M. A., and Liss, S. A., 1981, Assessment of thermal spring sites, Aleutian Arc, Atka Island to Becharof Lake--Preliminary results and evaluation: Alaska Division of Geological and Geophysical Surveys, Open File Report AOF-144, 173 p.
- Motyka, R. J., 1982, High-temperature hydrothermal resources in the Aleutian arc: Alaska Geological Society Symposium on Western Alaska Geology and Resource Potential, Anchorage, Proceedings, p. 87-99.
- Motyka, R. J., Moorman, M. A., and Poreda, Robert, 1983, Progress report - thermal fluid investigations of the Makushin geothermal area: Alaska Division of Geological and Geophysical Surveys Report of Investigations 83-15, 48 p.
- Muffler, L. J. P., White, D. E., and Truesdell, A. H., 1971, Hydrothermal explosion craters, Yellowstone National Park: *Geological Society of America Bulletin*, v. 82, p. 723-740.
- Nehring, N. L., Truesdell, A. H., and Janik, C. J., 1982, Procedure for collecting and analyzing gas samples from geothermal and volcanic systems: U.S. Geological Survey Open-file Report (in preparation).
- Nye, C. J., Queen, L. D., and Motyka, R. J., 1984, Geologic map of the Makushin geothermal area, Unalaska Island, Alaska: Alaska Division of Geological and Geophysical Surveys Report of Investigations 84-3, 2 sheets, 1:24,000.

- Nye, C. J., Swanson, S. E., and Reeder, J. W., 1985, Petrology and geochemistry of Quaternary volcanic rocks from Makushin Volcano, Central Aleutian Arc, (in preparation).
- Okko, V., 1955, Glacial drift in Iceland, it's origin and morphology: Comm. Geol. de Finlande Bull., no. 170, 133 p.
- O'Neil, J. R., Clayton, R. N., and Mayeda, T., 1969, Oxygen isotope fractionation in divalent metal carbonates: Journal of Chemical Physics, v. 51, p. 902-909.
- Panichi, C., and Gonfiantini, R., 1978, Environmental isotopes in geothermal studies: Geothermics, v. 6, p. 143-161.
- Parmentier, P. P., Reeder, J. W., and Henning, M. W., 1983, Geology and hydrothermal resources of Makushin geothermal area, Unalaska Island, Alaska: Geothermal Resource Council Transactions, v. 7, p. 181-185.
- Perfit, M. R. and Lawrence, J. R., 1979, Oxygen isotope evidence for meteoric water interaction with Captian's Bay pluton, Aleutian Islands: Earth and Planetary Science Letters, v. 45, p. 16-22.
- Poreda, R. J., 1983, Helium, neon, water and carbon in volcanic rocks and gases: University of California, San Diego, Ph. D. thesis, 215 p.
- Potter, II, R. W., Clynnne, M. A., and Brown, D. L., 1978, Freezing point depression of aqueous sodium chloride solutions: Economic Geology, v. 73, p. 284-285.
- Presser, T. S., and Barnes, Ivan, 1974, Special techniques for determining chemical properties of geothermal waters, U. S. Geological Survey Water-Resources Investigation Report 22-74, 11 p.
- Queen, L. D., 1984, Lithologic log and hydrothermal alteration of core from the Makushin Geothermal area, Unalaska, Alaska: Alaska Division of Geological and Geophysical Surveys Report of Investigations 84-23, 1 sheet.
- Reeder, J. W., 1982, Hydrothermal resources of the northern part of Unalaska Island, Alaska: Alaska Division of Geological and Geophysical Surveys Open File Report AOF-163, 17 p.

- Republic Geothermal Inc., 1983, The Unalaska Geothermal Exploration Project, Phase 1B, Final Report, prepared for the Alaska Power Authority.
- Republic Geothermal Inc., 1984, The Unalaska Geothermal Exploration Project, Phase II Final Report, prepared for the Alaska Power Authority.
- Republic Geothermal Inc., 1985, The Unalaska Geothermal Exploration Project, Phase III Final Report, prepared for the Alaska Power Authority.
- Roedder, E., 1984, Fluid Inclusions: Reviews in Mineralogy, v. 12, Mineralogical Society of America, 664.
- Shore, R.A., 1985, Resistivity survey and interpretation, in Republic Geothermal Inc., The Unalaska Geothermal Exploration Project, Phase III Final Report, prepared for Alaska Power Authority, Appendix E.
- Taguchi, S., 1983, Study on Geothermal Geology of the Kirishima Volcanic Region: Ph. D. dissertation, Kyushu University, 131 p.
- Taguchi, S., Okaguchi, M., and Yamasaki, T., 1980, Reduction in the lengths of fission tracks by geothermal heating and its application to thermal history: Rept. Res. Inst. Industrial Sci., Kyushu University, No. 72, p. 21-26 (in Japanese; English abstr.).
- Torgersen, T., Lupton, J. E., Sheppard, D. S., and Giggenbach, W. F., 1982, Helium isotope variations in the thermal areas of New Zealand, Journal of Volcanology and Geothermal Research, v. 12, p. 283-298.
- Torgersen, T., and Jenkins, W. J., 1982, Helium isotopes in geothermal systems: Iceland, The Geysers, Raft River, and Steamboat Springs, Geochimica et Cosmochimica Acta, v. 46, p. 739-48.
- Truesdell, A. H., and Singers, Wendy, 1973, Computer calculation of downhole chemistry in geothermal areas: New Zealand Department of Science and Industry. Research Chemistry Division Report CD2136, 145 p.
- Truesdell, A. H., 1976, Geochemical techniques in exploration: United Nations Symposium on the Development and Use of Geothermal Resources, 2nd, San Francisco, 1975, Proceedings, v. 1, p. liii-lxxix.

- Truesdell, A. H., and Fournier, R. O., 1977, Procedure for estimating the temperature of a hot-water component in a mixed water by using a plot of dissolved silica versus enthalpy: *Journal of Research, U. S. Geological Survey*, v. 5, no. 1, p. 49-52.
- Truesdell, A. H., and Hulston, J. R., 1980, Isotopic evidence on environments of geothermal systems: in *Handbook of Environmental Isotope Geochemistry*: Elsevier, p. 1979-219.
- Welhan, J. A., 1981, Carbon and Hydrogen Gases in Hydrothermal Systems: the Search for a Mantle Source: University of California, San Diego, Ph. D. thesis, 182 p.

TABLES

Table 1. Fraction of Steam Separated from Flashed Well Fluids¹

<u>Sample #</u>		<u>Date</u>	<u>Time</u> ²	<u>Collection Pressure, Bars</u> ³	<u>Collection Temperature, °C</u> ⁴	<u>Steam Fraction</u> ⁵
<u>DGGS</u>	<u>USGS</u>					
71	1	8-27-83	(+1.5 hr)	2.00	120	0.144
74	2A	9-1-83	17:30	3.17	135.5	0.116
75	3B	9-2-83	10:10	3.03	134	0.119
76	4B	9-2-83	16:20	4.48	147.5	0.093
77	5A	9-3-83	19:50	4.55	147.5	0.092
84-1	-	8-4-84	15:00	2.65	129.5	0.127
84-2	-	8-7-84	13:00	2.79	131	0.124

1. Fluids collected using Webre type mini-cyclone separator.

2. Parenthetical value for 71 is the time elapsed after initial discharge from fracture zone at 593 m depth. Well was then shut-off until 9-1-83. Well was re-opened at 14:40, 9-1-83 and was run continuously until about 22:00, 9-3-83. Well was re-opened again on 7-4-84 and run nearly continuously until 8-8-84.

3. At the separator. These are absolute values calculated from gauge pressure plus atmosphere pressure which was assumed to be 0.96 bars.

4. Determined from the collection pressure assuming liquid-vapor equilibrium (Keenan et al., 1969).

5. Steam fraction calculated using a BHT=193°C and reservoir enthalpy value of 821 kJ/kg (Keenan et al., 1969).

Table 2. Chemical analyses of waters collected from Makushin Valley test well ST-1, 1983^a.
(Concentrations in mg/l unless otherwise specified).

	From Webre-separator ^b					Off End of Exhaust				
	71	74	75	76	77	64	74	75	76	77
Cations										
Na	2120	2020	2010	1900	2010	2840	2400	2470	2420	2460
K	270	280	270	250	250	360	180	310	300	310
Ca	150	139	140	128	144	216	175	175	175	181
Mg	0.2	0.1	0.1	0.1	0.1	0.3	0.2	0.2	0.2	0.2
Li	11	11	11	10	10	14	13	13	13	13
Sr	2.4	2.3	2.8	2.5	2.6	3.1	3.2	3.3	3.3	3.1
Cs	1.4	1.4	1.4	1.4	1.4	1.6	nd	nd	nd	nd
NH ₄	nd	nd	nd	nd	<1	nd	nd	nd	nd	nd
Total ^c	108.5	103.5	103.0	97.0	102.6	145.6	119.6	126.0	123.7	125.7
Anions										
HCO ₃	<5	<5	<5	<5	<1.0	<5	nd	nd	nd	nd
SO ₄	91	86	85	77	80	190	nd	nd	nd	nd
Cl	1.2	1.2	1.2	1.0	1.0	1.6	nd	nd	nd	nd
Br	3670	3540	3500	3230	3370	4870	4160	4240	4200	4220
Total ^c	14	13	12	12	13	19	nd	nd	nd	nd
	105.7	101.8	100.6	93.0	96.9	141.8	117.3	119.7	118.5	119.1
Balance per cent	2.6	1.7	2.4	4.2	5.7	2.7	1.9	5.2	4.3	5.4
SiO ₂	343	335	340	306	323	450	393	395	402	395
H ₂ S	nd	2.7	1.5	nd	nd	nd	nd	nd	nd	nd
Zn	68	64	65	59	62	86	74	76	77	78
Al	nd	nd	nd	nd	0.02	nd	nd	nd	nd	nd
As	12	11	13	12	12	16	14	15	15	15
Fe	nd	nd	nd	nd	0.13	nd	nd	nd	nd	nd
TDS ^d	6760	6500	6450	5990	6280	9070	---	---	---	---
pH, field ^e	8.1	8.0	7.8	7.6	7.9	7.8	nd	nd	nd	nd
Date	8/27/83	9/1/83	9/2/83	9/2/83	9/3/83	8/24/83	9/1/83	9/2/83	9/2/83	9/3/83

a) Alaska Division of Geological and Geophysical Surveys, Fairbanks, M.A. Moorman and R.J. Motyka, analysts.

b) Sampling conditions and steam fraction given in Table 1.

c) Cation and anion totals in milliequivalents/liter.

d) Calculated.

e) Sample 64 measured at T=50°C; all others measured after cooling to 15°C.

nd= not determined

Table 3. Chemical analyses of waters collected from Makushin Valley test well ST-1, 1984.^a (Concentrations in mg/l unless otherwise specified).

	From Webre-separator ^b		Off end of exhaust	
	1W	2W	1E	2E
Cations				
Na	1910	1930	2290	2290
K	260	250	300	310
Ca	129	133	155	149
Mg	0.2	0.2	1.3	0.6
Li	10	10	12	11.5
Sr	2.7	2.7	3.2	3.2
Cs	1.4	1.3	1.6	1.5
NH ₄	< 1	< 1	nd	nd
Total ^c	97.6	98.5	116.9	116.7
Anions				
HCO ₃	26	12	nd	nd
SO ₄	95	97	115	112
F	1.2	1.2	1.4	1.4
Cl	3480	3500	4180	4170
Br	12	12	14	14
Total ^c	100.9	101.3	120.5	120.2
Balance per cent	-3.3	-2.8	-3.1	-3.0
SiO ₂	--	328	397	384
H ₂ S	< 1	1	nd	nd
B	--	67	78	79
Al	nd	0.004	nd	nd
As	12	11	15	14
Fe	0.26	0.20	0.32	0.24
TDS ^d	nd	6360	7560	7540
pH, field ^e	7.7	7.6	nd	nd
Date				
Sampled	8/4/84	8/7/84	8/4/84	8/7/84

a) Alaska Division of Geological and Geophysical Surveys, Fairbanks, R.J. Motyka and M.A. Moorman, analysts.

b) Sampling conditions and steam fraction given in Table 1.

c) Cation and anion totals in milliequivalents/liter.

d) Calculated.

e) pH measured after waters cooled to 15°C.

nd= not determined

Table 4. Chemical analyses of 1983 waters from Makushin Valley
test well ST-1, corrected to reservoir conditions.
(Concentrations in mg/l unless otherwise specified)

	71	74	75	76	77	Average
Cations						
Na	1820	1780	1780	1730	1820	1790
K	230	250	240	230	230	240
Ca	128	123	124	116	131	124
Mg	0.2	0.1	0.1	0.1	0.1	0.1
Li	9	9	10	9	9	9
Sr	2.1	2.0	2.5	2.3	2.4	2.3
Cs	1.2	1.2	1.2	1.3	1.3	1.2
NH ₄	nd	nd	nd	nd	1.0	1.0
Anions						
HCO ₃	< 5	< 5	< 5	< 5	< 1.0	< 5
SO ₄	78	76	75	70	73	74
F	1.0	1.1	1.1	1.1	0.9	1.0
Cl	3140	3130	3080	2930	3060	3070
Br	12	11	11	11	12	11
SiO ₂	294	296	300	278	293	292
H ₂ S	nd	2.4	1.3	nd	nd	1.9
B	58	57	57	54	56	56
Trace						
Al	nd	nd	nd	nd	0.02	0.02
As	11	10	11	11	11	10.5
Fe	nd	nd	nd	nd	0.12	0.12
TDS	5790	5750	5680	5430	5700	5670
Date						
Sampled	8/27/83	9/1/83	9/2/83	9/2/83	9/3/83	

nd = not determined

Table 5. Chemical analyses of 1984 waters collected from the Makushin Valley test well ST-1, corrected to reservoir conditions.
(Concentrations in mg/l unless otherwise specified).

	<u>1W</u>	<u>2W</u>	<u>Average</u>
Cations			
Na	1670.	1690.	1680.
K	230.	220.	225.
Ca	112.	116.	114.
Mg	0.2	0.2	0.2
Li	9.	9.	9.
Sr	2.3	2.4	2.4
Cs	1.2	1.1	1.2
NH ₄	< 1.	< 1.	< 1.
Anions			
HCO ₃	23.	11.	17.
SO ₄	83.	85.	84.
F	1.0	1.1	1.1
Cl	3040.	3070.	3060.
Br	10.	10.	10.
SiO ₂	nd	287.	287.
H ₂ S	nd	1.	1.
B	nd	59.	59.
Al	nd	0.004	0.004
As	10.	10.	10.
Fe	0.23	0.18	0.2
TDS		5570.	5570.
Date			
Sampled	8/4/84	8/7/84	

nd= not determined

Table 6. Chemical analyses of exhaust pipe waters from Makushin Valley test well ST-1 corrected for reservoir conditions assuming 60°C and point flash temperature.^a
(Concentrations in mg/l unless otherwise specified).

Sample #	Date	Na	K	Cations		Li	Sr	Ca	HCO ₃	SO ₄	Anions		Br	SiO ₂	B	As	Fe	TDS	Steam Fraction
				Ca	Mg						F	Cl							
RM83-64	8-24-83	2120	270	160	0.2	11	2.3	1.2	nd	140	1.2	3650	14	337	64	12	nd	6780	0.252
RM83-74	9-01-83	1800	130	130	0.1	9.4	2.4	nd	nd	nd	nd	3110	nd	294	55	11	nd	5540	0.252
RM83-75	9-02-83	1850	230	130	0.2	9.6	2.5	nd	nd	nd	nd	3170	nd	296	57	11	nd	5760	0.252
RM83-76	9-02-83	1810	230	130	0.1	9.7	2.5	nd	nd	nd	nd	3140	nd	301	58	11	nd	5690	0.252
RM83-77	9-03-83	1840	230	140	0.1	9.7	2.3	nd	nd	nd	nd	3160	nd	296	58	11	nd	5740	0.252
RM84-01	8-04-84	1710	220	120	1.0	8.8	2.4	1.2	nd	86	1.0	3130	10	297	58	11	0.24	5660	0.252
RM84-02	8-07-84	1710	230	110	0.5	8.5	2.4	1.1	nd	84	1.0	3120	10	287	59	10	0.18	5640	0.252

a) Alaska Division of Geological and Geophysical Surveys, Fairbanks, Alaska, M.A. Moorman, analyst.

Table 7. Makushin test well, air corrected gas analyses, mole per cent.

Sample Code	Date Sampled	RO ₂	Xg	CO ₂	H ₂ S	H ₂	CH ₄	NH ₃	N ₂	Ar	N ₂ /Ar	C/S
MVTW-1 DS/CJ	8-27-83	0.00	0.070	87.74	1.80	0.28	0.006	0.76	9.24	0.18	50.4	48.9
MVTW-2A DS/CJ	9-01-83	0.00	0.098	89.61	2.71	0.46	0.007	0.18	6.92	0.10	67.3	33.0
MVTW-3B DS/CJ	9-02-83	0.00	0.081	92.54	2.27	0.17	0.006	0.25	4.68	0.07	66.8	40.7
MVTW-4B DS/CJ	9-02-83	0.00	0.109	91.61	3.15	0.12	0.007	0.20	4.84	0.08	63.8	29.1
MVTW-5A DS/CJ	9-03-83	0.00	0.105	92.73	2.28	0.10	0.006	0.18	4.63	0.07	63.2	40.7
MVTW-1G-C RM/CJ	8-04-84	0.27	0.089	86.26	2.52	0.04	tr	0.46	10.57	0.15	70.5	34.2
MVTW-2G-A RM/CJ	8-07-84	0.50	0.056	85.94	2.52	0.06	tr	0.67	10.69	0.12	89.6	34.1
MVTW-2G-B RM/CJ	8-07-84	0.14	0.064	93.81	2.02	0.02	tr	0.30	3.77	0.07	51.7	46.3

DS/CJ = D. Sheppard, Department of Scientific and Industrial Research, New Zealand, and C. Janik,
U.S. Geological Survey, Menlo Park, analysts.

RM/CJ = R. Motyka, Alaska Division of Geological and Geophysical Surveys, Fairbanks, and C. Janik,
U.S. Geological Survey, Menlo Park, analysts.

Xg = Ratio, moles gas to moles steam in per cent.

RO₂ = Ratio, oxygen in sample to oxygen in air.

Table 8. Mass per cent gas content of total discharge,
using O_2 corrected gas analyses.

Sample #	Steam Fraction	Mass per cent gas in Steam	Mass per cent gas Total Discharge
MVTW-1 DS/CJ	0.144	0.163	0.023
MVTW-2A DS/CJ	0.116	0.231	0.027
MVTW-3B DS/CJ	0.119	0.192	0.023
MVTW-4B DS/CJ	0.093	0.260	0.024
MVTW-5A DS/CJ	0.092	0.252	0.023
MVTW-1G-C RM/CJ	0.127	0.208	0.026
MVTW-2G-A RM/CJ	0.124	0.132	0.016
MVTW-2G-B RM/CJ	0.124	0.154	0.019

Table 9. Concentrations of chemical species in m moles/1000 gm H₂O for reservoir waters at 193°C.

Sample	pH	Li	Na	K	Cs	Mg	Ca
MVTW-1	5.9	1.4	76.6	5.9	0.009	0.004	2.9
MVTW-2A	5.9	1.4	75.3	6.3	0.009	0.002	2.8
MVTW-3B	5.7	1.4	74.7	6.0	0.009	0.002	2.9
MVTW-4B	5.4	1.3	72.7	5.7	0.010	0.002	2.7
MVTW-5A	5.7	1.3	77.0	5.7	0.010	0.002	3.0
MVTW-1W	5.1	1.3	70.2	5.7	0.009	0.004	2.7
MVTW2G-A	5.9	1.3	71.2	5.5	0.009	0.004	2.7
MVTW2G-B	5.8	1.3	71.2	5.5	0.009	0.004	2.7

Sample	Fe	Al	F	HF	Cl	NaCl	KCl
MVTW-1	nd	nd	0.052	0.002	86.7	2.41	0.077
MVTW-2A	nd	nd	0.053	0.003	86.3	2.36	0.083
MVTW-3B	nd	nd	0.051	0.005	85.1	2.32	0.079
MVTW-4B	nd	nd	0.041	0.006	80.8	2.17	0.072
MVTW-5A	0.002	0.001	0.045	0.003	84.3	2.36	0.074
MVTW-1W	0.004	nd	0.040	0.015	83.9	2.17	0.075
MVTW2G-A	0.003	0.001	0.053	0.003	84.7	2.21	0.073
MVTW2G-B	0.003	0.001	0.052	0.003	84.7	2.21	0.073

Sample	Br	SO ₄	HSO ₄	NaSO ₄	KSO ₄	MgSO ₄	CaSO ₄
MVTW-1	0.15	0.22	0.002	0.44	0.021	0.003	0.13
MVTW-2A	0.14	0.22	0.003	0.43	0.022	0.002	0.12
MVTW-3B	0.13	0.21	0.004	0.42	0.021	0.002	0.12
MVTW-4B	0.14	0.20	0.006	0.39	0.019	0.002	0.11
MVTW-5A	0.15	0.20	0.003	0.41	0.019	0.002	0.12
MVTW-1W	0.13	0.24	0.017	0.45	0.023	0.003	0.13
MVTW2G-A	0.13	0.25	0.002	0.48	0.023	0.003	0.14
MVTW2G-B	0.12	0.25	0.003	0.48	0.023	0.003	0.14

Sample	HBO ₂	BO ₂	SiO ₂	H ₄ SiO ₄	H ₃ SiO ₄	As
MVTW-1	5.4	0.007	4.9	4.9	0.009	0.14
MVTW-2A	5.3	0.005	5.0	5.0	0.007	0.13
MVTW-3B	5.3	0.004	5.0	5.0	0.005	0.15
MVTW-4B	5.0	0.002	4.6	4.6	0.002	0.15
MVTW-5A	5.2	0.004	4.9	4.9	0.006	0.15
MVTW-1W	nd	nd	4.8	4.8	6.001	0.14
MVTW2G-A	5.5	0.006	4.8	4.8	0.008	0.13
MVTW2G-B	5.5	0.005	4.8	4.8	0.006	0.13

Table 9. Continued.

Sample	H_2CO_3	HCO_3	CaCO_3	CaHCO_3	H_2S	HS
MVTW-1	4.3	0.38	0.0010	0.20	0.09	0.009
MVTW-2A	5.2	0.34	0.0007	0.17	0.23	0.017
MVTW-3B	4.6	0.22	0.0003	0.11	0.15	0.008
MVTW-4B	5.0	0.13	0.0001	0.06	0.18	0.005
MVTW-5A	4.7	0.25	0.0043	0.14	0.14	0.009
MVTW-1W	5.3	0.06	0.0002	0.03	0.16	0.002
MVTW2G-A	3.1	0.25	0.0006	0.12	0.11	0.010
MVTW2G-B	4.0	0.25	0.0005	0.12	0.11	0.008

Table 10. Partial Pressure of CO_2 and H_2S in solution, reservoir conditions.

Sample	millimole fraction in total fluid		Partial pressure bars	
	CO_2	H_2S	CO_2	H_2S
MVTW-1	0.0882	0.0018	0.55	0.0036
MVTW-2A	0.1026	0.0031	0.64	0.0062
MVTW-3B	0.0893	0.0022	0.56	0.0043
MVTW-4B	0.0943	0.0033	0.60	0.0065
MVTW-5A	0.0909	0.0023	0.57	0.0045
MVTW-1W	0.0979	0.0029	0.62	0.0057
MVTW2G-A	0.0601	0.0018	0.38	0.0035
MVTW2G-B	0.0749	0.0016	0.47	0.0032

Table 11. $^{18}\text{O}/^{16}\text{O}$ in anhydrite obtained from test well core.^a

Depth, m(ft)	$^{18}\text{O}/^{16}\text{O} - \text{CaSO}_4$, WRT SMOW	T °C, equil. ^b	
		(c)	(d)
148 (486)	-2.98	351	249
592.5 (1944)	-1.87	319	226
593.1 (1946)	-0.91	295	208

a) Analyzed at U.S. Geological Survey, Menlo Park.

b) T °C, equil. = equilibration fractionation temperature assuming $^{18}\text{O}/^{16}\text{O}$ for H_2O is -10.2, the current reservoir water value (U.S. Geological Survey analysis).

c) Temperature computed using Lloyd (1968) fractionation equation:

$$1000 \ln \alpha = 3.88 (10^6)/T^2 - 2.90, T = ^\circ\text{K}.$$

d) Temperature computed using fractionation equation of Chiba and others (1981):

$$1000 \ln \alpha = 3.21 (10^6)/T^2 - 4.72, T = ^\circ\text{K}.$$

Table 12. Makushin Valley test well ST-1, oxygen
and deuterium isotope analyses - steam and water.
(Parts per mil with respect to SMOW).

Sample #			Water			Steam		
DGGS	USGS	Date	D/H (SMU)	$^{18}\text{O}/^{16}\text{O}$ (SMU)	$^{18}\text{O}/^{16}\text{O}$ (USGS)	D/H (SMU)	$^{18}\text{O}/^{16}\text{O}$ (SMU)	$^{18}\text{O}/^{16}\text{O}$ (USGS)
71	1	8/27/83	-79	-9.7	-9.2	-97	-13.9	-13.45
74	2	9/1/83	-77	-10.05	-9.5	-90	-13.2	-13.05
75	3	9/2/83	-77.5	-9.95	-9.6	-90	-13.2	-13.05
76	4	9/2/83	-77.5	-8.4	-9.6	-87.3	-13.15	-12.85
77	5	9/3/83	-77.6	-9.8	-9.6	-88.3	-13.1	-13.0
84-1		8/4/84	-66	-10.25	-	-86	-11.25	-
84-2		8/7/84	-81.5	-9.95	-	-90	-12.3	-

SMU = Southern Methodist University, Stable Isotope Laboratory, R. Harmon and J. Borthwick, analysts.

USGS = U.S. Geological Survey, Menlo Park, C. Janik, analyst.

Table 13. Makushin Valley test well ST-1, stable isotope analyses
corrected to reservoir conditions.
(Parts per mil with respect to SMOW).

<u>1983</u>	<u>71</u>	<u>74</u>	<u>75</u>	<u>76</u>	<u>77</u>	<u>Average</u>
D/H (SMU)	-81	-78.5	-79	-78.5	-78.5	-79
$^{18}\text{O}/^{16}\text{O}$ (SMU)	-10.3	-10.4	-10.3	$(-8.8)^a$	-10.1	-10.3
$^{18}\text{O}/^{16}\text{O}$ (USGS)	-10.2	-9.9	-10.0	-9.9	-9.9	-10.0
<u>1984</u>	<u>84-1^b</u>	<u>84-2</u>				
D/H (SMU)	-69	-83				
$^{18}\text{O}/^{16}\text{O}$ (SMU)	-10.4	-10.2				

a) Suspect value; not used in computing average.

b) A large amount of chloride was detected in the 84-1 condensate indicating incomplete separation. Values for this sample are therefore not considered to accurately represent reservoir isotope composition.

Table 14. ST-1 whole rock oxygen isotope data.^a

Sample #	$^{18}\text{O}/^{16}\text{O}$	Description
ST-1-201	-4.0	Gabbro. Plagioclase altered to clays.
ST-1-664	-2.7	Gabbro altered to wairakite. Steam entry.
ST-1-1066	-2.0	Albite-K spar-biotite-epidote vein.
ST-1-1638	+2.8	"Unaltered" gabbro. Pyroxenes altered to anthophyllite-cummingtonite.
ST-1-1937	-0.1	Chloritically altered gabbro.
- -	+6.4	Average of 11 Makushin area volcanic rocks.

a) Analyzed at U.S. Geological Survey, Menlo Park, CA., I. Barnes lab.

Table 15. Analyses of tritium in waters from Makushin geothermal area.

Sample code	Locality	Date collected	TU
MVTW-3	ST-1	9-02-83	0.46±0.08
MVTW-5	ST-1	9-03-83	0.29±0.08
RM82MV-cs	cold str., Mk. Val	7-21-82	11.3±0.3
RM82MV-ru	hot spr. M-c	7-22-82	16.4±0.4
RM82GV-E	hot spr. G-j	7-20-82	36.5±0.8
RM82GV-wv	hot spr. G-l	7-20-82	28.2±0.7
RM82GV-24	hot spr. G-m	7-20-82	10.5±0.3
RM82PV	hot spr. G-p	7-20-82	6.1±0.2

Analyst: H. Gote Ostlund, U. of Miami, Miami, Florida.

TU = Tritium units

Table 16. Makushin Valley test well ST-1, Unalaska Island, Alaska, carbon isotope analyses, CO₂ in gas and steam.^a

<u>Sample #</u>	<u>Date Collected</u>	<u>T, °C Sep</u>	<u>$\delta^{13}\text{C}_{\text{PDB}}$</u>
MVTW-1	8/27/83	120	-13.3
MVTW-3	9/02/83	134	-13.5
MVTW-4	9/02/83	148	-13.3
MVTW-5	9/03/83	148	-13.3
MVTW-1G-C	8/04/84	130	-15.1
MVTW-2G-A	8/07/84	131	-15.0
MVTW-2G-B	8/07/84	131	-15.1

a) C. Janik, U.S. Geological Survey, Menlo Park, analyst.

Table 17. Helium isotope data, Makushin geothermal area.^a

Location	Year Collected	R/Ra ^b	(He/Ne)/air ^c	Rc/Ra ^d
Fum. field #1	1980	6.6	110.0	6.6
Fum. field #2	1980	4.9	37.0	5.1
Fum. field #2	1981	5.0	94.0	5.1
Fum. field #3, sp	1981	3.8	24.0	4.0
Fum. field #3	1981	4.4	53.0	4.5
Fum. field #3, SH	1982	4.1	11.4	4.4
Fum. field #5	1982	5.0	50.0	5.1
Fum. field #6, SU	1982	7.8	1500.0	7.8
Fum. field #7	1983	5.9	300.0	5.9
Spring G-p	1983	(1.3) ^e	(1.5) ^e	(1.9) ^e
Test well ST-1	1983	3.6	41.0	3.7

a) R. Poreda analyst, Scripps Institute of Oceanography, Stable Isotope Lab.

b) $R = {}^3\text{He}/{}^4\text{He}$ ratio in sample.

c) $Ra = {}^3\text{He}/{}^4\text{He}$ ratio in air.

d) Rc = Sample ratio corrected for air contamination using He/Ne ratios.

e) Helium concentration in sample was extremely low.

Table 18. Geothermometry for Webre separator waters from Makushin Valley test well ST-1 corrected for reservoir conditions. (Temperatures in °C).

Sample #	Date	Qz. cond (1)	Chal. cond (2)	Na/K (3)	Na/K (4)	Na/K (5)	Na-K-Ca (6)	Na/Li (7)
RM83-71	8-27-83	208	191	240	216	222	224	193
RM83-74	9-01-83	208	192	247	226	231	229	194
RM83-75	9-02-83	209	193	243	221	227	227	196
RM83-76	9-02-83	203	186	241	218	224	225	194
RM83-77	9-03-83	208	191	238	213	220	223	193
RM84-01	8-04-84	nd	nd	245	223	229	227	194
RM84-02	8-07-84	206	189	240	217	223	224	193

(1) Fournier and Potter, 1982, improved SiO_2 (quartz).

(2) Fournier, 1981, chalcedony.

(3) Fournier, 1981, Na/K.

(4) Truesdell, 1976, Na/K.

(5) Arnorsson, 1983, Na/K, Basalt.

(6) Fournier & Truesdell, 1973.

(7) Fouillie & Michard, 1981.

Table 19. Sulfate-water $^{18}\text{O}/^{16}\text{O}$ isotope temperatures, Makushin Valley test well, ST-1.^a

Sample #	Date Collected	Temp sep, °C	$^{18}\text{O}/^{16}\text{O}$ -SO ₄ , WRT SMOW	$^{18}\text{O}/^{16}\text{O}$ -H ₂ O WRT SMOW at sep	$^{18}\text{O}/^{16}\text{O}$ -H ₂ O WRT SMOW, res	T ₁ , °C ^c	T ₂ , °C ^d
MVTW-74	9-01-83	135	-3.8	-9.5	-9.9	245	256
MVTW-75	9-02-83	134	-3.4	-9.6	-10.0	235	245
MVTW-76	9-02-83	148	-3.4	-9.6	-9.9	235	248
MVTW-77	9-03-83	148	-3.3	-9.6	-9.9	235	244
MVTW-1W	8-04-84	130	-3.9	-10.3 ^b	-10.4 ^b	230	246
MVTW-2W	8-07-84	131	-3.6	-10.0 ^b	-10.2 ^b	232	246

a) Isotope analyses performed at U.S. Geological Survey, Menlo Park, except as noted.

b) Analysis performed at Southern Methodist University, Stable Isotope Laboratory.

c) Temperature calculated using method described in McKenzie and Truesdell (1977) for the case of single-stop steam-loss. The separator water composition was used for $^{18}\text{O}/^{16}\text{O}$ - H₂O.

d) Temperature calculated using the $^{18}\text{O}/^{16}\text{O}$ - H₂O value determined for the reservoir water and the equilibrium fractionation equation of Mizutani and Rafter (1969): $1000 \ln \alpha = 2.88 (10^6/T^2) - 4.1$, T=°K.

Table 20. Gas geothermometers applied to Makushin test well.

Sample #	Date Sampled	T°C (a)	T°C (b)	T°C (c)
MVTW-1 DS/CJ	8-27-83	228	212	220
MVTW-2A DS/CJ	9-01-83	250	222	227
MVTW-3B DS/CJ	9-02-83	217	216	222
MVTW-4B DS/CJ	9-02-83	213	223	223
MVTW-5A DS/CJ	9-03-83	204	216	222
MVTW-1G-C RM/CJ	8-04-84	218	220	225
MVTW-2G-A RM/CJ	8-07-84	216	211	199
MVTW-2G-B RM/CJ	8-07-84	190	212	213

(a) Gas geothermometer of D'Amore and Panachi, 1980.

(b) H₂S geothermometer of D'Amore and Truesdell, 1980.

(c) CO₂ geothermometer of Arnorsson and others, 1983.

Table 21. Description of fluid inclusion samples.

Sample Number	Description
ST-277	Clear, euhedral quartz crystals (0.5 cm diam.) from a vuggy anhydrite, quartz, magnetite breccia infilling. Primary and pseudo-secondary inclusions present. Some primary inclusions form phantoms within the quartz crystals.
ST-295	Clear, euhedral quartz crystal (1.0 cm diameter) from an anhydrite, quartz, calcite, magnetite breccia infilling. Inclusions are rare. Primary and secondary inclusions.
E-1-791	Quartz from a calcite, quartz, epidote vein. Quartz grains are euhedral and surrounded by calcite. Some epidote grains in the calcite. Surrounding gabbro only slightly altered. Plagioclase to montmorillonite. Mafics to chlorite and pyrite.
E-1-1155	Quartz crystals from sealed quartz vein. Vein is 2 cm wide. Individual quartz crystals are subhedral. Crystals are 1 cm long and 0.3-0.5 cm wide. Surrounding rock is extensively altered.
E-1-1396	Quartz vein. Wairakite is present in vug along one side of vein. The wairakite is younger than the quartz vein.
I-1-164	Fine grained quartz vein (2.5 cm wide). Much of the sample can not be used because of numerous clay inclusions and most of the inclusions are too small. Acceptable inclusions are present in the small (1.0-0.5 mm) subhedral crystals which project into the occasional small vugs. The host rock is highly altered to the argillic assemblage and only pyrite traces of the mafic minerals remain.

FIGURES

- Figure 1. Location map for Makushin Geothermal Area.
- Figure 2. Geologic map of the Makushin Geothermal Area.
- Figure 3. Webre mini-cyclone separator in use at well ST-1, Makushin Geothermal Area.
- Figure 4. $\text{CO}_2\text{-H}_2\text{S-N}_2$ compositions of well ST-1 and fumarolic gases from Makushin Geothermal Area.
- Figure 5. N_2/Ar vs H_2/Ar plot for well ST-1 gases, Makushin Geothermal Area.
- Figure 6. Quartz solubility curve and values for well ST-1, Makushin Geothermal Area .
- Figure 7. Calcite saturation curve and values for well ST-1, Makushin Geothermal Area.
- Figure 8. Anhydrite saturation curve and values for well ST-1, Makushin Geothermal Area.
- Figure 9. Stable isotope analyses of well ST-1, thermal springs, and meteoric waters from the Makushin Geothermal Area.
- Figure 10. Tritium analyses of well ST-1, thermal springs, and ground water streams in the Makushin Geothermal Area. The three values at right give 1980 data from Anchorage for comparison.
- Figure 11. ^{13}C compositions of CO_2 in gases from well ST-1, fumaroles, and hot springs in the Makushin Geothermal Area.
- Figure 12. He isotope analyses from well ST-1, fumaroles, and hot springs in the Makushin Geothermal Area compared with values from various tectonic settings.
- Figure 13. Comparison of geothermometry of well ST-1, Makushin Geothermal Area.
- Figure 14. Lithologic log and temperature profile of geothermal gradient hole D-1, Makushin Geothermal Area.

- Figure 15. Lithologic log and temperature profile of geothermal gradient hole E-1, Makushin Geothermal Area.
- Figure 16. Lithologic log and temperature profile of geothermal gradient hole I-1, Makushin Geothermal Area.
- Figure 17. Lithologic log and temperature profile of geothermal well ST-1, Makushin Geothermal Area.
- Figure 18. Lithologic log and temperature profile of geothermal gradient hole A-1, Makushin Geothermal Area.
- Figure 19. Paragenetic chart of Makushin alteration minerals.
- Figure 20. Fluid inclusions in quartz from the Makushin Geothermal Area.
- Figure 21. Fluid inclusions showing daughter minerals.
- Figure 22. Histogram of fluid inclusions last ice melting.
- Figure 23. Temperatures of fluid inclusion homogenization.
- Figure 24. Chemical potential diagram for the system $\text{CaO-Al}_2\text{O}_3\text{-SiO}_2\text{-H}_2\text{O}$.
- Figure 25. Makushin reservoir waters plotted on the activity diagram for the system $\text{CaO-Al}_2\text{O}_3\text{-SiO}_2\text{-H}_2\text{O}$.
- Figure 26. Makushin reservoir waters plotted on the activity diagram for the system $\text{CaO-K}_2\text{O-Al}_2\text{O}_3\text{-SiO}_2\text{-H}_2\text{O}$ at 200 deg. C.
- Figure 27. Makushin reservoir waters plotted on the activity diagram for the system $\text{CaO-Na}_2\text{O-Al}_2\text{O}_3\text{-SiO}_2\text{-H}_2\text{O}$ at 200 deg. C.
- Figure 28. Fugacity of oxygen vs pH diagram for the system $\text{Fe-S-H}_2\text{O}$ at 250 deg. C (after Crerar and Barnes, 1970).
- Figure 29. Boundaries and generalized results of E-scan electrical resistivity survey of the Makushin Geothermal Area performed by

Premier Geophysics, Inc. of Vancouver, Canada (taken from appendix E of RGI final report to APA, 1985).

- Figure 30. Model of resistivity section through E-1 and ST-1 by Premier Geophysics, Inc. of Vancouver, Canada (taken from appendix E of RGI final report to APA, 1985).
- Figure 31. Generalized model of a geothermal system typical of active island-arc andesite volcanoes (reproduced from Henley and Ellis, 1983).
- Figure 32. Cross-section of Makushin Geothermal system. Location of section AA' is shown on figure 2. Isotherms are based on locations of fumaroles and hot springs and on temperature data from thermal gradient holes and well ST-1. Geology is from Nye and others, 1984.

NORTHERN UNALASKA ISLAND

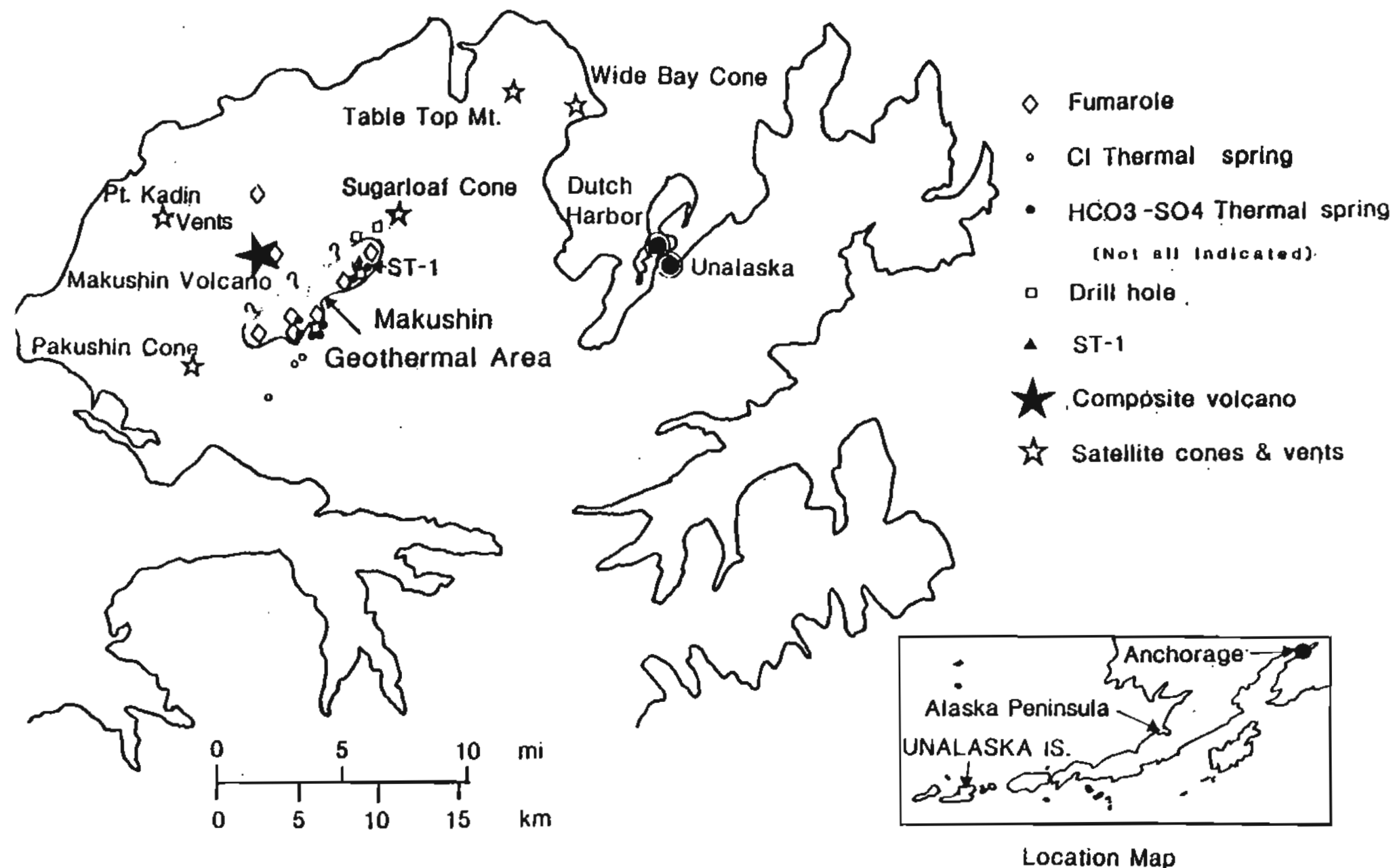


Fig. 1

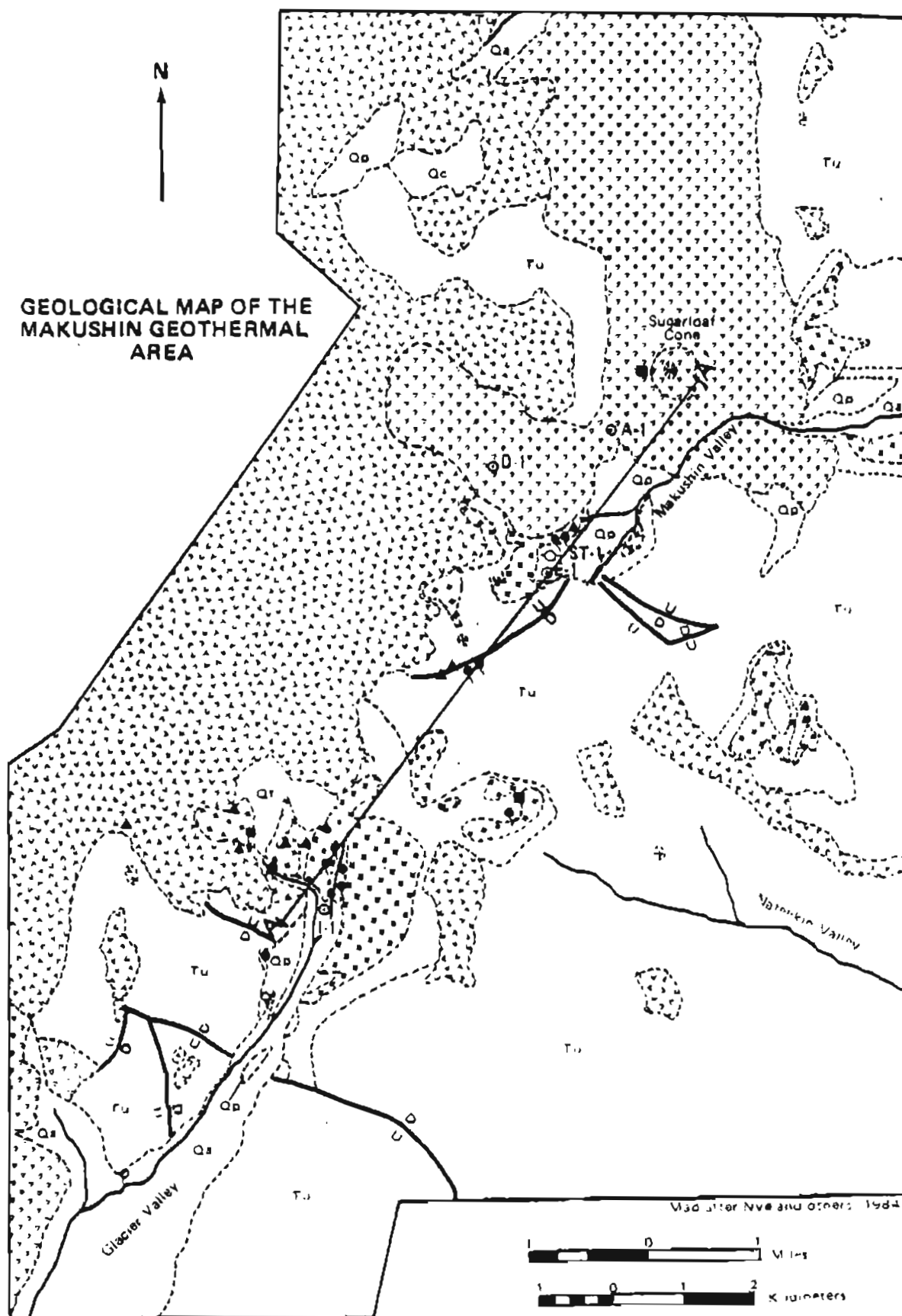


Fig. 2

EXPLANATION OF MAP SYMBOLS




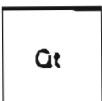


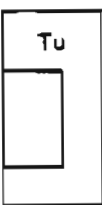

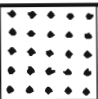

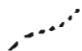






		Alluvium	
		Solluvium	
		Pyroclastic Debris	
		Glacial Till	
		Homogeneous Volcanics	
		Inhomogeneous Volcanics	
		Unalaska Formation	
		Contact Metamorphosed Unalaska Formation	
Gabbroonorite			
Fumarole		Contact	
Warm Ground		Fault	
$\text{HCO}_3\text{-SO}_4$ Thermal Springs		Test Well	
Cl-Thermal Springs		Thermal Gradient Well	

Fig. 2

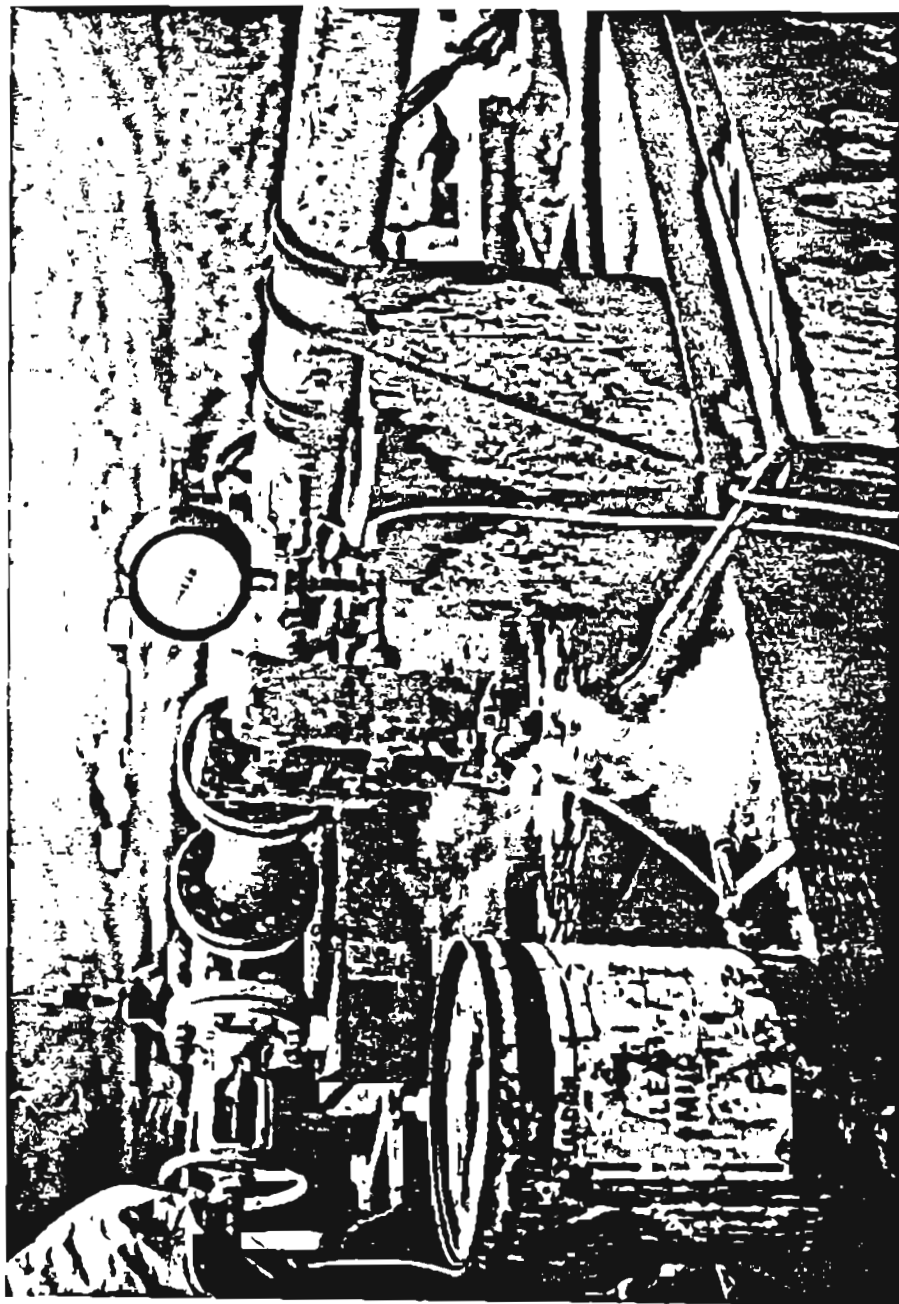


Fig. 3

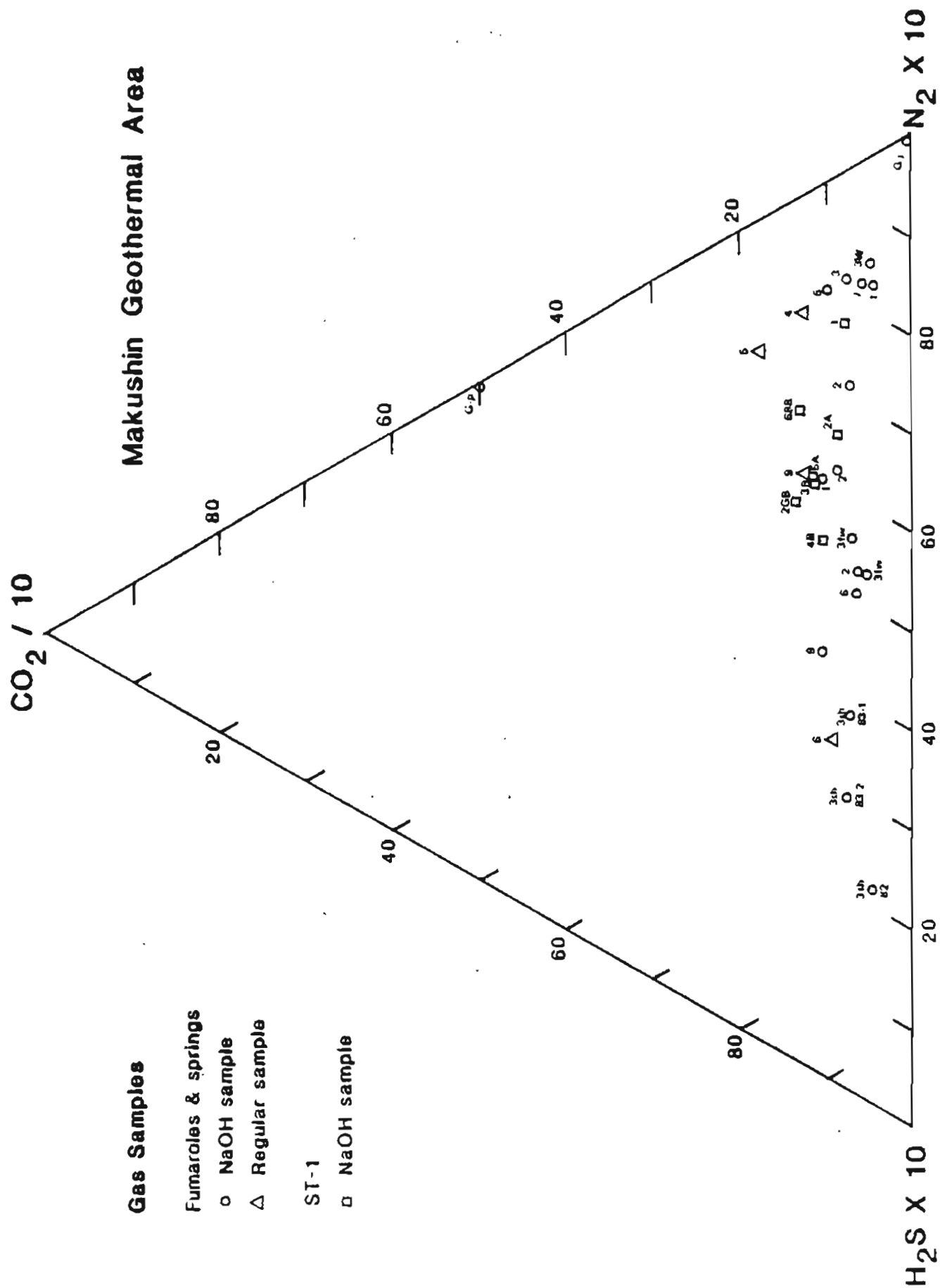


Fig. 4

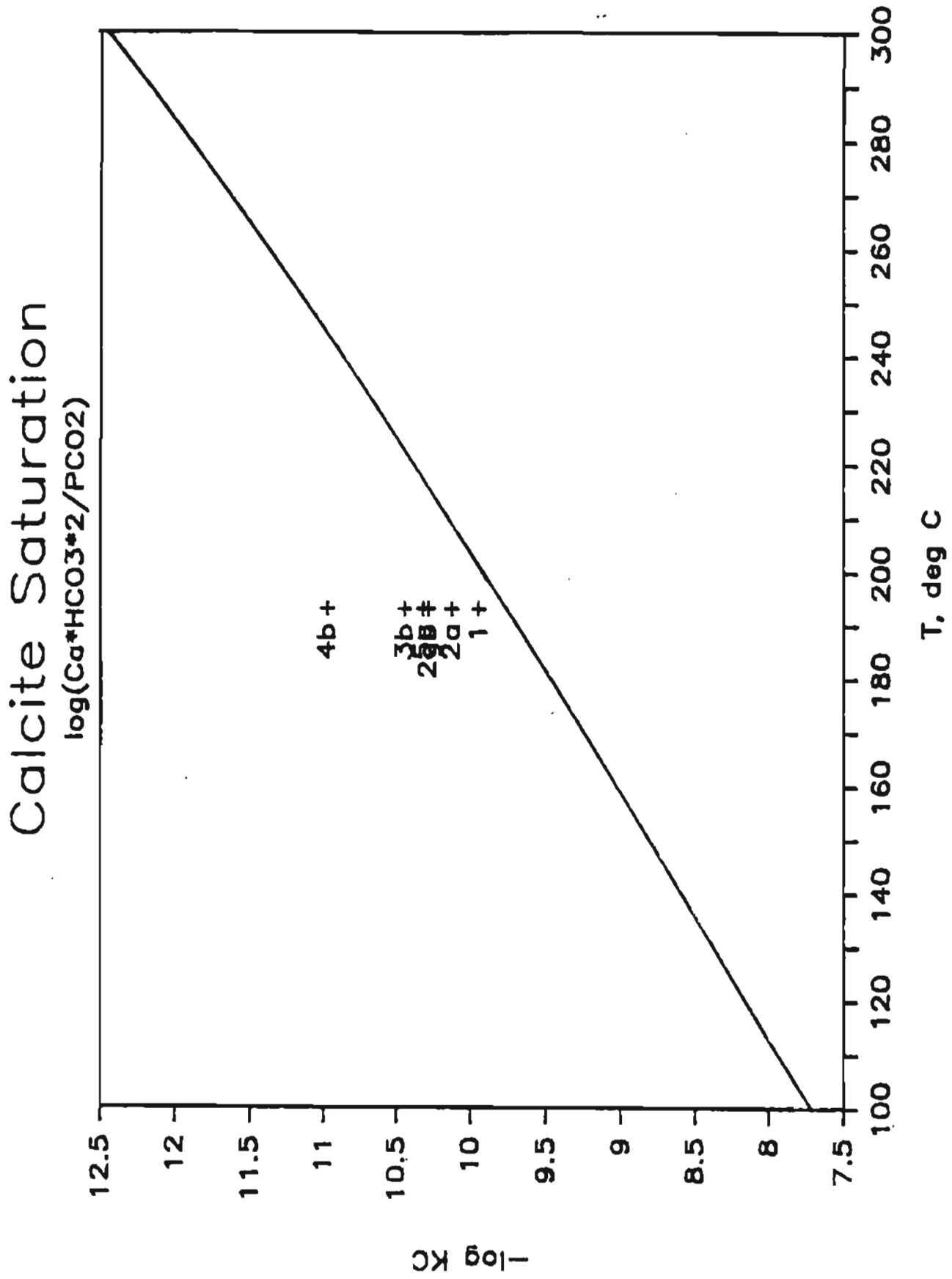


Fig. 7

Anhydrite Saturation

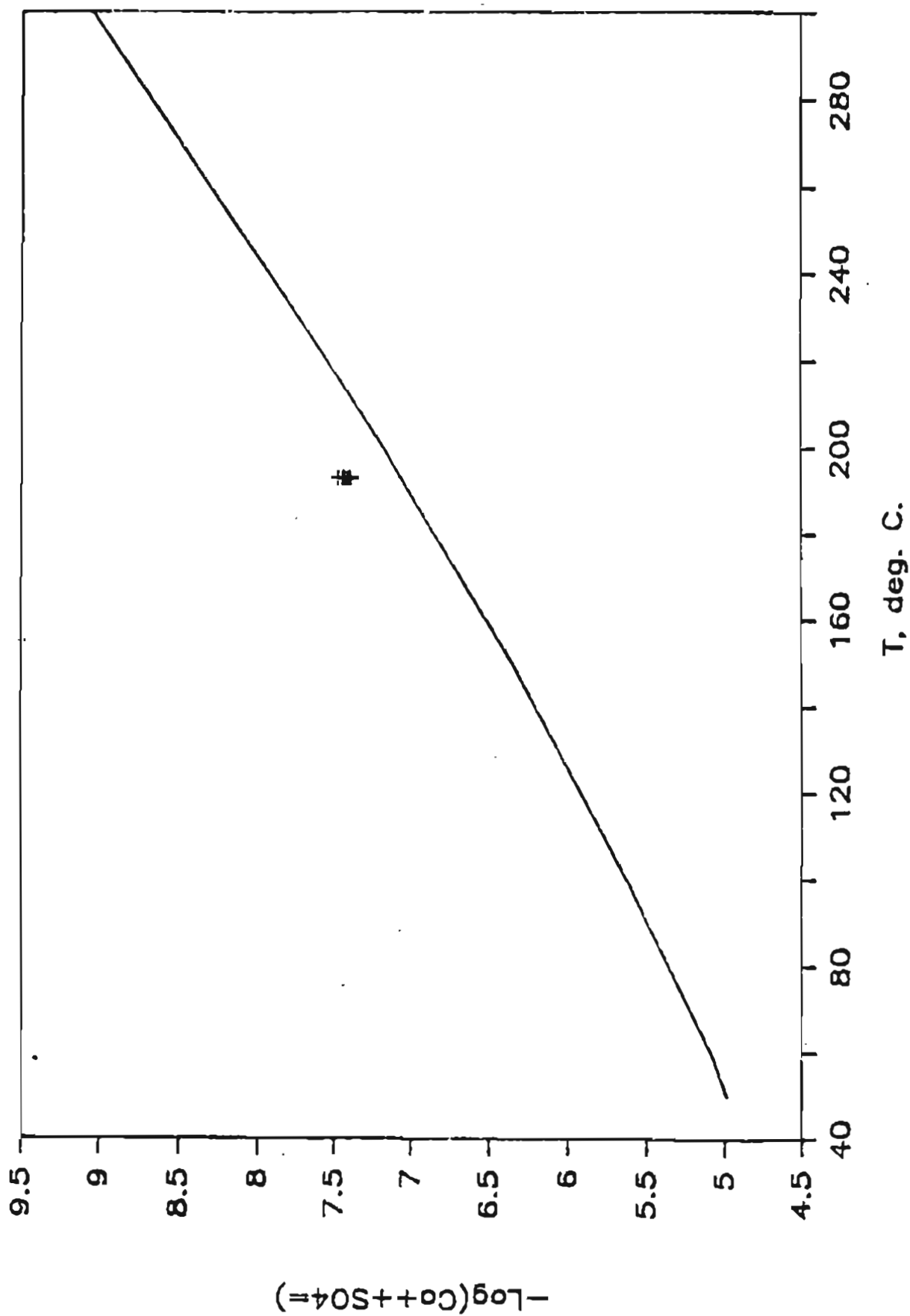


Fig. 8

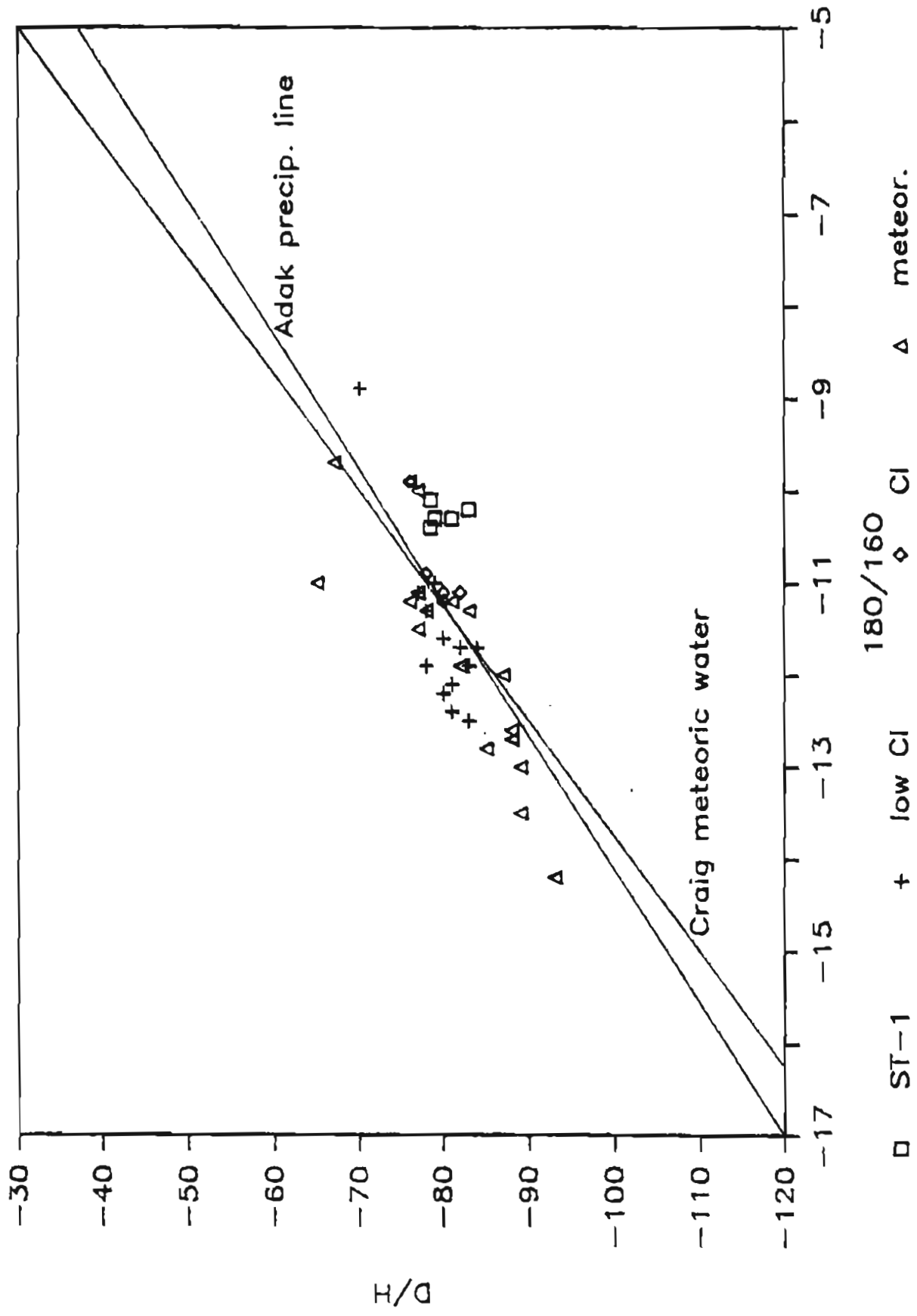


Fig. 9

MAKUSHIN GEOTHERMAL AREA

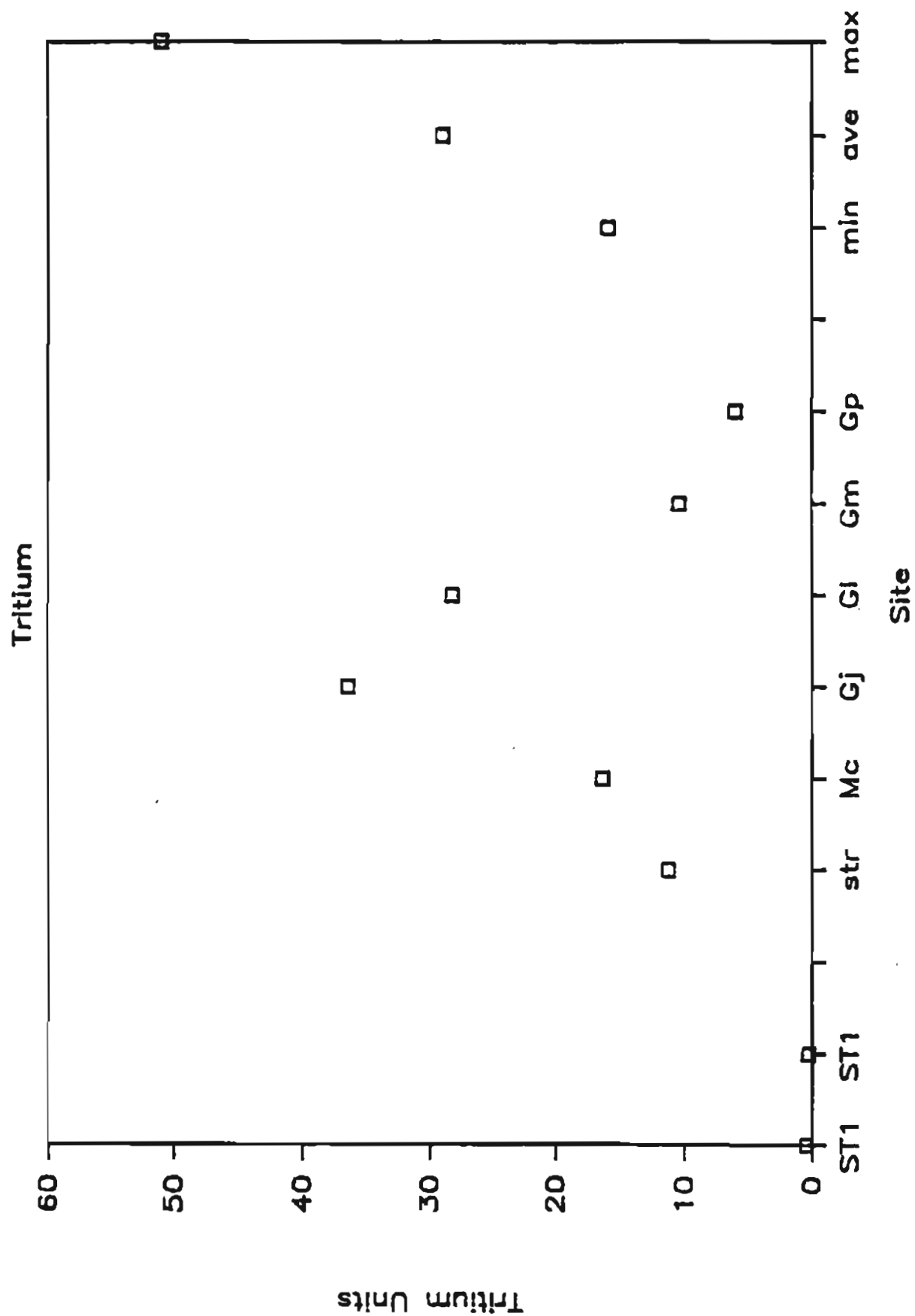


Fig. 10

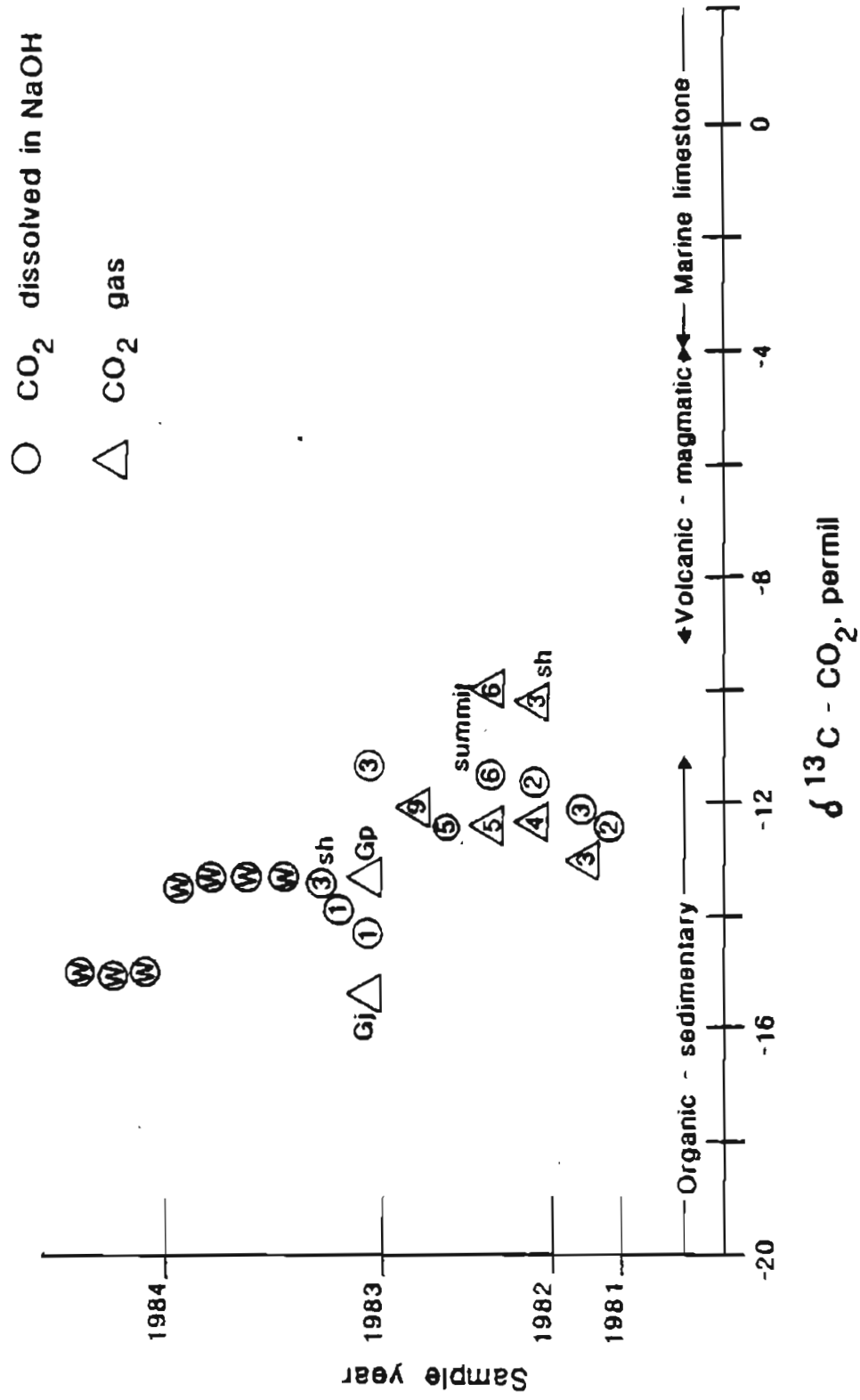


Fig. 11

Makushin Geothermal Area

Helium Isotope Data

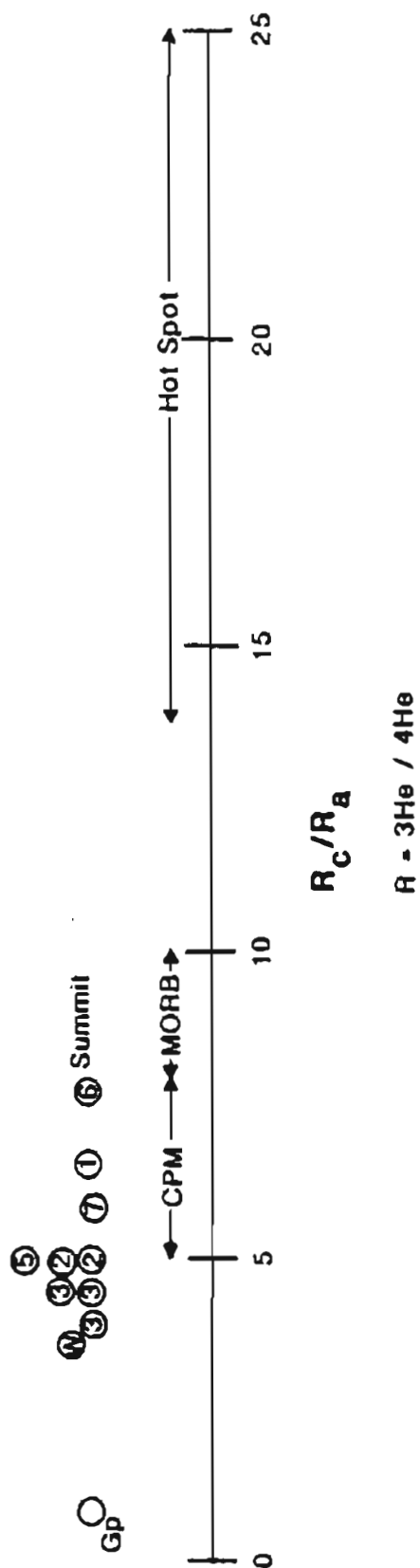


Fig. 12

GEOTHERMOMETRY ST-1

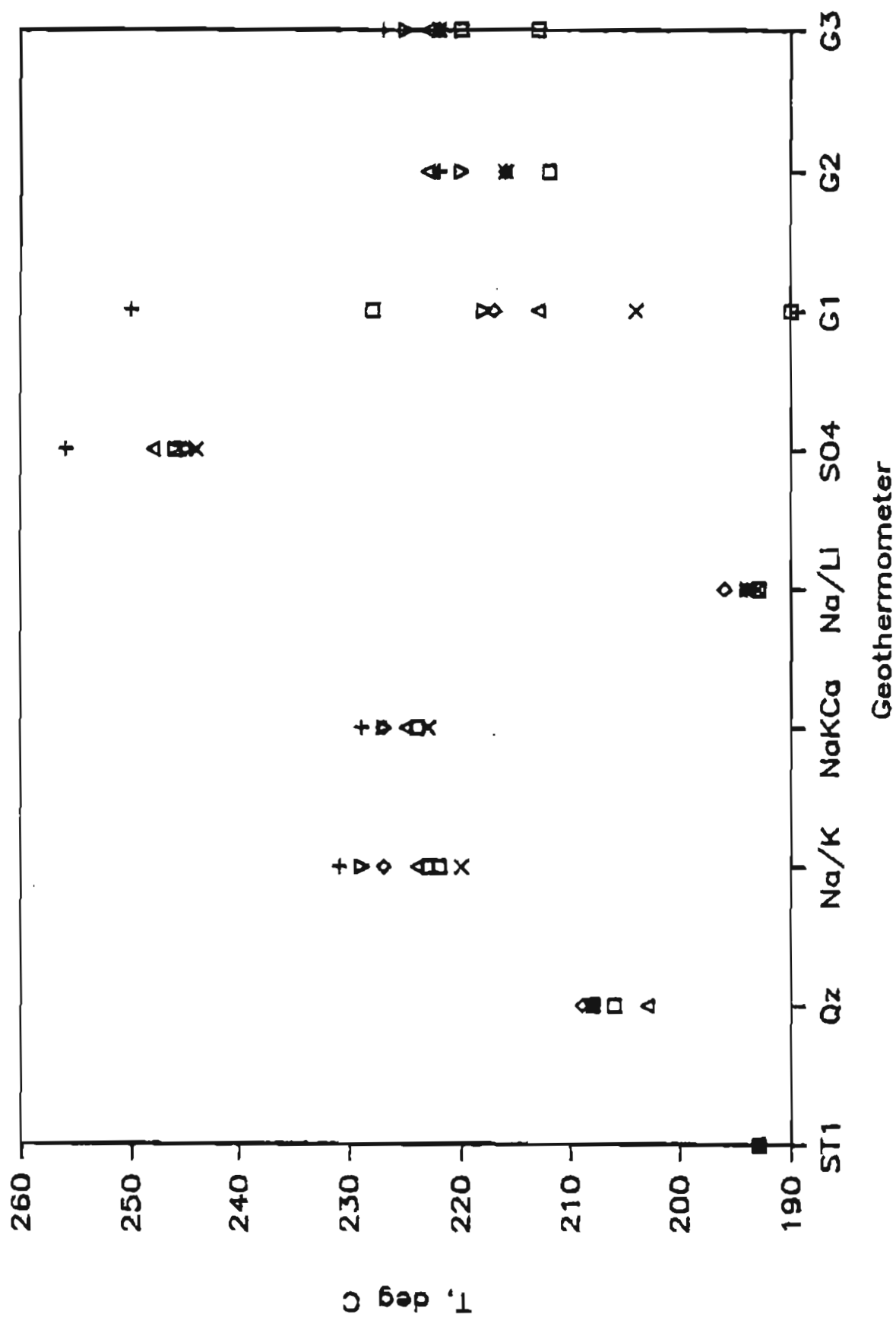
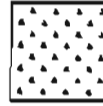


Fig. 13

EXPLANATION OF LOG SYMBOLS

Homogeneous Volcanics



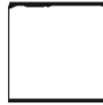
Gravel, Lahar, Till



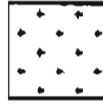
Cinders



Unalaska Hornfels



Gabbro-norite



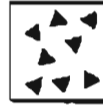
Unalaska Clastics



Unalaska Flows



Hydrothermal Breccia



Sharp Contact



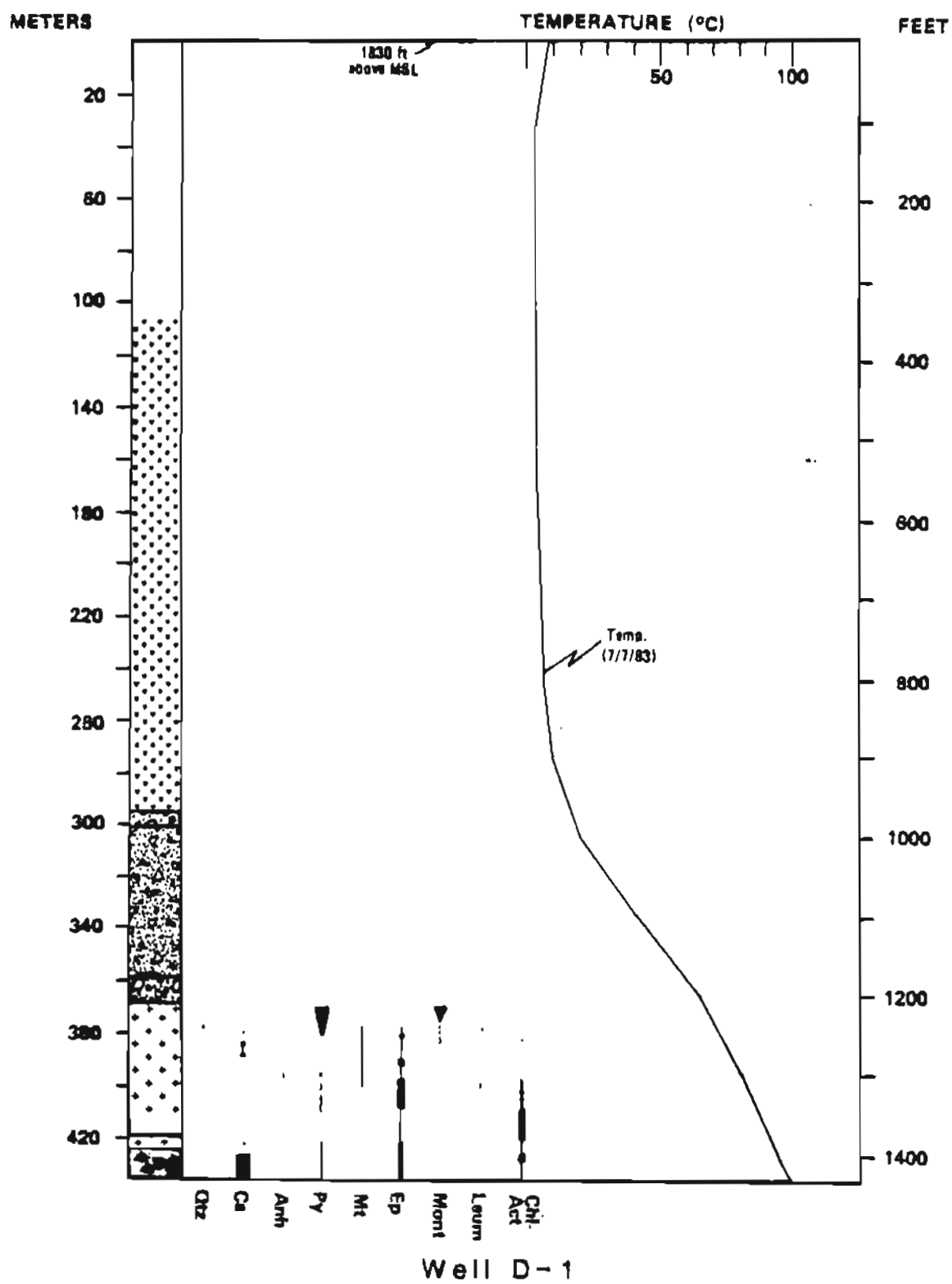


Fig. 14

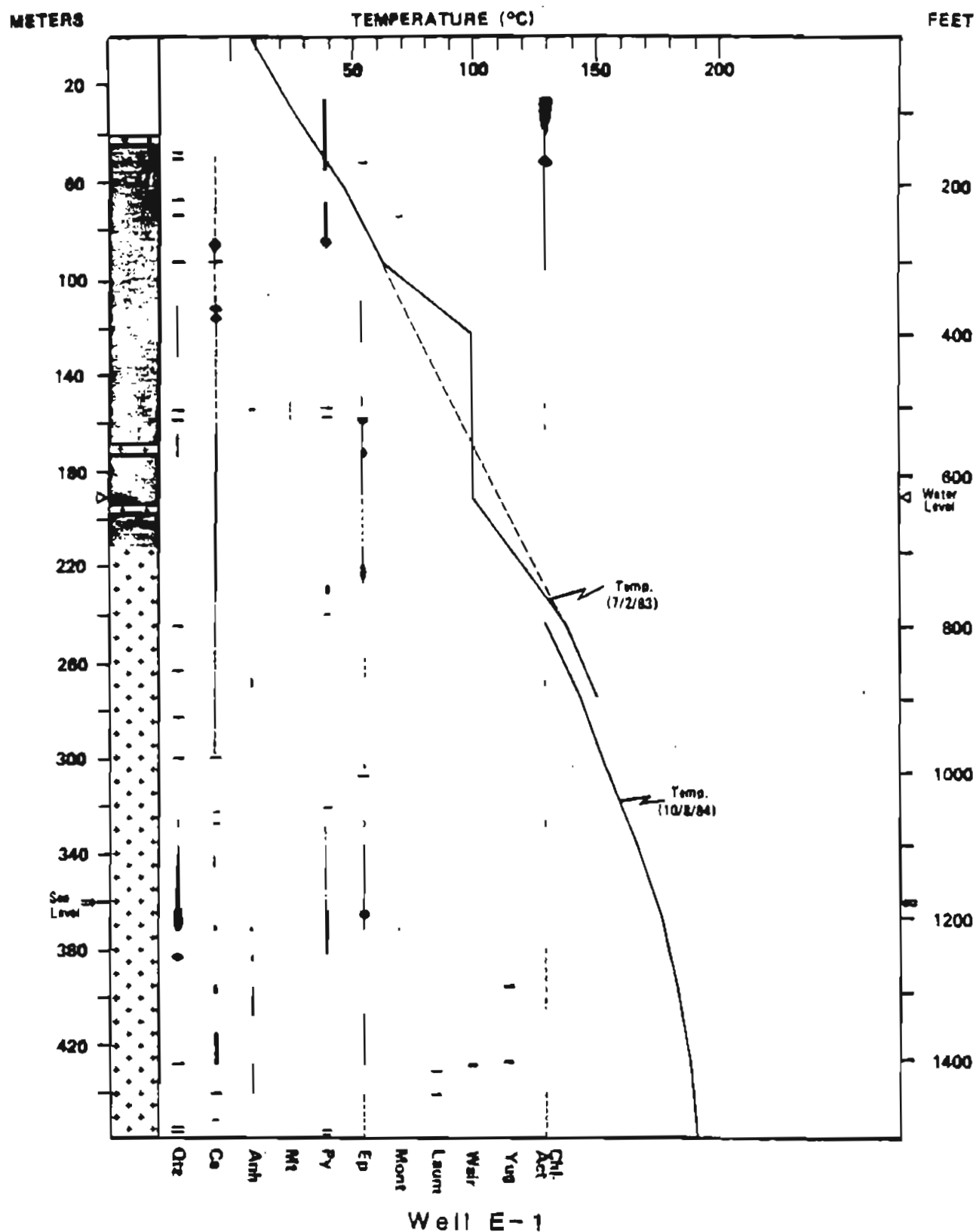


Fig. 15

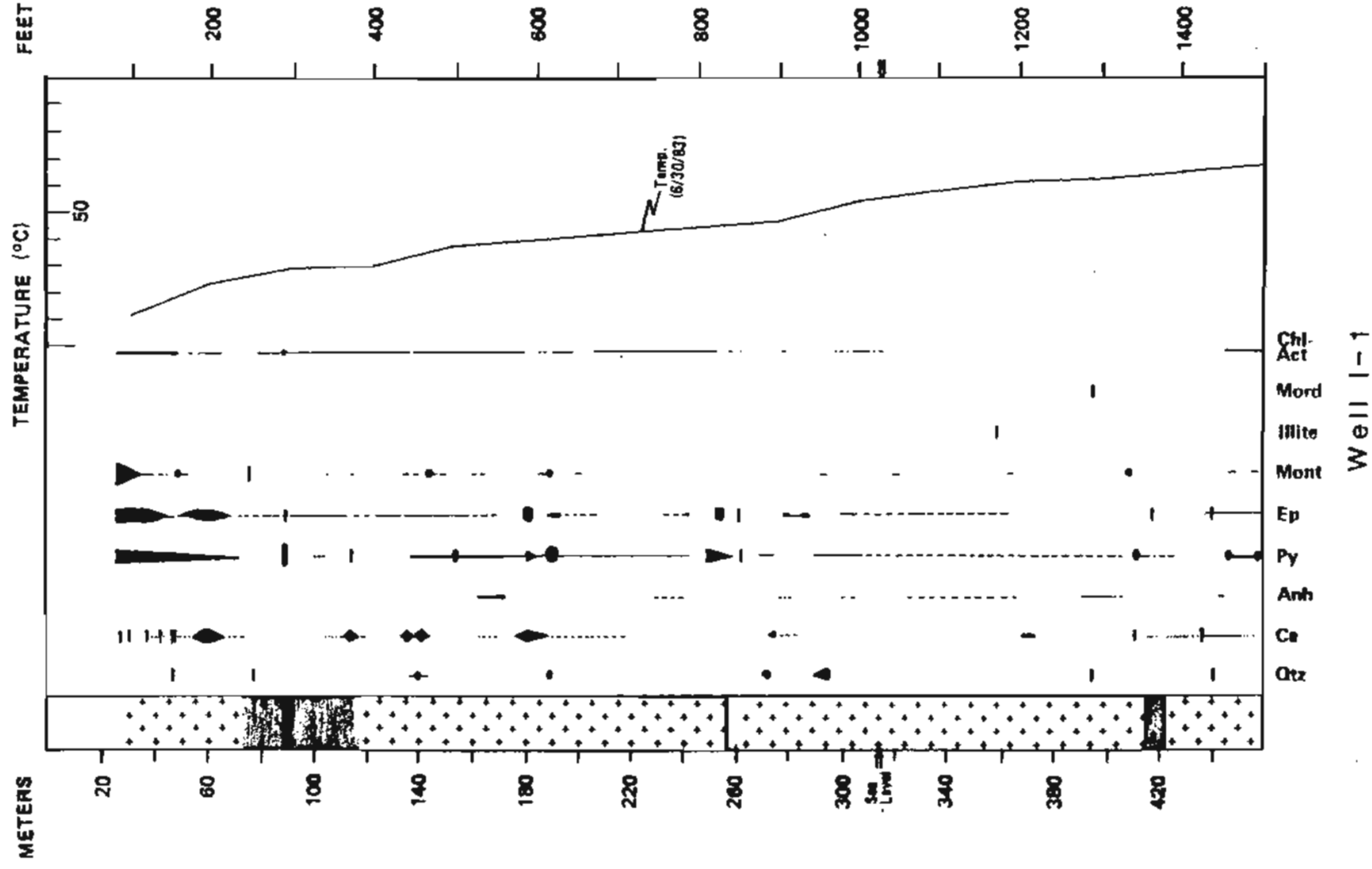


Fig. 16

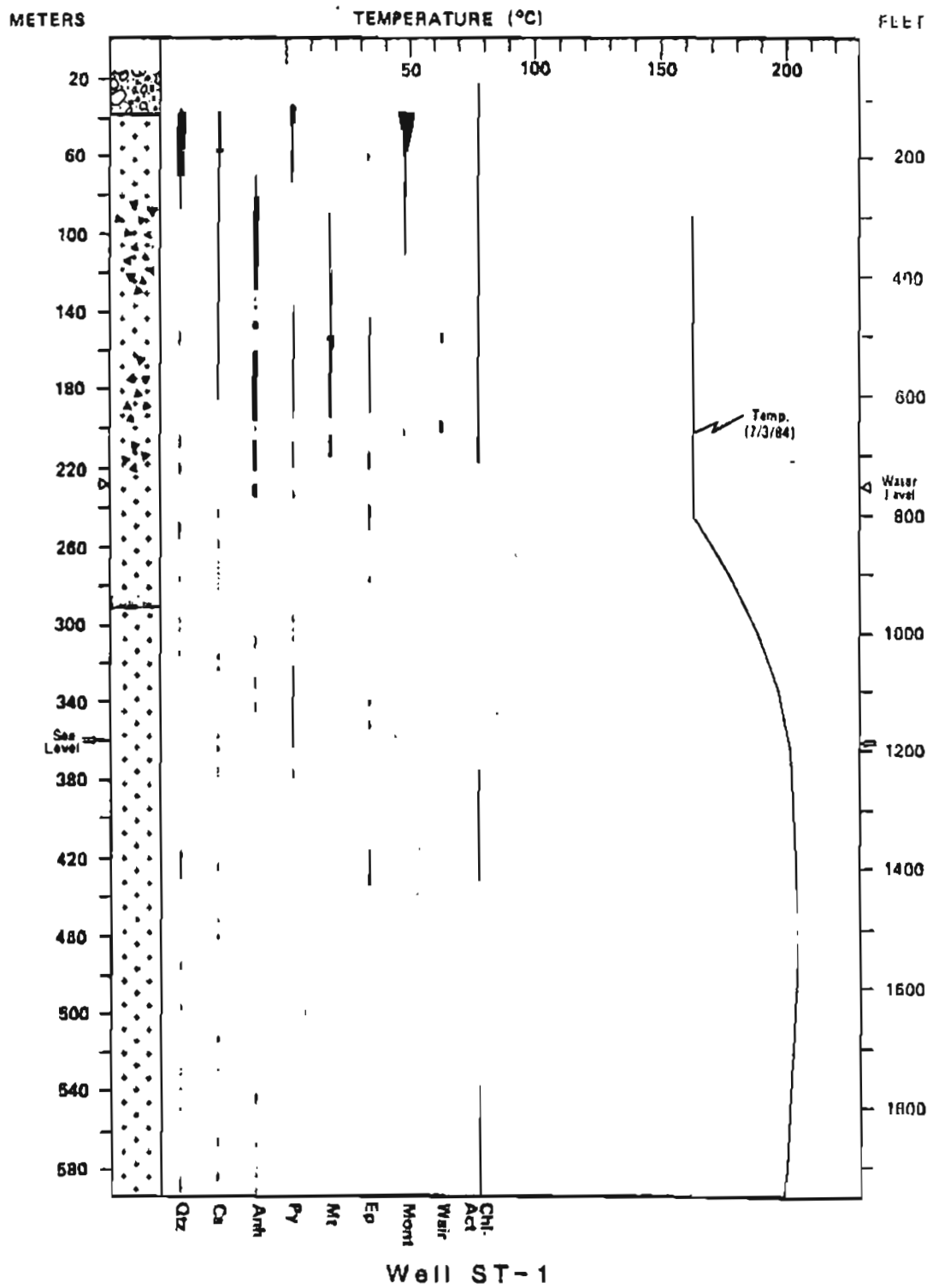


Fig. 17

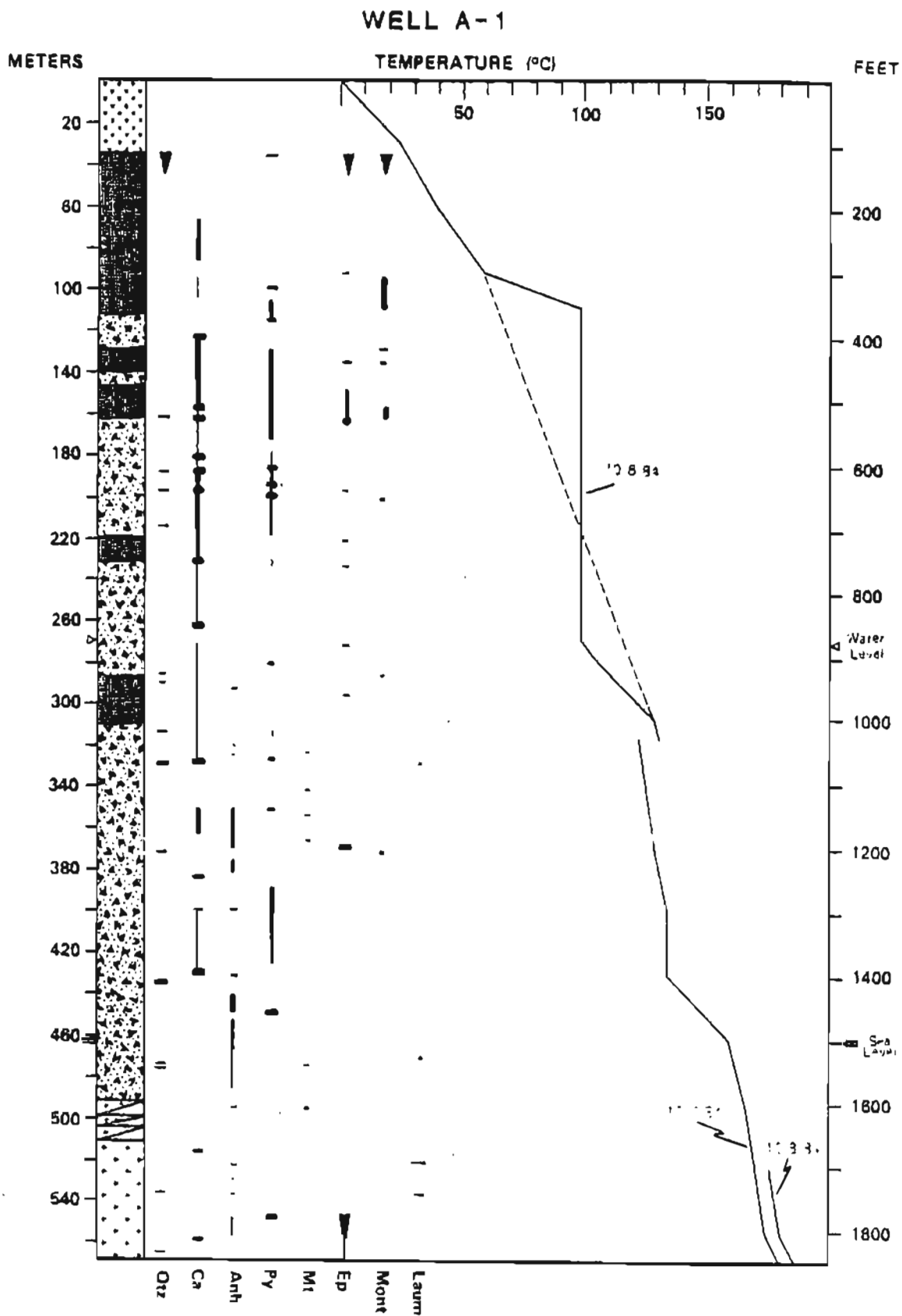
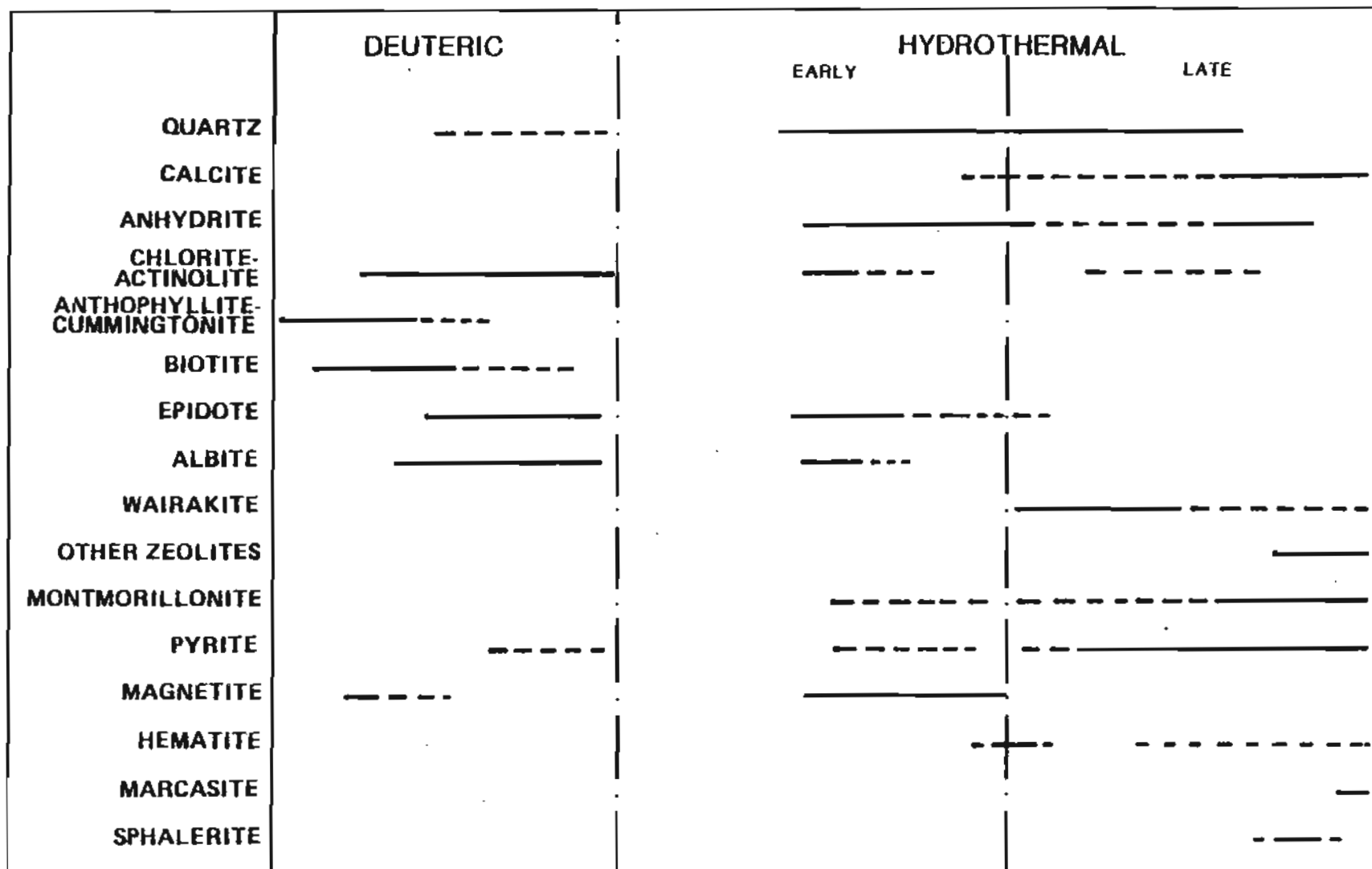


Fig. 18



Paragenetic Chart of Makushin Alteration Minerals

Fig. 19



Fig. 20

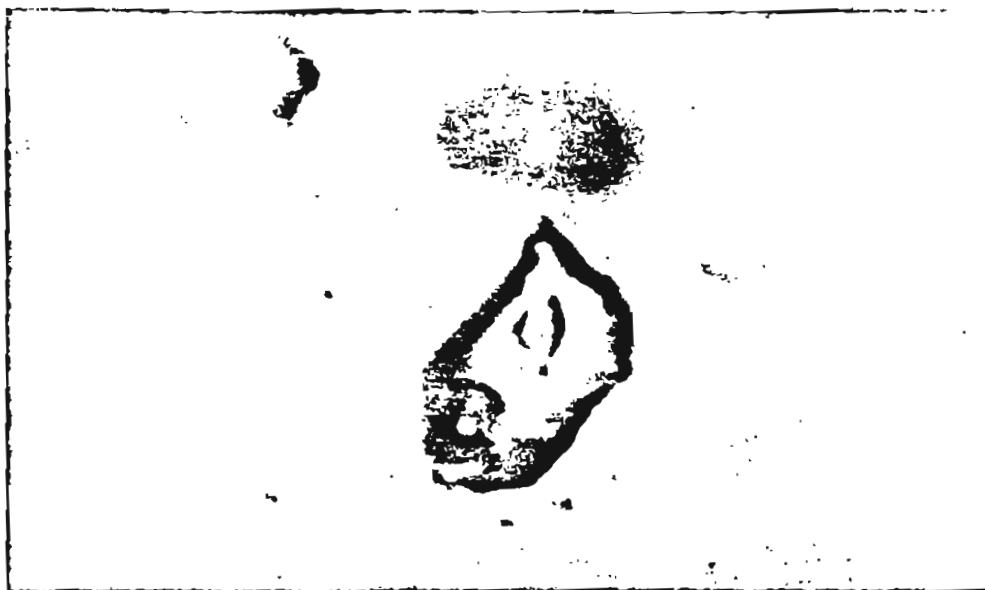


Fig. 21

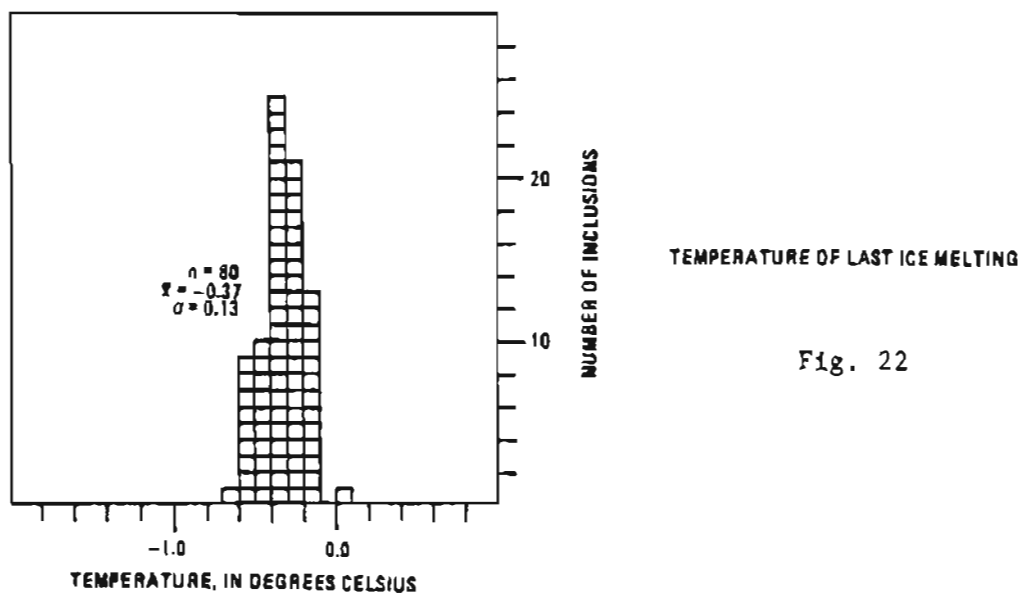


Fig. 22

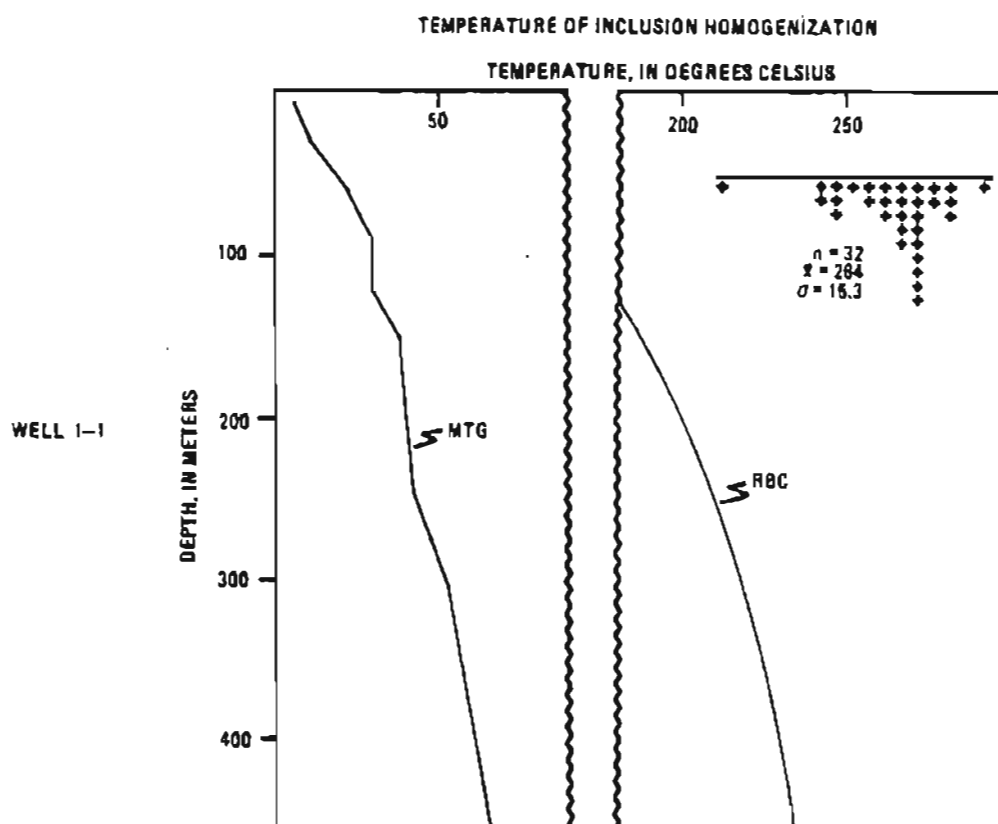
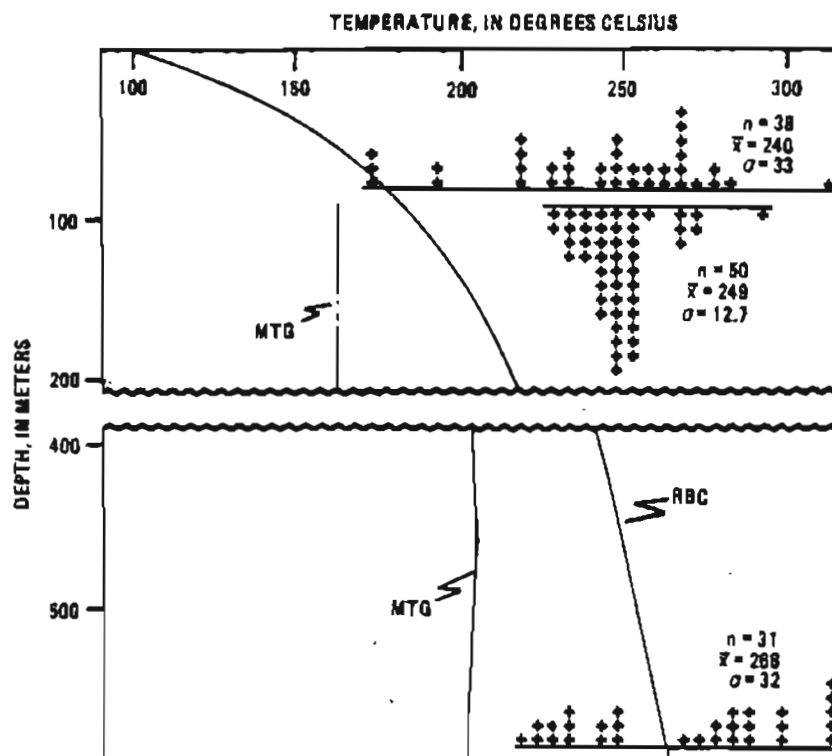


Fig. 23a

WELL ST-1

Fig. 23b



WELL E-1

Fig. 23c

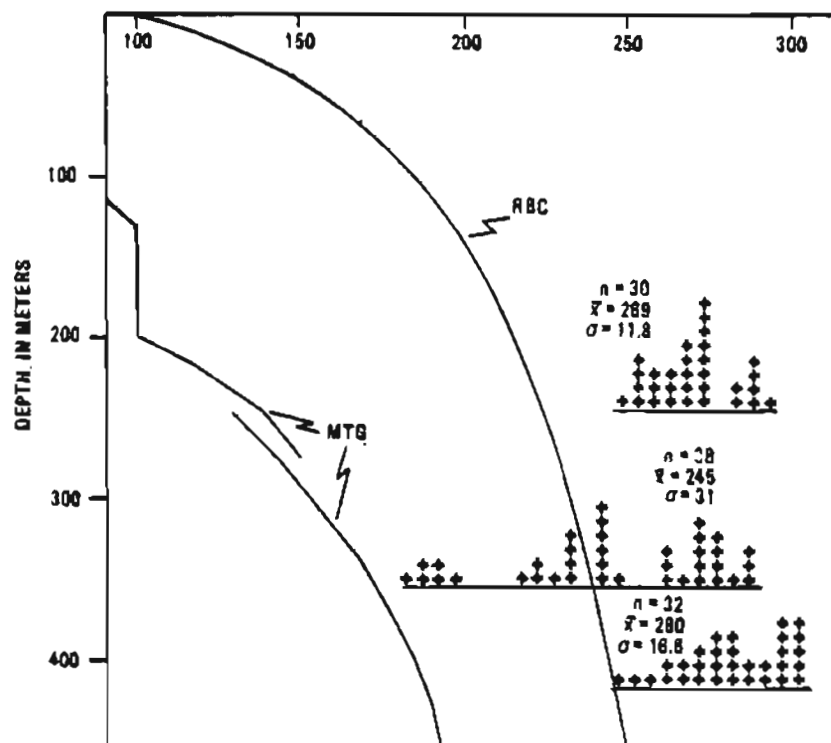


Fig. 24

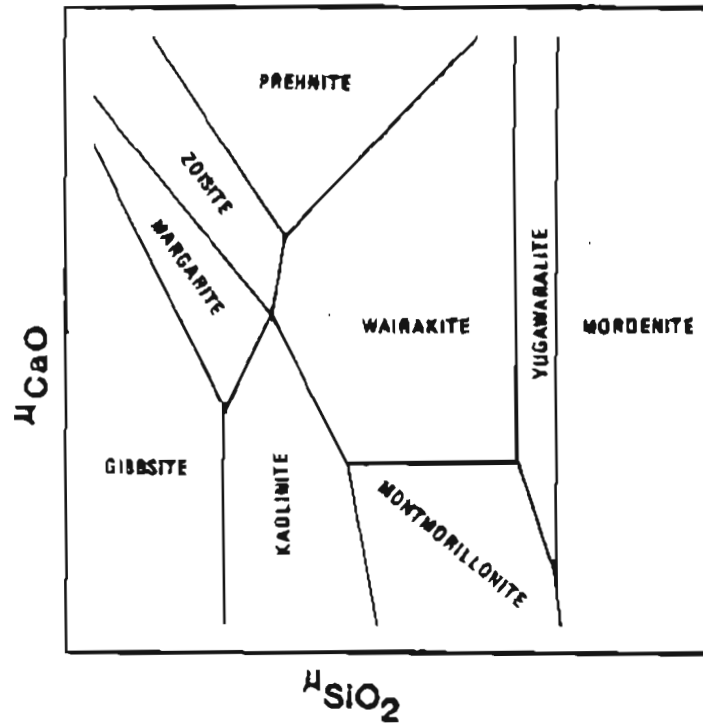


Fig. 25

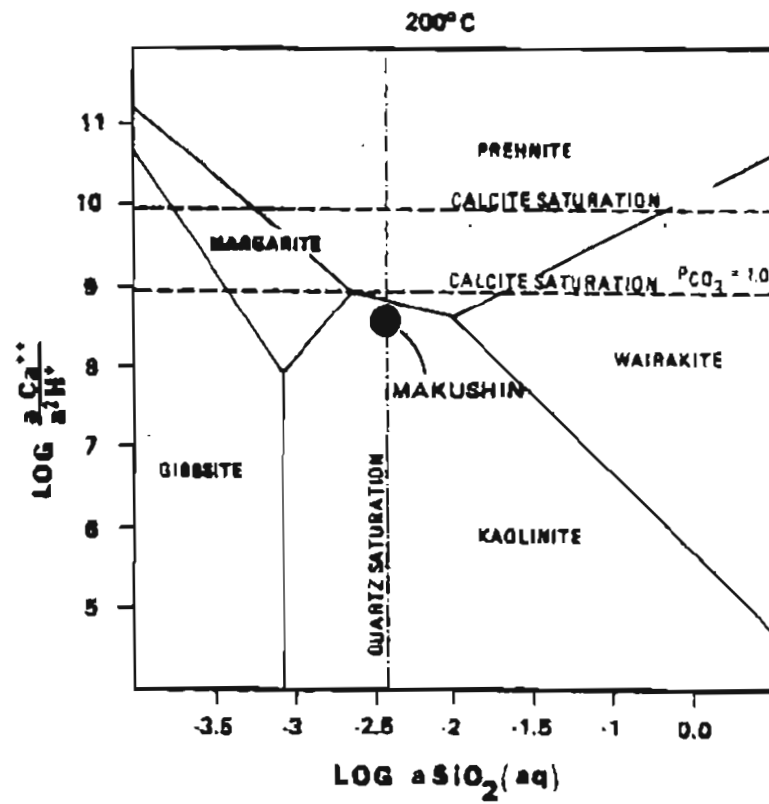


Fig. 26

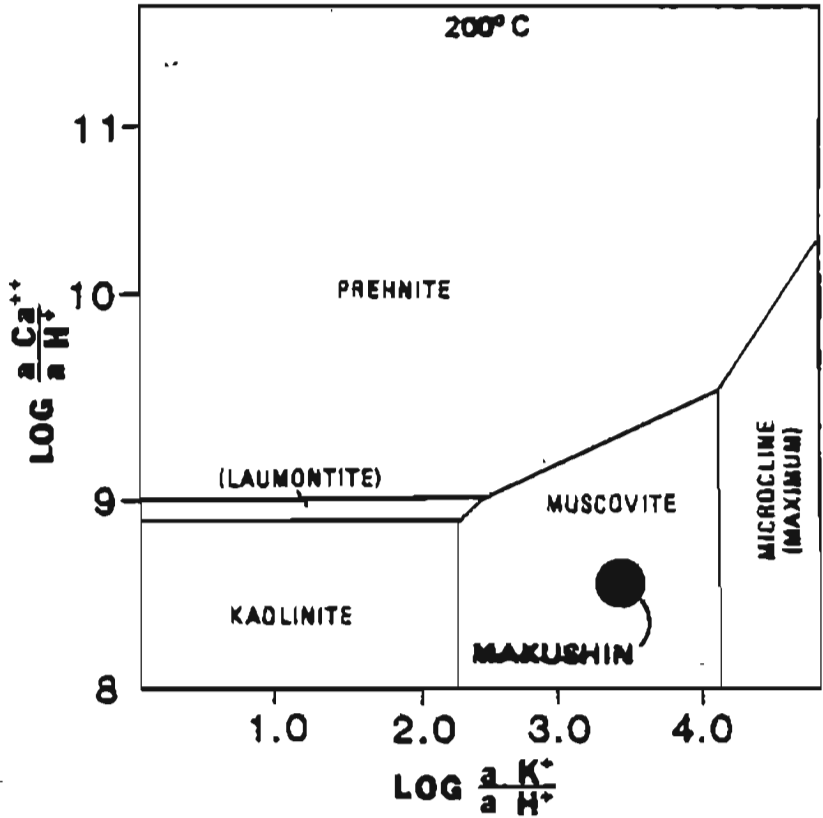
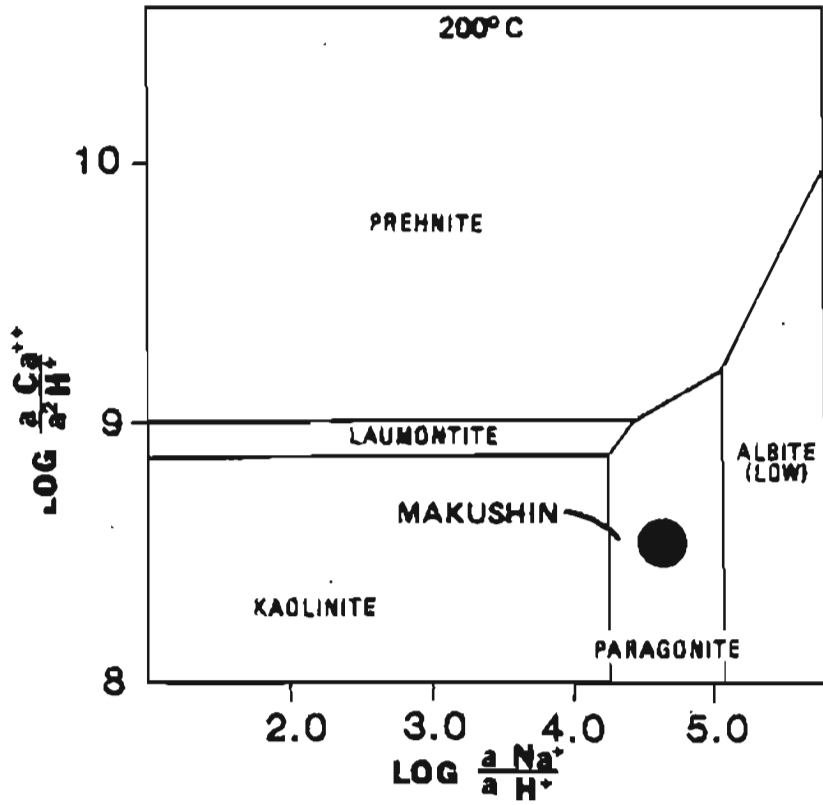


Fig. 27



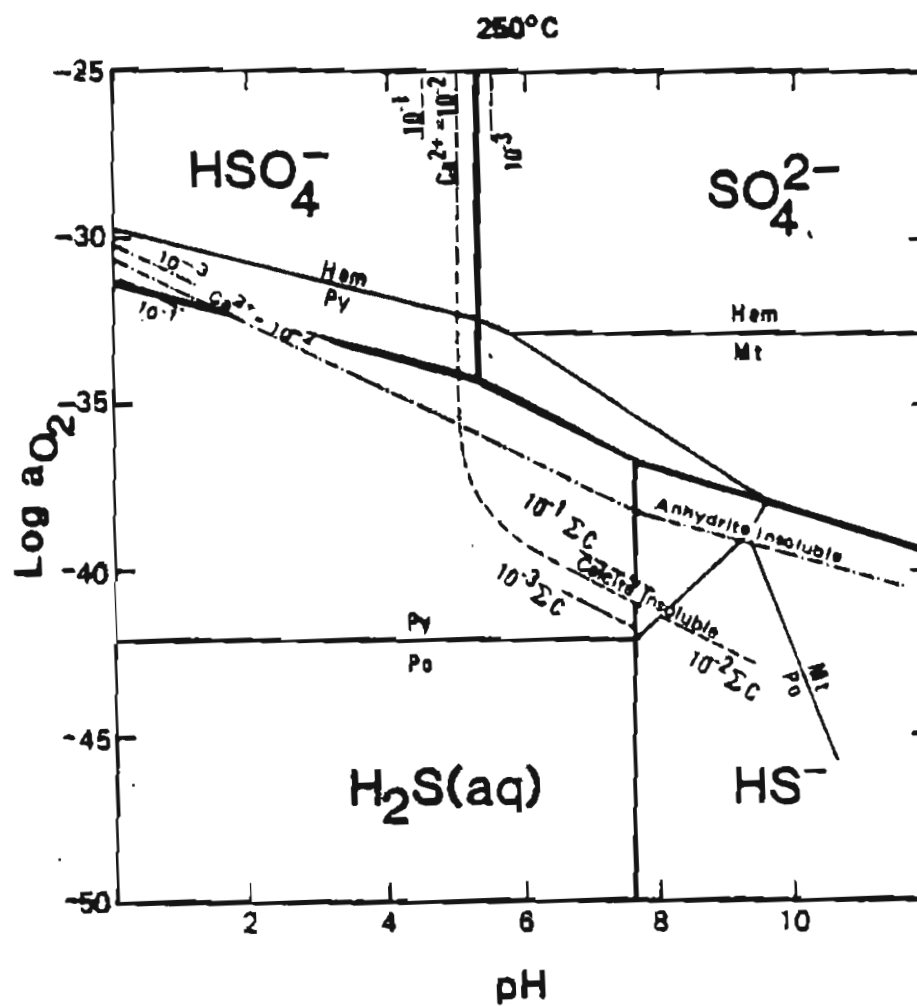


Fig. 28

REF

GEOL

UNAL

E-SCAN

MAK

LOC

RESI

SHOW

FIGUR

POSSIBLE LARGE SCALE FAULT
OBTAINED IN TRIAL 2-D MODEL

FOX CANYON

LOWER ROCK RESISTIVITIES

HIGHER ROCK RESISTIVITIES

DRIFTWOOD VALLEY

SHEAR ZONE

EVIDENCE OF HYDROTHERMAL ACTIVITY

BOUNDARY UNDEFINED

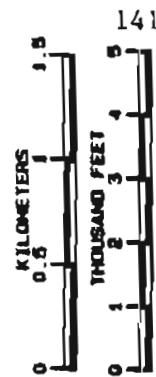
BOUNDARY DEFINED

MAKUSHIN VALLEY

LOCATION OF INTERPRETED
RESISTIVITY CROSS SECTIONS
SHOWN ON UNALTERED SUMMARY
FIGURE 2 OF THE 1984 REPORT
----- SECTION LOCATION. #

RESISTIVITY CONTACT OR
FAULT IMPLICATION DERIVED
FROM SHALLOW (<700 METERS)
DATA ONLY. NO STRUCTURAL
INFERENCES FROM DEEPER
DATA ARE SHOWN.
(1984 Report)

- SURVEY ELECTRODE SITE
- DRILL HOLE SITE



**PREMIER GEOPHYSICS INC.
VANCOUVER, CANADA**

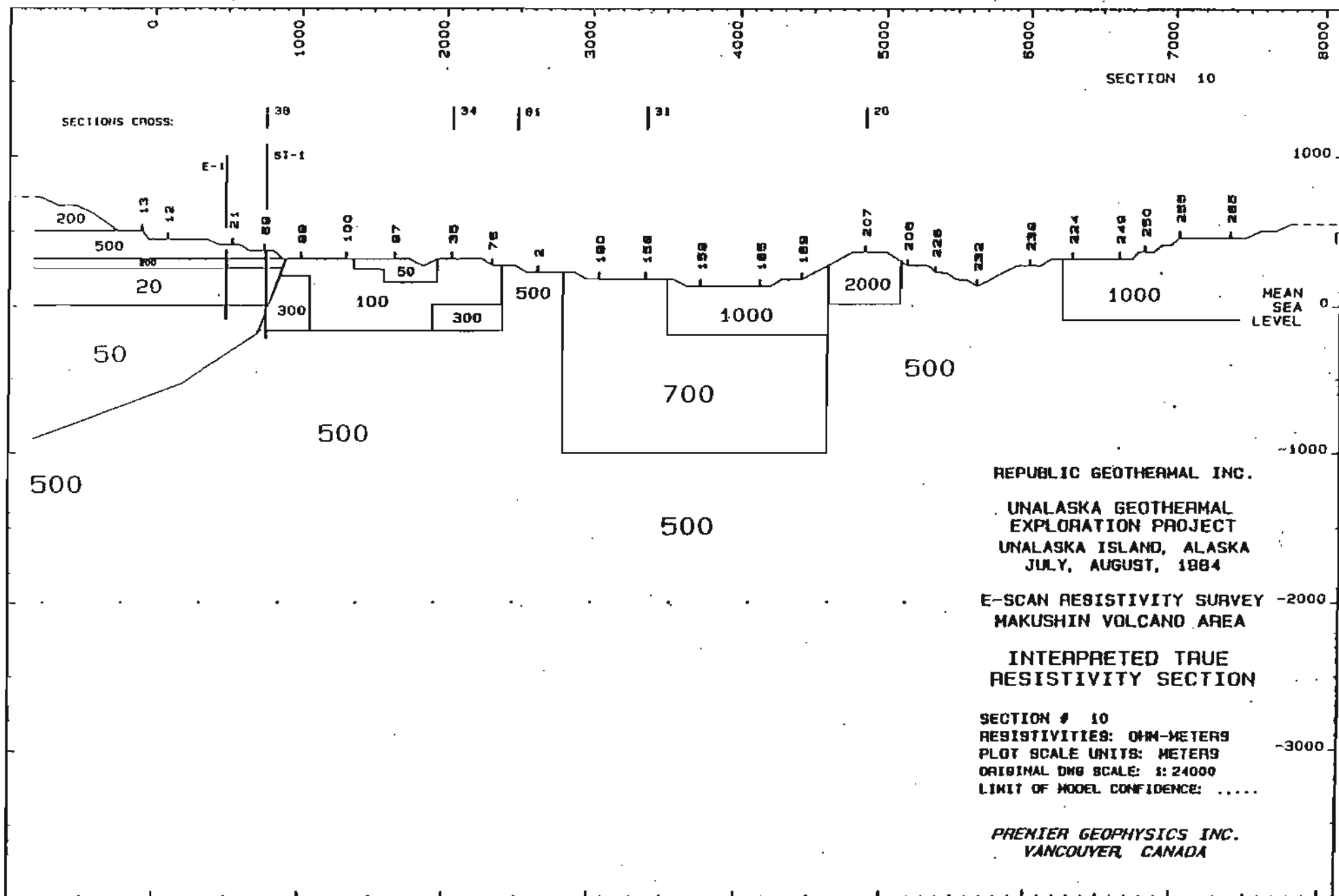


Fig. 30

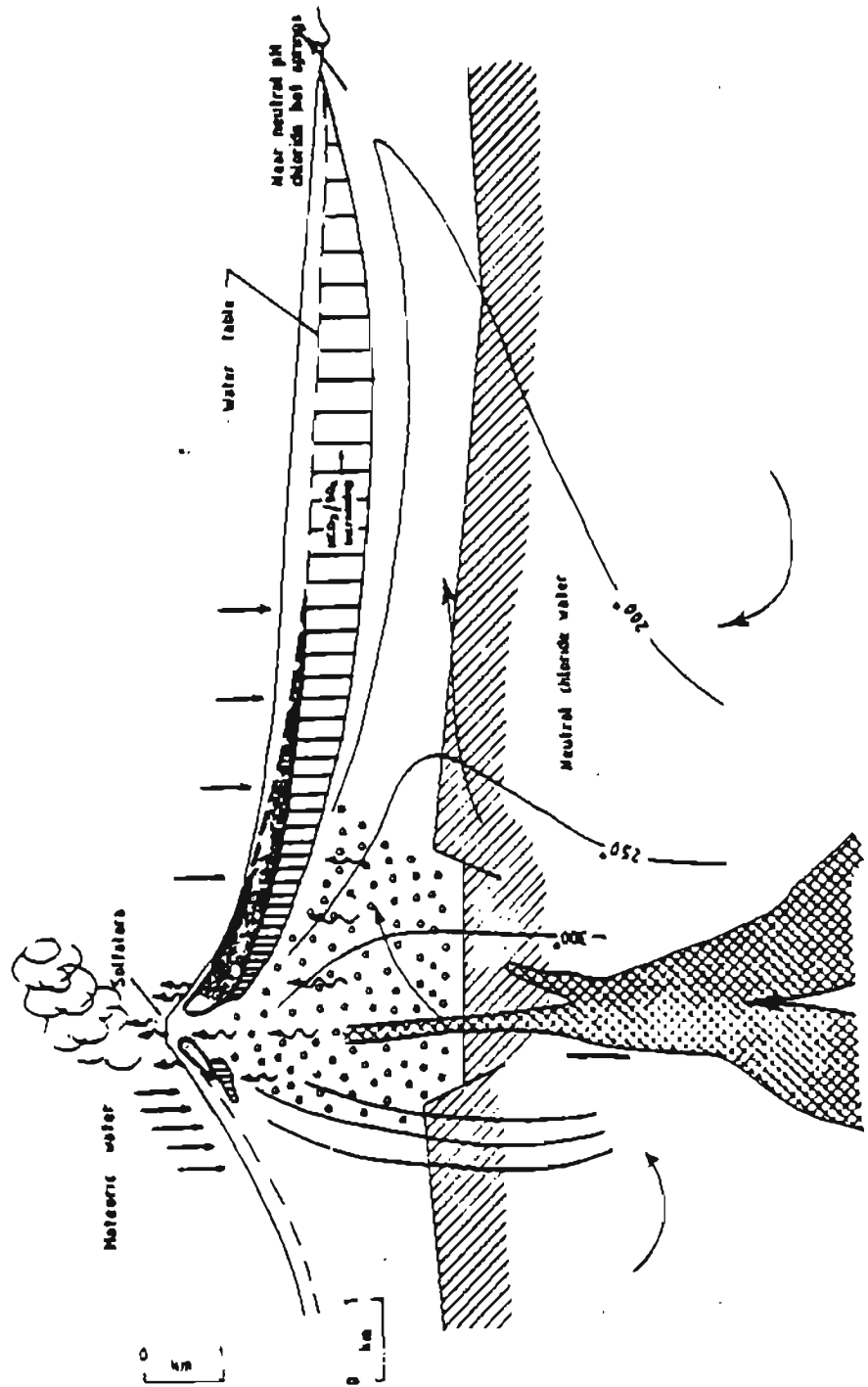


Fig. 31

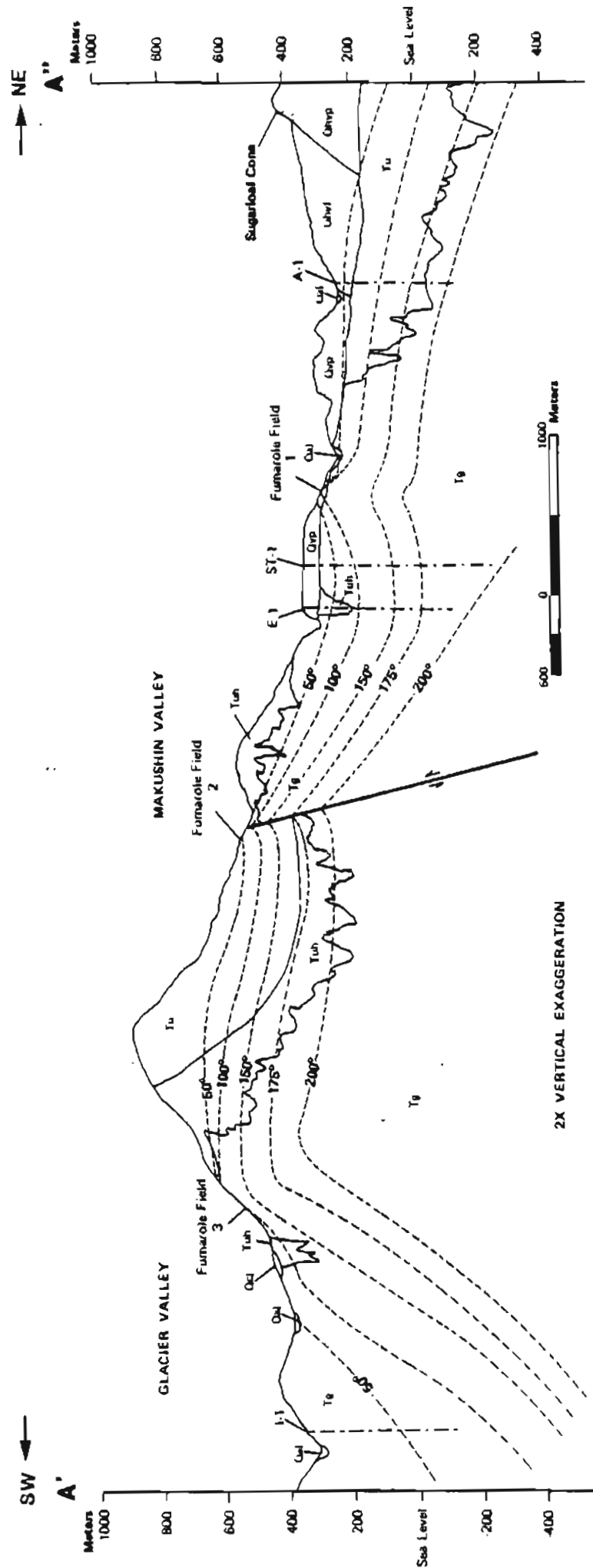


Fig. 32

APPENDIX A

Fluid Geochemistry Data Tables for Fumaroles and Hot Springs

Table A1. Chemical analyses of sulfate-carbonate spring waters in the Makushin geothermal area.^a
(Values in mg/l unless otherwise specified).

Site Name	Date	T ^b	pH ^b	Na	K	Ca	Mg	Li	Sr	HCO ₃ ^b	SO ₄	F	Cl	SiO ₂	B	Fe	TDS	SC
CV-Gd1	8-11-80	97	6.4	52	4.8	12	4.0	0.01	0.1	37	129	0.1	10.0	94	0.5	0.10	325	360
GV-Gd2	8-11-80	82	6.5	87	5.7	32	1	0.02	0.3	288	95	0.3	5.0	125	0.5	0.01	504	580
GV-Gd3	7-05-81	78	4.3	62	5.2	25	8.0	0.01	0.2	3	218	0.1	6.1	120	0.5	nd	447	9250
GV-Ge	7-05-81	68	nd	61	3.3	260	9.6	0.04	1.1	nd	491	0.3	2.3	138	0.5	0.02	nd	1400
GV-Gf	8-11-80	70	6.1	78	4.5	nd	nd	nd	nd	42	nd	nd	10.0	125	nd	nd	nd	nd
GV-Gf	7-05-81	79	6.4	81	4.8	210	7.8	0.03	1.1	256	476	0.2	7.5	142	0.5	0.21	1050	1200
GV-Gh	7-11-82	61	6.0	64	3.8	240	11	0.03	1.2	358	472	1.0	5.8	145	0.5	0.40	1120	1320
GV-Gj	7-10-82	41	6.1	53	3.4	280	11	0.03	1.4	332	581	1.0	6.6	120	0.5	0.70	1220	1430
GV-Gl	7-13-82	62	6.0	63	4.5	260	10	0.03	1.2	325	542	1.0	6.6	135	0.5	0.50	1190	1370
MV-Ma	7-17-82	84	6.0	54	9.0	65	13	0.02	0.3	nd	344	1.0	nd	155	0.5	2.5	nd	nd
MV-Mb	8-13-80	87	5.5	28	5.9	67	12	0.01	0.3	191	155	0.1	5.0	140	nd	0.09	508	600
MV-Mc	7-04-81	58	5.3	24	3.2	23	5.5	0.01	0.1	nd	25	0.1	7.8	88	0.5	0.07	nd	250
MV-Mc	7-18-82	55	6.8	32	4.3	34	6.1	0.01	0.1	201	15	1.0	7.9	105	0.5	0.10	305	351
MV-Md	8-13-80	67	5.3	14	3.4	23	8.0	0.01	0.1	116	21	0.1	5.0	88	nd	0.03	220	255
NV-Na	8-20-83	23	6.1	88	4.2	390	36	0.14	3.1	678	710	0.7	5.6	110	0.5	nd	1680	nd

CV = Glacier Valley, MV = Makushin Valley, NV = Nareekin Valley

a) Alaska Division of Geological and Geophysical Surveys, Fairbanks, Alaska, M.A. Moorman, analyst.

b) Determined in the field.

Table A2. Chemical analyses of chloride spring waters in the Makushin geothermal area.^a
(Values in mg/l unless otherwise specified)

Site Name	Date	T ^b	pH ^b	Na	K	Cations		Li	Sr	HCO ₃ ^b	Anions		Cl	SiO ₂	B	Fe	TDS	SC
						Ca	Mg				SO ₄	F						
DV - stream	8-21-83	14	6.9	36	3	8.8	2	0.15	0	35	6	nd	56	43.6	0.7	nd	175	nd
GV - Gm	7-20-82	39	5.9	180	19	200.0	15	0.48	1.1	463	360	1.0	160	113	4.2	1.7	1290	1380
GV - Gn	7-20-82	27	5.8	180	19	180.0	23	0.40	1.0	563	320	1.0	140	119	4.0	1.9	1260	1760
GV - Gp	7-20-82	40	6.3	300	31	160.0	39	0.86	1.4	590	180	1.0	380	104	9.9	2.1	1500	nd

DV - Driftwood Valley, GV - Glacier Valley

a) Alaska Division of Geological and Geophysical Surveys, Fairbanks, Alaska, M.A. Moorman, analyst.

b) Determined in the field.

Table A3. Chemical analyses of cold waters in the Makushin geothermal area.^a
(Values in mg/l unless otherwise specified)

Site name	Date	T ^b	pH ^b	Cations				Anions				Br	SiO ₂	B	As	Fe	TDS	SC
				Na	K	Ca	Mg	Li	Sr	HCO ₃ ^b	SO ₄ ^b	F	Cl					
DV - stream	8-21-83	14	6.9	36	3.4	8.8	2.0	0.15	.1	35	6	nd	56	nd	0.10	nd	175	nd
GV - Cd spring	7-05-81	5	nd	4.7	0.8	8.9	1.9	0.01	.1	nd	29	0.1	5.6	nd	nd	nd	nd	100
GV - Gd stream	8-11-80	7	6.0	78	4.5	nd	0.1	0.01	nd	nd	418	nd	10	nd	nd	nd	nd	nd
GV - Gk spring	7-15-82	16	6.6	4.1	0.3	20	1.1	0.01	0.1	38	27	1.0	5.9	nd	nd	0.10	88	161
GV - G1 stream	7-18-82	5	6.5	8.5	1.4	52	6.6	0.01	0.1	13	150	1.0	12	nd	nd	0.40	264	375
GV - Gn spring	7-09-83	6	6.4	5.6	0.2	6.4	1.0	0.01	0.2	26	4	nd	5.5	nd	0.002	nd	42	nd
GV - clear river mouth	7-19-83	7	6.4	7.5	0.5	53	1.8	0.01	.1	37	14	nd	8.8	nd	0.001	nd	117	nd
GV - kettle pond	8-19-84	nd	nd	1.9	0.1	0.5	0.3	0.01	.1	nd	1	nd	2.0	0.1	0.001	nd	nd	nd
GV - muddy river mouth	7-19-83	5	6.5	6.3	0.7	12	2.2	0.01	0.1	11	36	nd	7.0	nd	0.001	nd	82	nd
MV - spring	7-19-82	6	6.6	2.6	0.2	1.8	0.6	0.01	0.1	11	3	1.0	3.7	nd	0.1	0.1	32	34

DV - Driftwood Valley, GV - Glacier Valley, MV - Makushin Valley

a) Alaska Division of Geological and Geophysical Surveys, Fairbanks, M.A. Moorman, analyst.
b) Determined in the field.

Table A4. Stable isotope analyses of sulfate-carbonate spring waters in the Makushin geothermal area.^a

Site Name	Date	T°C	D/H ^b	¹⁸ O/ ¹⁶ O ^b
GV - Ga	7-05-81	nd	-83	-11.9
GV - Gb	7-05-81	nd	-80	-12.2
GV - Gc	7-05-81	nd	-83	-12.5
GV - Gd1	8-11-80	97	-70	-8.9
GV - Gd2	8-11-80	82	-80	-11.6
GV - Gd3	7-05-81	78	-83	-11.9
GV - Ge	7-05-81	68	-80	-12.2
GV - Gf	7-05-81	79	-83	-12.5
GV - Gh	7-11-82	61	-82	-11.7
GV - Gj	7-10-82	41	-79	-11.0
GV - Gl	7-13-82	62	-83	-11.9
MV - Ma	7-17-82	84	-77	-11.1
MV - Mb	7-04-81	nd	-81	-12.4
MV - Mb	8-13-80	87	-78	-11.9
MV - Mc	7-04-81	58	-81	-12.4
MV - Mc	7-18-82	55	-84	-11.7
MV - Md	8-13-80	67	-81	-12.1
NV - Na	8-20-83	23	-78	-11.3

GV - Glacier Valley

MV - Makushin Valley

NV - Nateekin Valley

a) Analyzed at Stable Isotope Laboratory, Southern Methodist U., Dallas, Texas.

b) Values are in permil with respect to SMOW.

Table A5. Stable isotope analyses of chloride spring waters in the Makushin geothermal area.^a

Site Name	Date	T°C	D/H ^b	$^{18}\text{O}/^{16}\text{O}^b$
DV - stream	8-21-83	14	-76	-9.9
GV - Gm	7-20-82	39	-80	-11.1
GV - Gn	7-20-82	27	-82	-11.1
GV - Gp	7-20-82	40	-78	-10.9
GV - Gp	7-16-83	44	-80	-11.2

DV - Driftwood Valley

GV - Glacier Valley

a) Analyzed at State Isotope Laboratory, Southern Methodist U., Dallas, Texas.

b) Values are in permil with respect to SMOW.

Table A6. Stable isotope analyses of cold waters in the Makushin geothermal area.^a

Site Name	Date	T°C	D/H ^b	¹⁸ O/ ¹⁶ O ^b
DV - stream	8-21-83	14	-76	-9.9
FF 1 - stream	7-18-83	nd	-81	-11.2
FF 3 - stream	7-11-83	nd	-89	-13.5
FF 6 - snow	7-18-82	nd	-121	-15.9
FF 7 - snow melt	8-20-83	nd	-88	-12.7
FF 9 - snow melt	7-11-83	nd	-65	-11.0
GV - Gd spring	7-05-81	5	-93	-14.2
GV - Gd spring	8-11-80	nd	-77	-11.1
GV - Gd stream	8-11-80	7	-87	-12.0
GV - Gk spring	7-15-82	16	-77	-10.0
GV - Gl stream	7-18-82	5	-88	-12.6
GV - Gn spring	7-09-83	nd	-78	-11.3
GV - West Fork River	7-05-81	5	-93	-14.2
GV - clear river mouth	7-19-83	7	-77	-11.5
GV - muddy river mouth	7-19-83	5	-85	-12.8
GV - snow melt	8-11-80	nd	-76	-11.2
MV - Camp spring	7-19-82	nd	-67	-9.7
MV - Mb stream	8-13-80	nd	-89	-13.0
MV - Mc stream	7-04-81	nd	-82	-11.9
MV - Md stream	8-11-80	nd	-83	-11.3
MV - spring	7-19-82	6	-82	-11.9
NV - stream	8-20-83	nd	-88	-12.7

DV - Driftwood Valley

FF - Fumarole field

GV - Glacier Valley

MV - Makushin Valley

NV - Nateekin Valley

a) Analyzed at Stable Isotope Laboratory, Southern Methodist U., Dallas, Texas.

b) Values are in permil with respect to SMOW.

Table A7. Geothermometry of chloride spring waters in Makushin geothermal area.
(Temperatures in °C).

Site Name	Date	Qz. cond. (1)	Chal. cond. (2)	Na/K (3)	Na/K (4)	Na/K (5)	Na-K-Ca (6)	Na-K-Ca (7)	Ni/Li (8)
DV - stream	8-21-83	96	65	210	178	187	157	71	171
GV - Cm	7-20-82	144	118	225	197	205	166	129	139
GV - Gn	7-20-82	147	122	225	197	204	167	99	126
GV - Cp	7-20-82	139	113	221	192	200	175	64	143

DV = Driftwood Valley, GV = Glacier Valley

- (1) Fournier and Potter, 1982, improved SiO_2 (quartz).
- (2) Fournier, 1981 (chalcedony).
- (3) Fournier, 1981, Na/K.
- (4) Truesdell, 1976, Na/K.
- (5) Arnorsson, 1983, Na/K, Basalt.
- (6) Fournier & Truesdell, 1973.
- (7) Fournier & Potter, 1979, Mg-corrected.
- (8) Fouillie & Michard, 1981.

Table A8. Analyses of gases collected from fumaroles and hot springs, Makushin geothermal area, in mole per cent.
Analyses corrected for air contamination using ratio of O_2 in sample to O_2 in air (RO_2).

Sample code	Location	Date sample	RO ₂	Xg	CO ₂	H ₂ S	H ₂	CH ₄	NH ₃	N ₂	Ar	N ₂ /Ar	C/S	Gas geothermometer ^c	
														T ₁	T ₂
Sodium-hydroxide charged flasks: ^a															
RM 83-46	FF#1	7-17-83	0.01	0.17	82.19	2.28	0.21	0.039	0.38	14.73	0.17	86.4	36.1	227	206
RM 83-GV1-A	FF#3 Superheated	7-08-83	0.00	0.16	88.04	6.38	0.95	0.010	0.13	4.43	0.06	80.2	13.8	298	272
RM 83-11b	FF#3 West	7-10-83	0.06	0.50	83.72	1.69	0.22	0.001	0.04	14.16	0.17	84.1	49.4	256	234
RM 83-31	FF#3 Far west	7-13-83	0.05	0.36	88.10	4.58	0.25	0.001	0.01	6.94	0.14	51.3	19.3	273	249
RM 83-57	FF#7	8-20-83	0.01	2.63	82.15	1.81	1.10	2.482	0.18	12.21	0.08	161.9	46.7	230	210
RM 83-19	FF#9	7-11-83	0.00	0.78	91.55	3.94	0.85	0.004	0.01	3.63	0.02	146.3	23.2	294	268
DS 83 BN7 DS	FF#3 superheated (98°C)	8-29-83	0.00	0.18	88.93	6.85	0.88	0.006	0.08	3.22	0.03	113.1	13.0	302	275
DS 83 BN13 DS	FF#3 Far west	8-29-83	0.00	0.25	84.93	6.25	0.66	0.003	0.06	8.06	0.01	--	13.6	299	273
RM 82-GV1	FF#3 Superheated	7-09-82	0.02	0.15	82.29	12.25	1.84	0.070	nd	3.56	0.07	54.7	6.7	313	285
RM 82-Ma sum	FF#6 Summit	7-18-82	0.00	1.67	87.47	5.53	0.21	0.047	nd	6.63	0.11	60.2	15.8	235	214
RM 82-MV FF#2	FF#2	7-17-82	0.00	--	90.40	2.92	0.35	0.012	nd	6.24	0.07	87.8	30.9	252	229
RM 82 Ma west fl.	FF#5	7-13-82	0.01	1.39	91.16	0.95	0.51	0.004	0.03	7.29	0.05	137.0	96.4	257	234
RP 81-AL3	FF#2	7-14-81	0.00	0.00	87.17	5.26	0.75	0.002	nd	6.76	0.06	120.2	16.6	308	280
RP 81-A15	FF#3	7-05-81	0.00	0.00	87.42	1.23	1.80	0.002	nd	9.43	0.11	86.4	70.9	309	281
RM 80-MV2	FF#1	8-13-80	0.00	0.41	91.68	2.63	0.24	0.029	nd	5.36	0.07	78.4	34.9	231	210
RM 80-MV1	FF#2	8-13-80	0.00	0.59	87.90	2.65	0.54	0.002	nd	8.81	0.09	95.4	33.2	283	258
Uncharged, evacuated flasks: ^b															RM 83
G-p	Spring G-p	7-16-83	--	--	98.22	0.02	0.005	0.052	nd	0.96	0.02	48.0	--	--	--
RM 83 G-j	Spring G-j	7-21-83	0.04	--	25.43	0.02	0.02	0.010	nd	74.13	1.02	72.4	--	--	--
RM 82 GV UW	FF#4	7-14-82	0.01	--	92.73	0.82	1.21	0.01	nd	5.50	0.05	104.8	113.5	295	269
RM 82 Ma WF	FF#5	7-13-82	0.00	--	94.89	0.68	0.59	0.01	nd	3.78	0.05	77.6	139.3	268	244
RM 82 Ma Sum	FF#6	7-18-82	0.00	--	90.60	5.68	0.12	0.02	nd	3.43	0.01	--	16.0	226	206
RM 82 GV W	FF#9	7-14-82	0.00	--	93.36	2.01	0.72	0.01	nd	4.33	0.04	108.3	46.4	293	267

(a) Samples RM 83 and RM 82 analyzed by R.J. Motyka, Alaska Division of Geological and Geophysical Surveys; samples DS 83 analyzed by D.S. Sheppard, Department of Scientific and Industrial Research, New Zealand; samples RP 81 and RM 80 analyzed by J. Whelan, Scripps Institute of Oceanography, La Jolla, and R.J. Motyka, Alaska Division of Geological and Geophysical Surveys, Fairbanks.

(b) Analyzed by W. Evans, U.S. Geological Survey, Menlo Park, and R.J. Motyka, Alaska Division of Geological and Geophysical Surveys, Fairbanks.

(c) D'Amore and Panichi, 1980. T_1 uses $P CO_2 = 1$ bar; T_2 uses $P CO_2 = 0.5$ bar.

nd = not determined.

Table A9. Makushin geothermal area, analyses of $^{13}\text{C}/^{12}\text{C}$ in CO_2 emanating from fumaroles and hot springs.

Location	Year Collected	^{13}C , PDB	Type	Analyst
Fum. field #1	1983	-14.3	$\text{SrCO}_3/\text{NaOH}$	USGS
	1983	-13.9	$\text{SrCO}_3/\text{NaOH}$	USGS
Fum. field #2	1981	-12.2	$\text{SrCO}_3/\text{NaOH}$	GC
		-12.5	$\text{SrCO}_3/\text{NaOH}$	SMU
	1982	-11.6	$\text{SrCO}_3/\text{NaOH}$	USGS
Fum. field #3,sp	1981	-11.8	$\text{SrCO}_3/\text{NaOH}$	GC
		-12.4	$\text{SrCO}_3/\text{NaOH}$	SMU
lower	1981	-13.0	$\text{CO}_2\text{-gas}$	GC
super heated	1982	-10.2	$\text{CO}_2\text{-gas}$	SIO
	1983	-13.4	$\text{SrCO}_3/\text{NaOH}$	USGS
west	1983	-11.3	$\text{SrCO}_3/\text{NaOH}$	USGS
Fum. field #4	1982	-12.3	$\text{CO}_2\text{-gas}$	USGS
Fum. field #5	1982	-12.4	$\text{SrCO}_3/\text{NaOH}$	USGS
		-12.4	$\text{CO}_2\text{-gas}$	USGS
Fum. field #6	1982	-10.0	$\text{CO}_2\text{-gas}$	USGS
		-11.5	$\text{SrCO}_3/\text{NaOH}$	SMU
Fum. field #9	1982	-12.1	$\text{CO}_2\text{-gas}$	USGS
Spring G-j	1983	-15.4	$\text{CO}_2\text{-gas}$	USGS
Spring G-p	1983	-13.3	$\text{CO}_2\text{-gas}$	USGS

USGS = U.S. Geological Survey, Menlo Park, California.

SMU = Southern Methodist University, Stable Isotope Laboratory, Dallas, Texas.

GC = Global Geochemistry, Inc., Canoga Park, California.

SIO = Scripps Institute of Oceanography, Stable Isotope Laboratory, La Jolla, California.

Table A10. Makushin geothermal area, miscellaneous stable isotope analyses.

$^{13}\text{C}/^{12}\text{C} - \text{HCO}_3$, thermal waters (USGS).

Location	Year Collected	^{13}C , PDB
Spring G-h	1982	-11.1
Test well ST-1	1984	-23.0

$^{13}\text{C}/^{12}\text{C}$ and $^{18}\text{O}/^{16}\text{O}$ in CaCO_3 , calcite sinter deposited on downhole instrument cable in test well ST-1, mid-July, 1984. (SMU analysts).

	$^{13}\text{C}/^{12}\text{C}$, PDB	$^{18}\text{O}/^{16}\text{O}$, PDB: CO_2
RM84-MVTW CaCO_3	-12.5	-29.3

$^{13}\text{C}/^{12}\text{C}$ in methane, fumarole gases.

Location	Year Collected	^{13}C , PDB	Analyst
Fum. field #2	1982	-42.3	USGS
Fum. field #6	1982	-30.6	SIO

D/H in hydrogen and methane, fumarole gases.

Location	Year Collected	D/H - H_2 , SMOW	D/H - CH_4 , SMOW	Analyst
Fum. field #3, sp	1981	-601	---	GC
Fum. field #3, superheated	1982	-582	---	USGS
Fum field #6, summit	1982	-719	-132.6	USGS

USGS = U.S. Geological Survey, Menlo Park, California.

SMU = Southern Methodist University, Stable Isotope Laboratory, Dallas, Texas.

GC = Global Geochemistry, Inc., Canoga Park, California.

SIO = Scripps Institute of Oceanography, Stable Isotope Laboratory, La Jolla, California.